Direct Conversion of Benzene to Phenol over Zeolite Catalysts using N_2O

Dissertation

zur

Erlangung des akademischen Grades

doctor rerum naturalium (Dr. rer. nat.)

der Mathematisch-Naturwissenschaftlichen Fakultät

der Universität Rostock

vorgelegt von

M.Sc. Mansour Alotaibi

geboren am 13.08.1981 in Riyadh, Saudi Arabien

Rostock: 24.01.2017

urn:nbn:de:gbv:28-diss2018-0178-7

Referees:

1. PD Dr. habil. Andreas Martin
Leibniz Institute for Catalysis
University of Rostock
Germany

2. Prof. Hamid Almegren
Materials Science Research Institute
at King Abdulaziz City for Science and Technology
Saudi Arabia, Riyadh

Name: Mansour Alotaibi
Submission date: 24.01.2017
Defense date: 18.07.2017

Declaration

I declare that the work presented in this thesis entitled “Direct conversion of benzene to phenol over zeolite catalysts using N_2O” is original and carried out by myself to obtain the doctoral degree at Leibniz Institute for Catalysis e.V., Rostock, Germany, under the guidance of my supervisors PD Dr. habil. Andreas Martin (Head of Department of Heterogeneous Catalytic Processes) and Dr. V.N. Kalevaru (Group leader). I further declare that this thesis has not been submitted, either wholly or in part, to any academic institutions for the award of any other degree or qualifications.

Rostock: 24.01.2017
Mansour Alotaibi

Acknowledgment

It is my great pleasure to present the doctoral thesis on “Direct conversion benzene to phenol over zeolite using nitrous oxide”. I would like to acknowledge a number of people for their support during the research work for this thesis.

First and foremost, I would like to extend my ultimate gratitude and appreciation to my supervisor, **Dr. habil. Andreas Martin**, Head of the Department “Heterogeneous Catalytic Processes”, Leibniz Institute for Catalysis (LIKAT) for his support, encouragement and excellent guidance throughout my entire doctoral work.

I also take this opportunity to profusely thank **Dr. Narayana Kalevaru** (Group leader, LIKAT), for his enormous support and valuable discussion and follow up action, which gave me the opportunity to learn more during the course of my Ph.D. studies. His guidance is indeed an important part of my learning.

I would like to express my acknowledgements to Dr. M. Schneider, Mr. R. Eckelt, Dr. M.-M. Pohl, Ms. A. Simmula, Ms. A. Lehmann, and other analytical staffs of LIKAT for their help in characterization of my samples and valuable discussion

I gratefully acknowledge King Abdulaziz Center for Science and Technology (KACST), Ministry of higher education Saudi Arabia, for supporting the research project and financial funding.

Special thanks go to the colleagues from KACST especially **Dr. Turki Al-Saud**. It is my pleasant duty to thank him for his encouragement, useful discussions and all kind of support

Last, but not the least, I owe my deepest gratitude to my parents for encouragement and supporting me all my life; to my brothers, my sisters throughout my study and my life

Thanks again to all of you.

Mansour Alotaibi

Abstract

Phenol is indeed a highly industrially important intermediate for the manufacture of various commercially valuable chemicals such as plastics, agrochemicals, petrochemical products and so on. The existing commercial process for the production of phenol is the so-called “Cumene process” and the majority (ca. 90%) of the phenol is being produced worldwide by this three-step process starting from benzene. Even though this synthesises currently running on industrial scale, there are several disadvantages associated with this process. For instance, i) formation of explosive intermediates (e.g. cumene hydroperoxide), ii) formation of unwanted acetone (less market valued product) as a by-product in equimolar amounts, iii) multi-step process, iv) high energy requirement etc. are some of the disadvantages of this cumene-based process. This situation stimulated several researchers to develop alternative routes to produce phenol in one step and also to avoid explosive intermediates. Direct hydroxylation of benzene to phenol is one such good option and very attractive alternative. Various research groups across the globe have made intense efforts to produce phenol in one step from benzene using a variety of catalysts and oxidants such as O_2, H_2O_2, and N_2O. Nevertheless, the desire to produce phenol in one-step with high yields still remains a dream reaction and highly challenging topic in the field of heterogeneous catalysis. This is mainly due to the reason that the target product phenol is more reactive towards further oxidation than the reactant benzene under the conditions applied. Among the different oxidizing agents applied, N_2O has given more promising results. In view of this, in the present study N_2O was used as a suitable oxidising agent and ZSM-5 supported catalysts as efficient catalysts. The primary objective of the present study was to develop highly active and selective catalysts for one-step hydroxylation of benzene to phenol with a special emphasis devoted to enhance the yield of phenol. With such objective, a variety of catalysts (mono and bimetallic catalysts) were prepared, characterised and tested in a fixed bed stainless reactor under gas phase conditions in continuous mode. More details on this approach are described below in a systematic manner.

The practical work included the preparation of various zeolite catalysts, their characterization, and catalytic testing under different reaction conditions. Initially, a variety of ZSM-5 supported monometallic catalysts were prepared by impregnation method and tested. The active component selected for these monometallic catalysts comprises of metals such as Sc, Ti, V Cr, Mn, Fe, Co, Ni, Cu, Zn, Ru and Pd. The content of metal was kept constant at 1 wt%. These catalysts were characterized by various techniques such as ICP, TGA, N_2 adsorption

(BET-SA and pore size distribution), XRD, FTIR, TPR, TPD-NH_3, SEM/TEM etc. The Si/Al ratio of ZSM support was fixed to 25. ICP revealed that the measured metal contents are in good agreement with those of nominal values. XRD showed only the diffraction patterns of ZSM-5 support and no reflections corresponding to the doped metals. This fact suggests that the doped metals are probably X-ray amorphous and this is possible because the content of metal doped is very low, i.e. only 1 wt%. BET surface areas are found to depend upon the nature of metal doped and varied in the range from 353 to 394 m^2/g. Additionally, reducible properties and acidity characteristics were observed to depend upon the metal doped. In NH_3-TPD, the catalysts exhibited both weak and strong acidic sites. TEM results of this catalyst showed no clearly distinguishable morphology for the metal particles incorporated, which is again due to low contents of metals doped.

The catalytic tests were carried in a fixed bed tubular stainless steel reactor at ambient pressure using N_2O as an oxidising agent. The reactant feed mixture consists of benzene (BN), N_2O and N_2 (as diluent to maintain constant space velocity). Initially, one commercial Fe/ZSM-5 zeolite catalyst has been tested but it has given somewhat poor results during the preliminary studies. Fe/ZSM-5 catalyst gave a phenol yield of only 3% at a benzene conversion of 7%. Among, twelve different monometallic catalysts tested, V/ZSM-5 was the best and Ti/ZSM-5 was the second best catalyst. Then, optimization of reaction conditions were also investigated using this best monometallic V/ZSM-5 catalyst to improve the yield of phenol. For optimization studies, the influence of all possible reaction variables such as i) effect of reaction temperature, ii) the effect of space velocity (GHSV), iii) the impact of BN feed rate, iv) the effect of BN to N_2O mole ratio on the catalytic activity and selectivity were explored. The optimized reaction conditions are: mole ratio of BN: N_2O: N_2 = 1: 1.5: 82.3, Reaction T = 410 °C, GHSV = 2612 h^{-1}, contact time = 1.4 s. Additionally, catalyst calcination temperature was also optimized and found that a calcination temperature of 500 °C is optimum for this reaction. After optimization, the best monometallic V/ZSM-5 showed acceptably good phenol yield of 11.6% at a benzene conversion of 23.8%. After testing all monometallic catalysts, it was decided to combine both the first and second best metals and prepare bimetallic catalysts. With this objective, six different bimetallic catalysts were prepared by impregnation, characterized and tested in same way.

Among different bimetallic catalysts tested, the catalyst containing vanadium and titanium gave superior performance. Some selected reaction variables were optimized using this V-Ti/ZSM-5 catalyst. As a result, the yield of phenol improved from 10% (on monometallic catalyst) to 16% on bimetallic V-Ti catalyst. Later on the contents of each metal were also

optimized and found that a metal content of 0.25 wt% each gave best results. All bimetallic catalysts were calcined at 500 °C too. However, for the best catalyst composition (V-Ti/ZSM-5), three Si/Al ratios (25, 240 and 400) were taken and checked its influence on the catalytic performance. Among the three, a Si/Al ratio of 25 was found to give better performance.

After identifying the best bimetallic composition, the subsequent investigations were focused on the exploring the effect of support. This is again with the intention of improving further the yield of phenol. For this study, four different zeolite supports such as ZSM-5, Ga-ZSM-5, USY, and BEA were selected. Among these supports, Ga-ZSM-5 has shown astonishingly good catalytic performance. Consequently, the best V-Ti/Ga-ZSM-5 catalyst has given significantly higher yield of phenol (27.2%) at a benzene conversion of 33.6% due to high acidity and thermal stability. On the whole; the yield of phenol was improved from ca. 3% during the initial tests over Fe/ZSM-5 catalysts to an amazing value of 27.2% over V-Ti/Ga-ZSM-5 catalyst which is indeed a significant achievement of this study.

Zusammenfassung

Phenol ist ein industriell wichtiges Intermediat für die Herstellung verschiedener kommerziell bedeutsamer Chemikalien wie z. B. Kunststoffe, Agrochemikalien, Erdöl-basierte Produkte usw. Der existierende kommerzielle Prozess für die Produktion von Phenol ist das sogenannte Cumolhydroperoxid-Verfahren (Hock'sche Phenolsynthese) und die Hauptmenge (ca. 90%) an Phenol wird weltweit nach diesem Verfahren in einem Dreistufenprozess ausgehend von Benzol erzeugt. Obwohl die Synthese im industriellen Maßstab realisiert ist hat der Prozess einige Nachteile wie z. B. 1.) die Bildung von explosiven Intermediaten (z. B. Cumolhydroperoxid), 2.) die Bildung von nicht erwünschtem Aceton als Nebenprodukt in äquimolaren Mengen (Produkt mit niedrigem Marktpreis), 3.) einen Mehrstufenprozess, oder 4.) einen hohen Energiebedarf.

Diese Ausgangslage hat verschiedentlich Forschergruppen veranlasst, alternative Routen für die Produktion von Phenol in einem Syntheseschritt zu erforschen und gleichzeitig explosive Intermediate zu vermeiden. Unter anderen Wegen ist die direkte Hydroxylierung von Benzol zu Phenol eine sehr attraktive Alternative. Eine Vielzahl an verschiedenen Wissenschaftlergruppen weltweit haben große Anstrengungen unternommen, um Phenol in einem Schritt aus Benzol durch Verwendung einer Vielzahl an Katalysatoren und Oxidationsmittel wie z. B. O_2, H_2O_2 und N_2O zu synthetisieren. Dennoch bleibt die Produktion von Phenol in einer Einstufensynthese mit hohen Ausbeuten weiterhin eine "dream reaction" und damit ein höchst anspruchsvolles Thema auf dem Gebiet der heterogenen Katalyse. Dies liegt insbesondere daran, dass das Zielprodukt Phenol reaktiver in Hinblick auf Weiteroxidation als das eingesetzte Benzol unter Prozessbedingungen ist. Unter den verschiedenen angewendeten Oxidationsmitteln hat N_2O vielversprechende Resultate gezeigt. Mit dieser Kenntnis habe ich in meiner Arbeit N_2O als Oxidationsmittel und ZSM-5 geträgerte Materialien als effiziente Katalysatoren genutzt.

Das Primärziel meiner Untersuchungen war die Entwicklung hochaktiver und selektiver Katalysatoren für die Einschritt-Hydroxylierung von Benzol zu Phenol mit besonderer Berücksichtigung der Erhöhung der Phenolausbeute. Ausgehend von der Zielsetzung wurde eine Vielzahl an Katalysatoren (mono- und bimetallische Katalysatoren) synthetisiert, charakterisiert und in einem kontinuierlich betriebenen Festbettreaktor aus Edelstahl unter Gasphasenbedingungen ausgetestet. Detaillierte Information zur Herangehensweise sind im Folgenden systematisch erklärt.

Die praktischen Arbeiten umfassten die Synthese einer Vielzahl an Zeolith-Katalysatoren, deren Charakterisierung und katalytische Austestung unter verschiedenen Reaktionsbedingungen. Zuerst wurde eine Vielzahl an ZSM-5 geträgerten monometallischen Katalysatoren mittels Imprägniermethoden hergestellt und ausgetestet. Die Aktivkomponenten, die für diese monometallischen Katalysatoren ausgewählt wurden, waren Sc, Ti, Cr, V, Mn, Fe, Co, Ni, Cu, Zn, Pd und Ru. Der Metallgehalt wurde bei konstant 1 Gew.-% gehalten. Diese Katalysatoren wurden mit einer Vielzahl an verschiedensten Techniken wie z. B. ICP, TGA, N_2-Adsorption (BET-SA und Porengrößeverteilung), XRD, FTIR, TPR, TPD-NH_3, SEM/TEM usw. charakterisiert. Das Si/Al-Verhältnis des ZSM-Trägers wurde auf 25 eingestellt. ICP-Untersuchungen zeigten, dass der gemessene Metallgehalt in guter Übereinstimmung mit den nominalen Werten war. XRD-Messungen zeigten ausschließlich Beugungsmuster des ZSM-5-Trägers und keinerlei Reflexe des entsprechenden, aufgebrachten Metalls. Dieser Fakt suggeriert, dass das aufgebrachte Metall röntgenamorph zu sein scheint und dies ist sehr wahrscheinlich, da der Anteil des aufgebrachten Metall mit 1 Gew.-% sehr klein ist. BET-Oberflächen scheinen von der Natur des aufgebrachten Metalls abzuhängen und variieren im Bereich von 353 bis 394 m²/g. Zusätzlich wurden Redoxeigenschaften bestimmt, die vom aufgebrachten Metall abhängen. Mittels NH_3-TPD zeigte sich, dass die Katalysatoren sowohl schwach als auch stark saure Zentren besitzen. TEM-Ergebnisse der Katalysatoren zeigten keinerlei klar zu unterscheidende Morphologien aufgrund des geringen Anteils für die eingebrachten Metallpartikel.

Die katalytischen Testungen wurden in einem Festbett-Edelstahlrohrreaktor unter Umgebungsdruck unter Verwendung von N_2O als Oxidationsmittel durchgeführt. Die Feedzusammensetzung der Eduktströme bestand aus Benzol (BN), N_2O und N_2 (als Verdünnungsmittel für konstante Raumgeschwindigkeiten). Zuerst wurde ein kommerzieller Fe/ZSM-5-Zeolith-Katalysator ausgetestet. Dieser Fe/ZSM-5-Katalysator zeigte eine geringe Phenolausbeute von nur 3% bei einem Benzolumsatz von 7%. Unter den selbst hergestellten zwölf verschiedenen monometallischen Katalysatoren waren V/ZSM-5 der beste und Ti/ZSM-5 der zweitbeste Katalysator. Anschließend wurde auch die Optimierung der Reaktionsbedingungen unter Verwendung des besten monometallischen Katalysators (V/ZSM-5) zur Steigerung der Phenolausbeute untersucht. Für die Optimierungen wurden sämtliche Reaktionsvariablen wie z. B. 1.) der Effekt der Reaktionstemperatur, 2.) der Effekt der Raumgeschwindigkeit (GHSV), 3.) die Auswirkung der BN-Feedrate, 4.) der Effekt des BN: N_2O-Molverhältnisses auf die katalytische Aktivität und Selektivität untersucht. Die

optimalen Reaktionsbedingungen sind: Molverhältnis BN: N_2O: N_2 = 1,0: 1,5: 82,3 Reaktionstemperatur T = 410 °C, GHSV = 2612 h^{-1}; Kontaktzeit = 1,4 s. Zusätzlich wurde auch die Kalziniertemperatur des Katalysators optimiert und es zeigte sich, dass bei einer Kalziniertemperatur von 500 °C ein Optimum für diese Reaktion besteht. Nach der Optimierung zeigte der beste monometallische V/ZSM-5 Katalysator eine akzeptable Phenolausbeute von 11,6% bei einem Benzolumsatz von 23,8%. Nach den Testungen an den monometallischen Katalysatoren wurde beschlossen, dass durch die Kombination der beiden besten Metalle ein bimetallischer Katalysator hergestellt werden sollte. Ausgehend davon wurden so sechs verschiedene bimetallische Katalysatoren mittels Imprägniermethoden synthetisiert, charakterisiert und in gleicher Weise ausgetestet.

Unter den verschiedenen bimetallischen, ausgetesteten Katalysatoren zeigten die Katalysatoren ausgezeichnete Leistungen, die Vanadium und Titan beinhalteten. Einige ausgewählte Reaktionsvariablen wurden mittels dieses V-Ti/ZSM-5-Katalysators optimiert. Demzufolge konnte die Phenolausbeute von 10% (monometallischer Katalysator) auf 16% unter Verwendung des bimetallischen V-Ti-Katalysators gesteigert werden. Später wurden auch die jeweiligen Metallgehalte optimiert und es zeigte sich, dass ein jeweiliger Metallgehalt von 0,25 Gew.-% die besten Ergebnisse liefert. Alle bimetallischen Katalysatoren wurden auch bei 500 °C kalziniert. Dennoch wurden für das beste Katalysatorverhältnis (V-Ti/ZSM-5) drei Si/Al-Verhältnisse (25, 240, 400) ausgewählt und deren Einfluss auf die katalytische Leistung untersucht. Es zeigte sich, dass bei einem Si/Al-Verhältnis von 25 eine bessere Leistung erzielt werden kann.

Nach Ermittlung des besten bimetallischen Verhältnisses wurden die Arbeiten auf den Effekt des Trägermaterials fokussiert. Dies erfolgte wiederum in Hinblick auf eine mögliche Verbesserung der Phenolausbeute. Für die Untersuchung wurden vier verschiedene Zeolith-Träger ausgewählt (ZSM-5, Ga-ZSM-5, USY, BEA). Unter diesen Trägern zeigte Ga-ZSM-5 eine erstaunlich gute katalytische Leistung. In der Konsequenz gab der beste V-Ti/Ga-ZSM-5-Katalysator eine signifikant höhere Phenolausbeute (27,2%) bei einem Benzolumsatz von 33,6% aufgrund hoher Acidität und thermischer Stabilität. Zusammenfassend kann festgestellt werden, dass die Phenolausbeute in Ausgangstests von ca. 3% unter Verwendung von industriell verfügbaren Fe/ZSM-5-Katalysatoren auf einen imposanten Wert von 27,2% bei Verwendung eines V-Ti/Ga-ZSM-5 Katalysators gesteigert werden konnte.

List of abbreviations, acronyms and symbols

POL	Phenol
BN	Benzene
MeOH	Methanol
FID	Flame Ionization Detector
GC	Gas Chromatography
TCD	Thermal Conductivity Detector
C-Bal	Carbon Balance
GHSV	Gas Hourly Space Velocity
BET	Brunauer – Emmet – Teller model
BJH	Barret – Joyner – Halenda model
CHNS	Carbon, Hydrogen, Nitrogen, Sulfur analysis
EDX	Energy Dispersive X-ray Spectroscopy
TGA	Thermogravimetric analysis
ICP-OES	Inductive Coupled Plasma Optical Electron Spectroscopy
XRD	X-ray Diffraction
NH_3-TPD	Temperature Programmed Desorption of Ammonia
TEM	Transmission Electron Microscopy
TPR	Temperature-programmed reduction
FTIR	Fourier transform infrared spectroscopy
UV-vis	Ultraviolet–visible spectroscopy
SEM	Scanning Electron Microscopy

Contents

1.	Introduction and objectives	1
1.1	Commercial applications of phenol	2
1.2	Phenol production and their processes	2
1.2.1	Sulfonation process	3
1.2.2	Chlorination process	3
1.2.3	Cyclohexanone process	3
1.2.4	Benzoic acid process	4
1.2.5	Cumene process	4
1.3	State of art	6
1.3.1	Direct conversion of benzene to phenol in the liquid phase	6
1.3.2	Direct conversion of benzene to phenol in the gas phase	6
1.4	Direct hydroxylation of benzene to phenol over zeolite using nitrous oxide	7
1.5	Zeolite catalysts	9
1.6	Transition metal ion doping in zeolite	10
1.7	Nitrous oxide	10
1.8	Objectives of the thesis	10
2.	Experimental Methods and Equipment	13
2.1	Preparation of monometallic and bimetallic catalysts	14
2.2	Catalyst Characterization	15
2.2.1	Thermogravimetric analysis (TGA)	16
2.2.2	Inductively coupled plasma optical emission spectroscopy (ICP-OES)	16
2.2.3	Nitrogen adsorption (BET-surface areas and pore size distribution)	17
2.2.4	X-ray powder diffraction (XRD)	19

2.2.5	Temperature programmed desorption of ammonia (TPDA)	20
2.2.6	Temperature-programmed reduction (TPR)	21
2.2.7	Fourier transform infrared spectroscopy (FTIR)	21
2.2.8	Ultraviolet–visible spectroscopy (UV-vis)	21
2.2.9	Scanning electron microscopy (SEM)	22
2.2.10	Transmission electron microscopy (TEM)	22
2.3	Experimental set up and catalytic test procedures	23
2.3.1	GC calibrations of educts/products	24
3.	Benzene hydroxylation over ZSM-5 supported monometallic catalysts	27
3.1	Studies on the ZSM-5 supported monometallic catalysts	28
3.2	Catalyst preparation	28
3.3	Characterization of ZSM-5 supported monometallic catalysts	29
3.3.1	Thermogravimetric analysis	29
3.3.1.1	ZSM-5 supported monometallic Fe, Ti, V and Sc catalysts	29
3.3.1.2	ZSM-5 supported monometallic Co, Ni, Cu and Zn catalysts	30
3.3.2	Textural properties and catalyst composition	31
3.3.3	Pore-Size distribution of ZSM-5 supported metal oxide catalysts	32
3.3.3.1	ZSM-5 supported Zn, Cu, Ni and Co catalysts	32
3.3.3.2	ZSM-5 supported Mn, Cr, V and Ti catalysts	33
3.3.3.3	ZSM-5 supported Sc and Pd catalysts	34
3.3.4	X-ray diffraction	35
3.3.4.1	ZSM-5 supported Co, Ni, Cu and Zn catalysts	35
3.3.4.2	ZSM-5 supported Mn, Cr, V and Ti catalysts	36
3.3.4.3	ZSM-5 supported Ru, Sc, Pd and Fe catalysts	37

3.3.5	Fourier transform infrared spectroscopy	38
3.3.5.1	ZSM-5 supported Mn, Cr, V and Ti catalysts	38
3.3.6	Temperature programmed desorption of ammonia	39
3.3.6.1	ZSM-5 supported Zn, Cu, Ni and Co catalysts	39
3.3.6.2	ZSM-5 supported Mn, Cr, V and Ti catalysts	41
3.3.7	Temperature programmed reduction	42
3.3.8	Ultraviolet visible spectroscopy	44
3.3.8.1	ZSM-5 supported Mn, Cr, V and Ti catalysts	44
3.3.8.2	ZSM-5 supported Zn, Cu, Ni and Co catalysts	45
3.3.9	Transmission electron microscopy and Energy dispersive X-ray spectroscopy	46
3.4	Catalytic results	48
3.4.1	General catalytic test conditions	48
3.4.2	Optimization of the reaction conditions	49
3.4.2.1	Effect of reaction temperature on the catalytic performance	49
3.4.2.2	Effect of benzene to N_2O mole ratio on the catalytic activity and selectivity	50
3.4.2.3	Effect of benzene feed rate on the catalytic performance	50
3.4.2.4	Effect of GHSV on the catalytic performance	51
3.4.2.5	Effect of Fe loading in Fe/ZSM-5 on the catalytic performance	52
3.4.3	Catalytic tests	53
3.4.3.1	Impact of V, Ti and Sc doping on the catalytic performance	53
3.4.3.2	Impact of Co, Mn, and Cr doping on the catalytic performance	54
3.4.3.3	Impact of Ni, Cu, and Zn doping on the catalytic performance	55
3.4.3.4	Impact of Pd, Ru, and Fe doping on the catalytic performance	56
3.5	Summary and conclusion	57

4.	Effect of second metal addition to V-ZSM-5 on benzene hydroxylation	61
4.1	Studies on the ZSM-5 supported bimetallic catalysts	62
4.2	Catalyst preparation	62
4.3	Characterization of bimetallic V-M/ZSM-5 catalysts	62
4.3.1	Textural properties and catalyst composition	62
4.3.2	XRD patterns	64
4.3.3	Temperature programmed desorption of ammonia	64
4.4	Catalytic results	66
4.4.1	Effect of V/Ti loading in 0.25V-0.25Ti/ZSM-5 catalyst on the performance	66
4.4.2	Catalytic results of V-Fe, V-Ni, V-Zn bimetallic catalysts	66
4.4.3	ZSM-5 supported V-Ti, V-Cr, V-Mn bimetallic catalysts	67
4.5	Conclusions	68
5.	Benzene hydroxylation over bimetallic V-Ti/ZSM-5 catalyst	71
5.1	Studies on the ZSM-5 supported bimetallic V-Ti/ZSM-5 catalyst	72
5.2.	Catalyst preparation	72
5.3	Characterization of bimetallic V-Ti/ZSM-5 catalyst	73
5.3.1	Thermogravimetric analysis	73
5.3.2	Textural properties and catalyst composition	74
5.3.3	Pore-Size distribution of pure ZSM-5 and V-Ti/ ZSM-5 samples	75
5.3.4	X-ray diffraction	75
5.3.5	Temperature programmed desorption of ammonia	76
5.3.6	Transmission electron microscopy and Energy dispersive X-ray spectroscopy	77
5.4	Catalytic tests	78
5.4.1	Optimization of reaction conditions	78

5.4.1.1	Influence of calcination temperature on the catalytic activity of V-Ti/ZSM-5	78
5.4.1.2	Impact of Si/Al ratio of ZSM-5 in V-Ti/ZSM-5 catalyst	79
5.4.1.3	Effect of reaction temperature on the catalytic performance of V-Ti/ZSM-5	80
5.4.1.4	Effect of GHSV on the catalytic performance of V-Ti/ZSM-5 catalyst	81
5.4.1.5	Effect of benzene feed rate on the catalytic performance V-Ti/ZSM-5 catalyst	82
5.4.1.6	Effect of N_2O molar portion on the catalytic activity of V-Ti/ZSM-5 catalyst	83
5.5	Conclusions	84
6.	Effect of support nature on the performance of bimetallic V-Ti/zeolite catalysts	85
6.1	Studies on different parent supported bimetallic catalysts	86
6.2	Catalyst preparation	86
6.3	Characterization of zeolite supported V-Ti catalysts	87
6.3.1	Thermogravimetric analysis	87
6.3.2	BET-surface areas and pore volumes	88
6.3.3	X-ray diffraction	88
6.3.4	TPR profiles of bimetallic V-Ti catalysts on various supports	89
6.3.5	Temperature programmed desorption of ammonia	90
6.3.6	Scanning electron microscopy	92
6.4	Catalytic results	93
6.4.1	Optimization of reaction conditions for direct conversion of benzene to phenol	93
6.4.1.1	Effect of support on the catalytic performance of bimetallic V-Ti catalysts	93
6.4.1.2	Effect of reaction temperature on the catalytic performance of V-Ti/Ga-ZSM-5	94
6.4.1.3	Effect of GHSV on the catalytic performance of V-Ti/Ga-ZSM-5 catalyst	95
6.4.1.4	Comparison of coke deposits in the spent V-Ti/S catalysts (S= support)	95
6.5	Conclusions	96

7. Overall summary and outlook 99

8. References 105

Chapter 1

Introduction and objectives

This chapter contains general information about the phenol industry, various processes for phenol manufacture, zeolite catalysts, properties and use of nitrous oxide, transition metal ion doping in zeolites and the objective of the present study. Literature survey supplies the information on the state of the art of promotion for gas phase hydroxylation of benzene to phenol. Comparison of cumene process and alternative routes is also given.

1. Introduction and objectives

1.1 Commercial applications of phenol

Phenol is indeed a large scale product in the chemical industry with a variety of commercial applications [1-10]. For instance, phenol is extensively used in the production of plastics, agrochemicals, pharmaceuticals, resins, etc. [11]. Furthermore, it is also used for the manufacture of a good number of intermediates, which include, bisphenol, alkylphenol, chlorophenol, and so on. In fact, the only convenient source of phenol until the early twentieth century was by-product retrieval from petroleum refinery processes. Nevertheless, in recent times, the phenol production is receiving enormous interest due to its high demand as well as commercial magnitude across the globe. Phenol is a white crystalline solid with the chemical formula C_6H_5OH. To large extent, phenol is produced by cumene process [12-19]. Figure 1.1 illustrates the commercial application of different types of products produced from phenol [20]. Phenol formaldehyde resin is a low cost product made through the condensation of phenol and formaldehyde. Bisphenol A is produced by the condensation reaction of acetone and phenol [21]. In addition, there are some other phenol derivatives such as aniline which also produced from phenol.

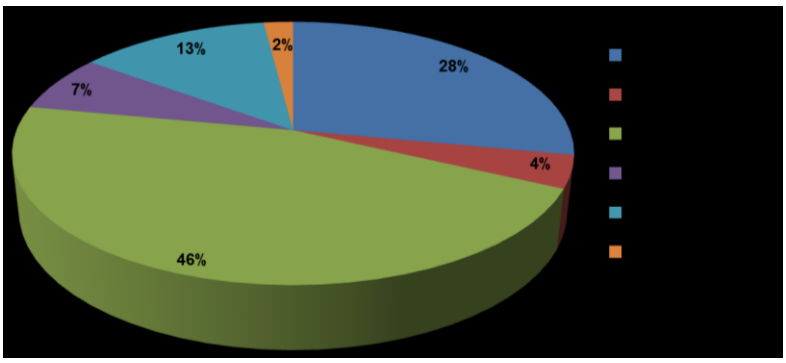

Figure 1.1. Application of phenol-based chemical products in 2015 [22]

1.2 Phenol production and their processes

Phenol was discovered in 1834 by German chemist F.F. Runge. He isolated it from coal tar and called it as carbolic acid. However, it is isolated from coal tar till date from hard-coal rich sources. There exist several processes to manufacture phenol synthetically, for example by i) benzene sulfonation process, ii) benzoic acid process and iii) cumene process [23]. All

these processes are briefly described below. Among them, cumene process is currently used on commercial scale. More than 90% of phenol is produced through this process.

1.2.1 Sulfonation process

The first industrial manufacture was carried out in 1899 by BASF. This process includes production of a large amount of Na_2SO_3 waste from corrosive H_2SO_4 to obtain benzenesulphonic acid which on reaction with a base (NaOH) produces phenol. Sulfonation process was applied for about eighty years [24].

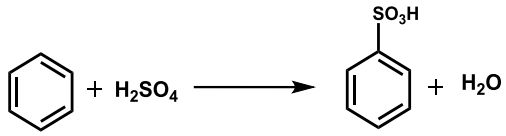

(Eq. 1.1)

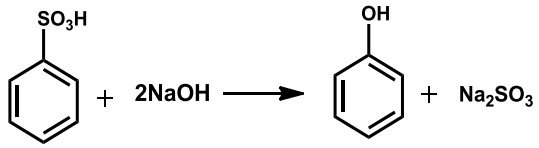

(Eq. 1.2)

1.2.2 Chlorination process

This process was developed in 1924 by Dow Chemical in US. It used in a first step chlorine and $FeCl_3$ as catalyst to obtain C_6H_5Cl that reacts consecutively with sodium hydroxide in the range of 300-390 °C to produce C_6H_5OH and NaCl as by-product [24, 25].

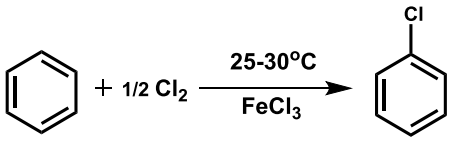

(Eq. 1.3)

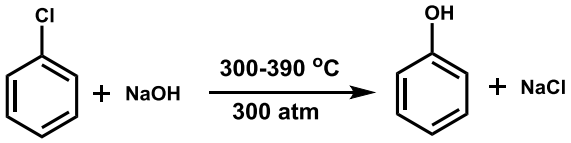

(Eq. 1.4)

1.2.3 Cyclohexanone process

Benzene is converted to phenol in a three-step process. First, benzene is hydrogenated to cyclohexane over Pt-containing catalyst. Afterwards the so-called KA-oil (ketone-alcohol oil) is produced by oxidation and in a third step such mixture might be dehydrogenated again to get phenol [24]. However, this process is not really economic.

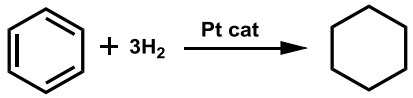

(Eq. 1.5)

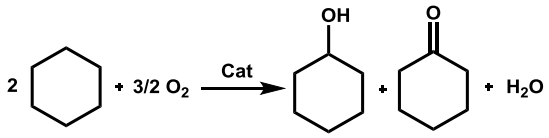

(Eq. 1.6)

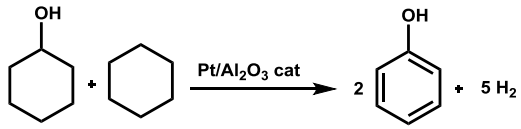

(Eq. 1.7)

1.2.4 Benzoic acid process

This process was used in Canada since1961. The benzoic acid of process consists of two stages: the first stage is formation benzoic acid from toluene with cobalt salt and air at 76-177 °C and the second processing; the formation of phenol was achieved from oxidation of benzoyl salicylic acid in presence of CuMg and air at 240 °C [24].

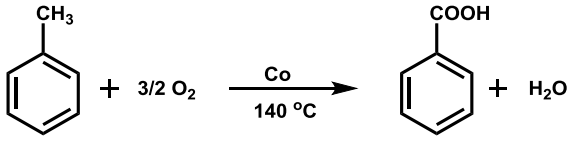

(Eq. 1.8)

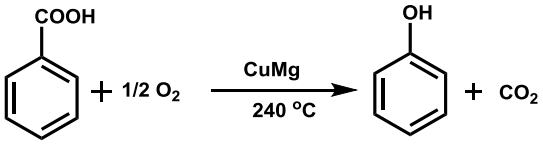

(Eq. 1.9)

1.2.5 Cumene process

The majority of the world phenol production is made at the moment by the so-called cumene process, which is of course a multi-step process (see Scheme 1.1.) [26]. In fact, alkylation of benzene with propene is the first step to produce cumene which is then further oxidized to cumene hydroperoxide ($C_6H_5C(CH_3)_2OOH$) by air [26]. The formation of phenol and acetone by means of an acidic cleavage of cumene hydroperoxide ($C_6H_5C(CH_3)_2OOH$) is the last step. This pathway is normally catalysed by H_2SO_4. In fact, this cumene process that is already running on commercial scale makes use of relatively cheaper feedstocks such as (propene and benzene), and at the same time, it also produces the unwanted acetone as by-product in considerably higher, i.e. equimolar amounts. Acetone market is somewhat limited

and hence this process is not really very attractive from economics point of view. One good improvement is the dehydration of acetone to get back propene that can be recycled. Even though this cumene process is commercially successful, there are several disadvantages: i) environmental unfriendly, ii) forming of an explosive mixture that consist of peroxides, iii) usage of a highly corrosive catalyst (e.g. aluminum chloride), iv) formation of unwanted acetone in high amounts as by-product, and v) the requirement of multi-step approach. Due to all these reasons, an increasing capital investment is also incurred. Based on these facts, it can be said that the economic competence of the cumene process depends essentially on the demand for acetone in the global market [27-29]. Therefore, there is a need to develop a suitable process for direct synthesis of phenol from benzene. Direct hydroxylation of benzene to phenol in one-step is one such good option. The phenol production by the cumene process is illustrated in Scheme 1.1.

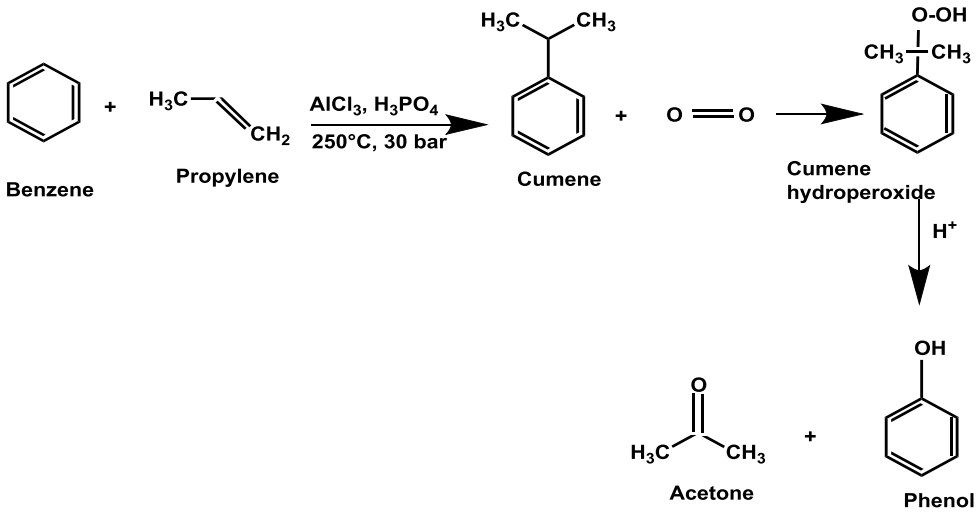

Scheme 1.1. Cumene process for the industrial production of phenol

1.3 State of art

1.3.1 Direct conversion of benzene to phenol in the liquid phase

Literature survey reveals that a variety of catalyst compositions related to both heterogeneous and homogenous processes of phenol production have been investigated in the past few decades. The reaction was carried out both in liquid phase and also in the gas phase. The reaction conditions of gas phase benzene hydroxylation are certainly much different from liquid phase hydroxylation. Moreover, various researchers have used different oxidants such as N_2O, molecular oxygen, and H_2O_2 etc. for benzene hydroxylation. It seems that H_2O_2 is widely used in liquid phase compared to others. However, better results in the gas phase were obtained with N_2O as an oxidant. Therefore, one step oxidation of benzene to phenol has shown somewhat better results. In the liquid phase, $V(acac)_3$ catalysts for benzene hydroxylation with H_2O_2 revealed a BN conversion of 26% and 26% yield of POL (i.e. phenol selectivity of 100%) at 65 °C [30]. Another example for liquid phase approach is the application of vanadyl pyrophosphate catalysts. These solids are also reported to be active and selective and gave a BN conversion of 67%, POL yield of 60% and POL selectivity of 90% at 60 °C using acetonitrile as solvent [31]. On the other hand, mesoporous materials based catalysts (e.g. V/MCM-41) for benzene hydroxylation with H_2O_2 showed a BN conversion of only 10%, with a POL yield of 8.1% that corresponds to a phenol selectivity of 81% at 70 °C [32]. Pd/Pt containing acid resin catalysts was used for benzene hydroxylation with a BN conversion of 7.5% with 4.2% POL yield (i.e. 57% phenol selectivity) at 43 °C [33]. VO_x/CuSBA-15 catalyst exhibits 27% BN conversion at 80 °C with selectivity to POL of 100% [34]. Cu-MCM-41 catalyst showed a BN conversion of 38.6%, with over 95% phenol selectivity at 65 °C using H_2O_2 [35]. On the other hand, TS-1 catalyst showed a BN conversion of 15.4%, POL yield 13% and selectivity 84.6% at 60 °C [36]. Based on neural network calculations, the authors claimed that TS-1 catalyst in BN hydroxylation with H_2O_2 gave a BN conversion of 81.2%, POL yield 78% that corresponds to a phenol selectivity of 96% at 50 °C [37].

1.3.2 Direct conversion of benzene to phenol in the gas phase

Our target is to develop novel catalyst compositions for gas phase hydroxylation of benzene to phenol. Fe/ZSM-5 catalyst was used for initial tests as bench mark catalyst and then modifies it in different ways using different components / modifiers / promoters. In addition, Fe/silicalite catalyst for benzene hydroxylation with N_2O exhibit a BN conversion of 12% and POL yield 11.7% at 450 °C, which is considerably good due to its very high POL selectivity

(98%) [38]. Fe/[B,Al]MFI catalysts for benzene hydroxylation with N_2O showed BN conversion of 14.3%, POL yield 13% with phenol selectivity 91% at 450 °C [39]. [Al]MFI+$FeCl_3$ catalysts for benzene hydroxylation with N_2O showed BN a conversion of 40% and POL yield of 33.2% (S = 83%) at 350 °C [40]. Efforts made by Hensen et al. [41] revealed only 14% BN conversion and 14% POL yield over [Fe,Al]MFI catalysts in benzene hydroxylation with N_2O at 350 °C. In other words, a POL selectivity of one 100% could be reached, which is indeed remarkable. Another such example is the application of H-Ga-FER zeolite catalyst where again 100% selectivity of POL is attained at a BN conversion of 21% at 500 °C [42]. Mo/Fe borosilicate molecular sieve catalyst for benzene hydroxylation with N_2O gave a BN conversion of 17% and POL yield of 16.5% (i.e S_{POL} = 97%) at 410 °C [43]. On the other hand, TS-1 catalyst showed relatively less conversion of BN (6.5%), and hence less yield of POL (6.4%) (i.e S_{phenol} = 99%) at 200 °C [44]. Titanium silicalite-1 (TS-1) and mesoporous Pd-TS-1 were also applied as catalysts for the direct conversion of BN to POL in a palladium membrane reactor. The BN conversion obtained was only 5.4% while the POL yield was 5.1% (i.e S_{phenol} = 95%) [45]. Similarly, Fe/Al-SBA-15 materials are reported to give poor performance in the hydroxylation of benzene to phenol with selectivity to phenol up to 40% at very low benzene conversion (2.3%) and phenol yield 0.9% [46]. Cu-Ca-PO_4 revealed less conversion of benzene 1.3% and hence less yield of phenol 1.3% with high selectivity 99% at 450 °C with O_2 as an oxidant [47].

1.4 Direct hydroxylation of benzene to phenol over zeolite using nitrous oxide

Hydroxylation of benzene to phenol is used in industry and in academic research such as selective oxidation of hydrocarbons, which is one of the important topics in heterogeneous and homogeneous catalysis [48-61]. Direct oxidation of benzene to phenol is highly attractive. Although different opportunities exist for the synthesis of phenol, the direct oxidation of benzene to phenol in one step (Scheme 1.2) using nitrous oxide as oxidant is indeed as an attractive and economic approach, which is also the main task of the present study. Moreover, gas phase hydroxylation also leads to the formation of some other by-products such as catechol, carbon oxides etc. In this approach, phenol is the major product of the reaction and the formation of various other by-products depends upon the reaction conditions and type of catalyst applied.

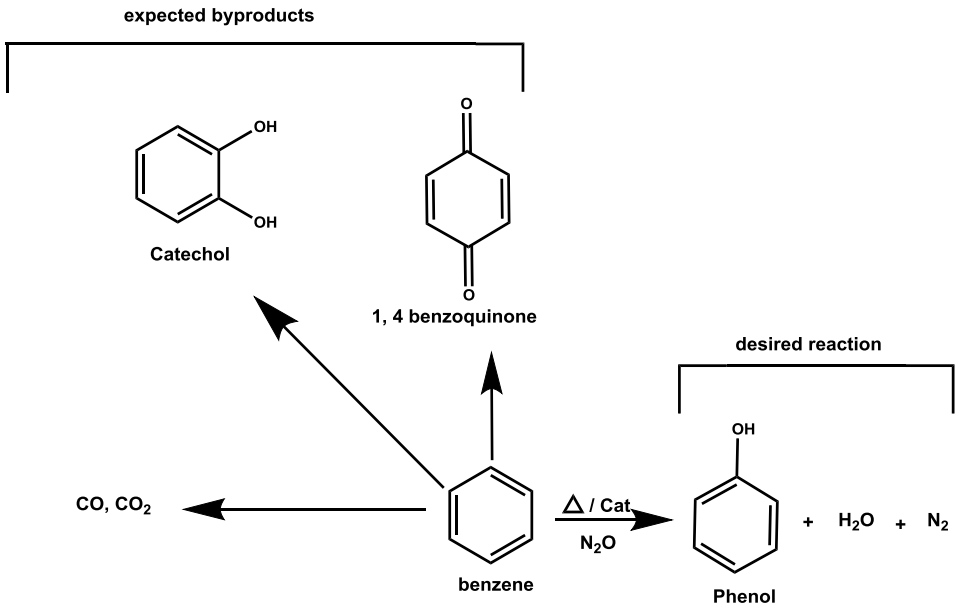

Scheme 1.2. An overview on the formation of desired product phenol and various by-products of the benzene to phenol reaction

Direct hydroxylation of benzene to phenol over zeolite using nitrous oxide is related to serious obstacle like deactivation which leads to the short lifespan of catalysts and lower phenol yield [62-66]. Accumulation interior the pore of catalyst leads to coke formation due to difficult diffusion and robust adsorption of molecule [67]. Gas phase hydroxylation of benzene to phenol in one step using monometallic and bimetallic zeolite catalysts is an attractive option. The strategy in this work is enhancing the yield of phenol using right composition of catalyst composition and zeolite support with different Si/Al ratio. At the same time the optimization of reaction conditions is also required for improving the yield of phenol. Extensive efforts have been made by various research groups for the past few decades to develop a suitable gas phase process for the direct synthesis of phenol from benzene using a variety of catalysts. As mentioned above, direct hydroxylation of benzene to produce phenol is an attractive alternative to the existing commercial process, i.e. Cumene process. The widely used catalysts for the direct hydroxylation of benzene are based on zeolites in general, ZSM-5 framework in particular. Doping of different transitional metals into various different zeolite frameworks are extensively applied and are certainly helpful to improve the yield of phenol.

In view of this, in the present study various novel catalyst compositions again based on zeolites were synthesized and tested for the present reaction. Some useful information on the zeolites and metal doping of such zeolites are briefly described below.

1.5 Zeolite catalysts

Zeolite is a class of solids based in general on crystalline aluminosilicates containing a microporous structure with uniform channels/cavities of SiO_4 and AlO_4 tetrahedra connected to each other by oxygen forming a three dimensional network enabling shape selective catalysis. There are various types of zeolite structures available, a few of them are ZSM-5, USY, BEA, Mordenite etc. [68-70]. Zeolites are widely used in industry for different catalytic and separation applications. They are mainly used for alkylation, isomerization, and dismutation reactions in refineries. Zeolites are important solids in heterogeneous catalysis due to their unique chemical properties such as good thermal stability, high acidity, tunable pore size, high surface areas and crystalline structure. Among them, acidity is one of the important factors that play a key role in catalytic activity and selectivity [71]. Literature survey reveals that Fe/ZSM-5 was widely applied for direct conversion of benzene to phenol and Lewis acid sites, Brønsted acid sites and the activity of ZSM-5 catalysts [72-92]. The main empirical formula of a zeolite maybe generally represented as:

$$M_{x/n}[(AlO_2)_x(SiO_2)_y].wH_2O \qquad \text{(eq. 1.10)}$$

Figure 1.2 shows the presence of Brønsted acid centers in the zeolite structure. Zeolites also contain both Lewis centers and Brønsted acid centers. The acidity and the shape selectivity play a crucial role on the catalytic performance of zeolite based catalysts. A change in Si/Al ratio also alters the catalytic properties [93].

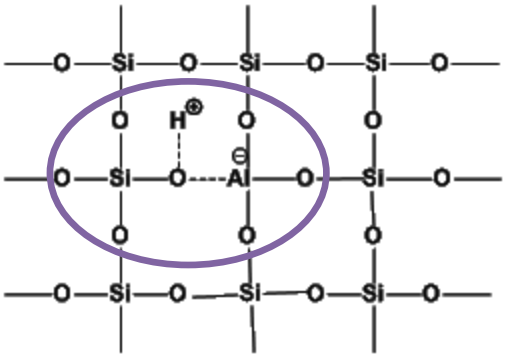

Figure 1.2. Brønsted acid center in the zeolite structure [94]

1.6 Transition metal ion doping in zeolite

It is favorable, at the starting, to know the chemical and physical properties of transition metals, for instance, i) the thermal stability of metals ii) variable oxidation states ii) charge radius ratio etc. [95] Several kinds of transition metals and some physical properties are compiled In Table 1.1. ZSM-5, BEA, and USY containing transition metal ions usually display a good activity in hydroxylation reactions. Moreover, there are two aspects of this study on the zeolites containing metals: i) activated oxygen species ii) coordination to the lattice [96]. In contrast, the high amount of transition metal ion loading will take place in the interior zeolite structure. The metals might be diffused to interior channels or partly located on the exterior surface of the ZSM-5 framework.

Table 1.1. Summary of physical properties used in this study.

Metals	Ionization energy kJ mol^{-1}	Density g cm^{-3}	M.P (°C)	B.P (°C)	Radius pm	At. Wt. of metal
Sc	631	2.99	1541	2836	164	44.96
Ti	658	4.50	1668	3287	147	47.90
V	650	5.96	1910	3407	135	50.94
Cr	653	7.20	1907	2671	129	51.99
Mn	717	7.21	1246	2061	137	54.94
Fe	759	7.87	1538	2862	126	55.85
Co	758	8.90	1495	2927	125	58.93
Ni	737	8.90	1455	2730	125	58.70
Cu	746	8.96	1084	2562	128	53.55
Zn	906	7.14	420	907	137	65.37

1.7 Nitrous oxide

The main industrial origin of nitrous oxide can be found the production of nitric acid and adipic acid [97-99]. N_2O is one of the suitable oxidizing agents and is also being widely studied for various oxidation reactions in general and hydroxylation of benzene to phenol. Nitrous oxide is categorized as one type of greenhouse gases and has prominent properties such as a colorless and nonflammable.

1.8 Objectives of the thesis

The main objective of the present study is to improve the direct oxidation of benzene to phenol over a zeolite catalyst using nitrous oxide as oxidant agent by i) identifying efficient catalyst compositions, better: identifying and characterising catalytic acitive sites and ii)

improve the yield of phenol compared to the state of the art by optimization of reaction conditions. The goal is to provide an improved and direct method for producing phenol from benzene in a single step. This thesis focuses on the application of various types of zeolite catalysts and their impact on hydroxylation of benzene to phenol.
The details of the objectives are

- To dope various metals onto zeolite (e.g. ZSM-5) channels and check their influence on the catalytic performance. For initial catalyst screening tests, a variety of transition metals (1 wt% each) such as Sc, Ti, V, Cr, Mn, Fe, Co, Ni, Cu, Zn, Ru and Pd should be impregnated separately onto ZSM-5 support.
- To prepare and test suitable bimetallic catalyst compositions (e.g. V-Ti/ZSM-5, V-Cr/ZSM-5, V-Mn/ZSM-5, V-Fe/ZSM-5, V-Ni/ZSM-5 and V-Zn/ZSM-5). To investigate the impact of metal loadings onto the zeolite by impregnation method and its effects on catalysis.
- Characterization of monometallic and bimetallic catalysts by various techniques such as TGA, ICP, BET-surface area, pore size distribution, XRD, NH_3-TPD, TPR, FTIR, UV-vis, SEM and TEM-EDX techniques.

Optimisation the reaction conditions for monometallic and bimetallic catalysts:

- Optimizing the calcination temperature to improve the efficiency of zeolite catalyst and for improving the yield of phenol.Discuss the effect of benzene to N_2O mole ratio on the catalytic activity and selectivity of V/ZSM-5 catalyst.
- Exploring the effect of benzene feed rate on the catalytic performance of V-ZSM-5 catalyst.
- Examining the effect of GHSV on the catalytic performance of V/ZSM-5 catalyst.
- On the whole, testing the catalytic performance for 12 different metals doped on ZSM-5 zeolite.
- Further to test the catalytic performance bimetallic such as V-Ti/ZSM-5, V-Cr/ZSM-5, V-Mn/ZSM-5, V-Fe/ZSM-5, V-Ni/ZSM-5 and V-Zn/ZSM-5.
- Finally, to test the catalytic performance of support nature on the performance of bimetallic V-Ti/Zeolite catalyst such as ZSM-5, Ga-ZSM-5, USY, and BEA.

Chapter 2

Experimental Methods and Equipment

This chapter provides detailed description of the experimental studies including catalyst preparation and characterization techniques applied. Reaction set up for hydroxylation of benzene to phenol using nitrous oxide as oxidant and evaluation procedure of the catalyst performance are also described.

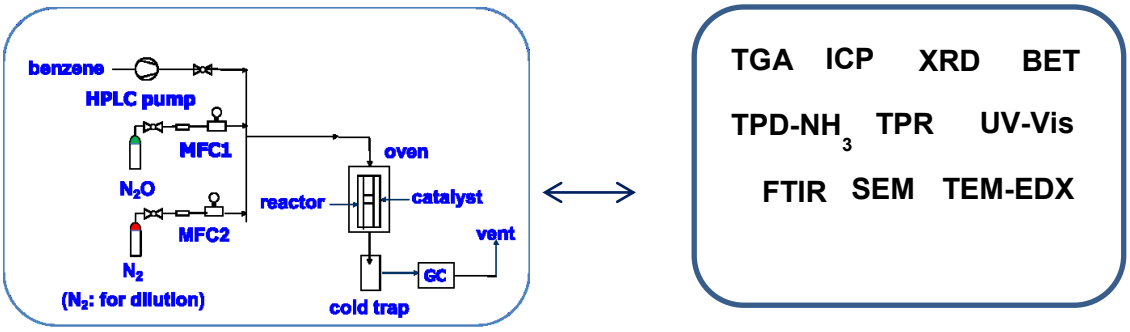

2. Experimental Methods and Equipment

Catalysis is a complex surface phenomenon occurring on the active sites on the surface of a catalyst. The adsorption of reactant molecules and their interaction to give the products on the active phase of the catalyst depends not only on the reaction variables/parameters, but also on the nature of active sites for reaction between the adsorbed and activated reactant molecules. The nature of adsorption sites and active sites on a supported metal oxide catalyst is expected to vary over a wide range with the content of metal(s) and also with the nature of the support. In order to understand the phenomena of adsorption and catalysis on a molecular basis, it is essential to investigate the nature of molecular structures. During the synthesis of commercial catalysts, even a minute change in the synthesis conditions can change the quality of the catalyst. Therefore, they must be thoroughly characterized before use. Measuring the same parameters after use often helps in understanding the cause of catalyst deactivation. Thus, the catalytic performance of the catalysts can be better understood if one knows as many of its physical properties as possible. With this background, several zeolite supported metal catalysts were prepared and tested towards a direct oxidation route for producing phenol from benzene using N_2O as oxidizing agent in the gas phase. In the present study, various characterization techniques such as TGA, ICP, XRD, N_2-adsorption, TPD-NH_3, TPR, FTIR, UV-Vis, SEM, and TEM-EDX were used. The principle and application of these techniques are briefly described below.

2.1 Preparation of monometallic and bimetallic catalysts

In this work all monometallic and bimetallic catalysts were prepared by impregnation method. For instance, M/ZSM-5, V-Ti/USY, V-Ti/BEA, and V-Ti/Ga-ZSM-5 etc. were prepared by this method. In this approach, a commercial ZSM-5, BEA and USY powder were used as catalyst supports for preparing various transition metal doped catalysts. Typically, in the model synthesis requisite quantity of suitable metal precursor (for bimetallic catalysts mixture of chloride precursor) was dissolved in distilled water. Then the solution of metal (V and Ti) was added to the support powder and stirred for 30 min at ambient conditions. Later on, the excess solvent was evaporated on a hotplate to dryness. Afterwards, the solid obtained was further dried at 120 °C for 12 h in an oven. Finally, the samples were calcined in a furnace at 500 °C (at a heating rate of 2 K/min) for 6 h in air. For all catalytic tests described below catalyst powder was used. Details on preparation of different catalyst groups are given below.

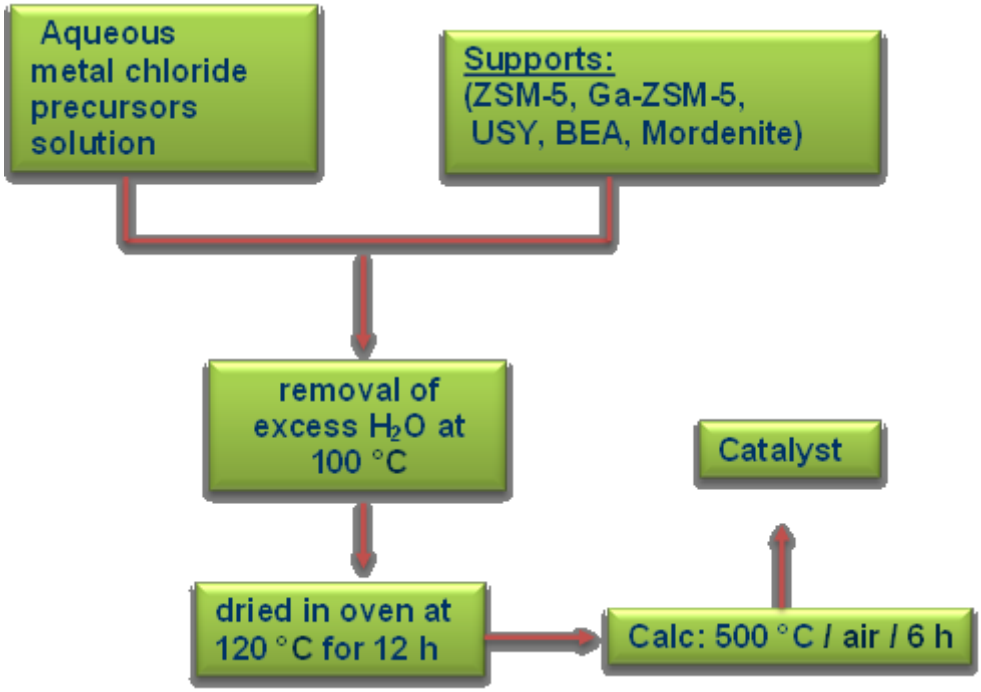

Figure. 2.1. Schematic representation of catalyst preparation

2.2 Catalyst Characterization

The following summary lists all characterization methods applied giving detailed insight in solid properties.

Characteristics	**Methods**
Surface area, pore volume & size	N_2 Adsorption-Desorption (BET, BJH)
Pore size distribution	PSD (BJH)
Elemental composition	ICP-OES
Phase composition & Crystallinity	XRD
Thermal stability, phase transformation	TG (TGA, DTA, DTG)
Particle size, shape and morphology,	SEM, TEM
Reducible properties	TPR
Acidic characteristics	NH_3-TPD
Coke measurement	CHNS

2.2.1 Thermogravimetric analysis (TGA)

In chemistry, thermography is used for determining phase composition, hydration, polymerisation, solvent retention, purity, melting, decomposition etc. The term thermal analysis incorporates those techniques in which some physical parameters of the system are determined or recorded as a function of temperature. Two most commonly used thermal methods are thermogravimetry (TG) and differential thermal analysis (DTA).

TG can be defined as a technique whereby the weight of a substance, in an environment (heated or cooled at a controlled rate), is recorded as a function of time or temperature. The principle of thermogravimetry is based on the fact that the sample is weighed continuously while it is being heated to higher temperatures. The instrument used for this purpose is called thermobalance. The results of thermobalance are represented by a plot of weight change vs temperature or time. The plot is called thermogravimetric curve or TG curve. The temperature or time is plotted on abscissa (X-axis) and weight is plotted as an ordinate (Y-axis). From the plot, the products formed at different timings or temperatures are identified.

The information that can be obtained from the TG curve is as follows: i) the curved portions in the graph suggest wt. loss, and with the help of this loss one can easily determine the composition of a compound, ii) the horizontal portions point out the regions where there is no weight change and from this information one can determine the thermal stability of the material, iii) it also gives the information about the procedural decomposition temperature. (It is the lowest temperature at which cumulative mass change attains a magnitude).

Sample weight, particle size of the sample, compactness of the sample, previous history of the sample, furnace atmosphere, instrumental factors, sample holder are some of the factors that are responsible for change in TG curve. TG analysis has been proved to be an important tool for fixing calcination temperature, determination of phase composition, % wt. loss, stability limits and evaluation of kinetic parameters etc.

In the present study, the TGA analysis performed in NETZSCH STA 449F3 TG equipped apparatus. The sample transferred into quartz tube and enhances the temperature from 20 °C to 1000 °C with heating rate of 5 K/min in air flow (25 ml/min).

2.2.2 Inductively coupled plasma optical emission spectroscopy (ICP-OES)

Metal contents of a catalyst were estimated by ICP-OES technique which works on the principles of atomic emission. In this method, all the samples are subjected to high pressure and temperature using argon plasma, and then atoms present in the samples are excited

and emit photons with particular wavelengths of electromagnetic radiation. The released photons intensity is proportional to the concentration of elements in the sample. ICP-OES is a simple, reliable, and fast multi-element analysis tool that can analyzed nearly 70 various elements (e.g. Cu, Cr, Ni and Zn). It is also efficient to determine the obstinate elements like Ti, V, W and non-metals like P, B etc. In this method, liquid samples are estimated in aqueous or acidic solution form, while the gaseous samples are analyzed with gas forming stable hydride elements (e.g. As, Se and Sb).

In a typical procedure, the samples were dissolved in a mixture of HF and aqua regia and then treated in a microwave assisted sample preparation apparatus at 200 °C and 60 bar. The sample solution will then be introduced into Ar plasma, and at this stage the sample solution gets converted into an aerosol of fine droplets by nebulizer in preheating zone at 8000 °C. At this temperature all elements become thermally excited and emit light at their characteristic wavelengths. This light is collected by the spectrometer and resolves the light into a spectrum of its constituent wavelengths. Elements were then analyzed using ICP-OES: Perkin Elmer OPTIMA 3000XL instrument using ICP−WinLAB software.

2.2.3 Nitrogen adsorption (BET-surface areas and pore size distribution)

Many catalysts and catalyst supports are porous in nature. Dubinin has classified pores according to their diameter as micropores (< 20 Å), mesopores (20-200 Å) and macropores (> 200 Å). Adsorption behaviour of a solid is largely determined by the number, shape and size of the pores [100]. The pore size can be determined either from an adsorption isotherm or by using a mercury porosity meter. In the present study, N_2 adsorption (using desorption branch / BJH method) is used for determining pore size distribution of the catalysts. Surface area determination is an important factor in predicting catalyst performance. The surface area measurements can be used to predict catalyst poisoning and also provide reasons for the deactivation of the catalysts either due to poisoning or due to sintering. It is also used as a method of assessing the efficiency of catalyst supports and promoters. There are various methods such as electron microscopy, mercury penetration etc. to estimate the total surface area and pore size distribution of porous materials. Among all, the BET method proposed by Brunauer, Emmett and Teller is the most commonly used one. The BET equation is based on an extension of the Langmuir theory to multilayer adsorption. The basic equation to determine the surface area is as follows:

$$\frac{P}{V\,(P_o-P)} = \frac{1}{V_M C} + \left[\frac{C-1}{V_M C}\right]\left(\frac{P}{P_o}\right) \qquad \text{(Eq. 2.1)}$$

Where, P is adsorption equilibrium pressure, P_0 is adsorbent saturated vapour pressure, V is volume of N_2 adsorbed at equilibrium pressure, V_m is monolayer volume of adsorbate, C is constant related to the heat of adsorption, Where $C = e^{E_q - E_L/RT}$

A plot between P/V (P_o-P) and P/P_o gives a straight line along with slope (C-1)/V_MC and intercept 1/V_MC. The values V_M and C are calculated from the slope and the intercept, to calculate the ET surface area of the sample from below relation,

$$S_{BET} = \frac{V_M A_M N_A}{V_{mol}} \qquad \text{(Eq. 2.2)}$$

Where, N_A refers to Avogadro number A_M refers to cross-sectional area of adsorbate molecule

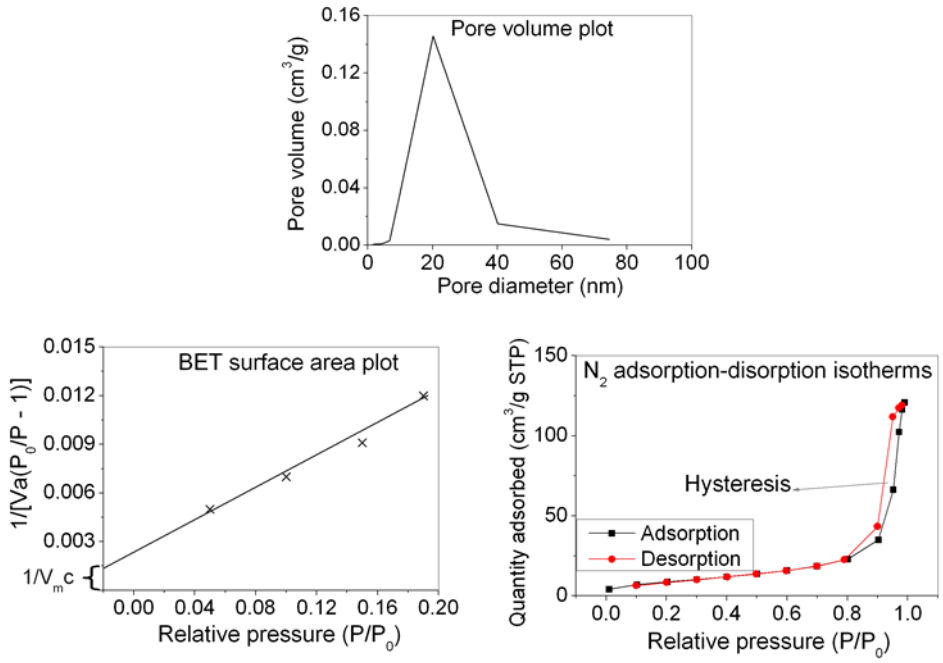

Figure 2.2. Pore volume plots and BET surface area derived from N_2-physisorption experiments

2.2.4 X-ray powder diffraction (XRD)

XRD is one of the most widely used and versatile techniques for the qualitative and quantitative analysis of solid phases of a powdered sample. It can provide the information i) about the crystallite size of the components present, ii) to identify the structure of substance, its allotropic transformation, iii) transition to different phases, iv) purity of the substance, v) lattice constants and vi) presence of foreign atoms in the crystal lattice of a component. X-rays are electromagnetic radiation with typical photon energies in the range of 100 eV-100 keV. For diffraction applications, only short wavelength X-rays 1 keV-100 keV is used. The phenomenon of diffraction arises from the interaction of X-ray with the periodic structure of polycrystalline material. In this technique, a fixed wavelength is chosen for the incident radiation and Bragg peaks are measured by observing the intensity of the scattered radiation as a function of scattering angle of 2 spacing's are calculated from the values of the peaks observed from the Bragg's equation.

$$n\lambda = 2d\sin\theta \qquad \text{(Eq. 2.3)}$$

where n = order of reflection and the values are 1, 2, 3 etc., λ = X-ray wave length (1.5406 Å for CuKα radiation), θ = is the angle between the incident beam and a lattice plane (i.e. Bragg's angle) with the d-values tabulated in decreasing order and the relative intensities recorded on a scale of 100 for the strongest line, the identification of the diffracting phases in the sample can be made. Designating the XRD reflections as the strongest, 2nd strongest, 3rd strongest etc. d- values of the pattern are termed as d1, d2, d3 etc.

In the present study, XRD powder patterns were recorded at ambient conditions in transmission mode using Cu Kα radiation (λ = 1.5406 Å) in the 2θ range of 10-60° (step width: 0.25°, 25 sec per step) on a Stoe STADI P diffractometer, equipped with a linear Position Sensitive Detector (PSD). Processing and assignment of the powder diffraction patterns was done using the software WinXpow (Stoe) and the Powder Diffraction File (PDF) database of the International Centre of Diffraction Data (ICDD). with the analysis of X-ray diffraction line broadening (XLB) of the peak shape of one or more diffraction lines crystallite size can be calculated using the Scherrer equation.

$$D_B = \frac{K\lambda}{\beta\cos\theta} \qquad \text{(Eq. 2.4)}$$

D_B = Mean crystallite diameter λ = X-ray wave length (1.5418 Å for CuKα radiation)

K = Scherrer's constant β = Full width at half maximum (FWHM)

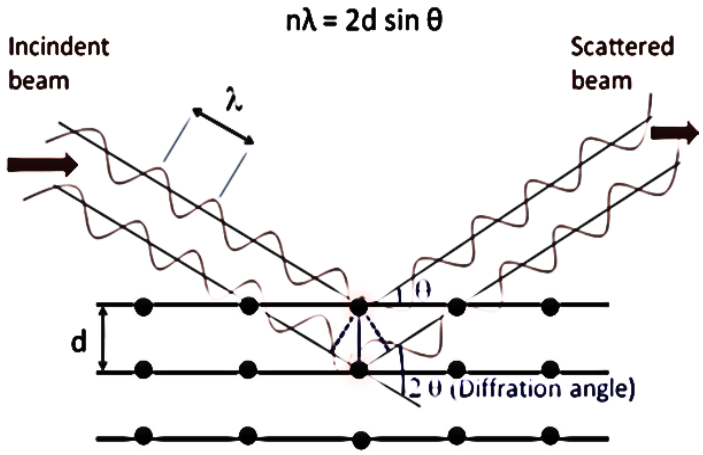

Figure 2.3. X-ray powder diffraction

2.2.5 Temperature programmed desorption of ammonia (TPDA)

Temperature-Programmed Desorption (TPD) is one of the most widely used techniques for characterizing the acid sites on solid catalysts. Estimation of the nature, quantity and strength of the acid sites will further help in predicting the catalytic performance of the heterogeneous catalysts. There are three types of molecular probes such as i) ammonia, ii) pyridine and iii) propyl amines that are generally used for characterizing the acidic sites of solids. Each probe has got its own merits and demerits. In the present study, NH_3 is used as probe molecule to estimate the total acidity of the catalysts. Normally, the samples are degassed at 100 °C for one hour in helium flow to remove physisorbed water vapor and also to avoid pore damage particularly in case of zeolite catalysts.

In a typical procedure, U shaped quartz reactor was filled with required amount of catalyst (70-100 mg, in general) and then heated the tube from RT to 400 °C in He flow (50 mL/min) at 10 K/min heating rate. At this stage, the temperature is kept constant for 30 min for removal of moisture from the catalyst and then decreased the temperature to 100 °C in He flow. Next, He gas was replaced by ammonia gas (1% NH_3 in He) with a flow rate of 50 mL/min for 120 min. After NH_3 adsorption, the catalyst sample was flushed again in He flow (50 mL/min) to remove physisorbed ammonia. Finally, raised the temperature gradually to 600 °C with 10 K/min heat rate in the flow, run for 30 min at 600 C. The Quadrupole mass spectrometer (Blazer Omnistar) instrument was used to explore the evolved gases. TPD measurements of the present catalysts are performed on Micromeritics Autochem II 2910

instrument. Unlike pyridine adsorption method by infrared spectroscopy, the currently applied NH_3-TPD technique gives the total acidity of the catalysts.

2.2.6 Temperature-programmed reduction (TPR)

Temperature Programmed Reduction (TPR) technique is a powerful tool to estimate the reducible properties of both supported and bulk metal oxide catalysts. In the present study, TPR profiles were recorded in a range from r.t. to 900 °C at a heating rate of 10 K/min on a Micromeritics AC 2920 instrument. Prior to TPR measurement, all the samples were pretreated under 5% O_2/He up to 450 °C with a rate at 20 K/min and kept at this temperature for 30 min and then cooled down to r.t. After this treatment, 5% H_2/Ar was passed through the sample tube during the measurement and increase the temperature from r.t. to 900 °C with a rate at 10 K/min.

2.2.7 Fourier transform infrared (FT-IR) spectroscopy

The atoms in a molecule are not still. They rotate and vibrate in different ways in certain quantized energy levels. The infrared spectrum causes when a molecule due to vibrations and rotations of atoms within the molecule produces a change in permanent dipole moment of the molecule. The most commonly used range of infrared spectrum is between 4000 cm^{-1} at high frequency end and 600 cm^{-1} at lower frequency end. IR spectra provide valuable information about the basic characteristics of the molecule, namely, the nature of atoms, their spatial arrangement and their chemical linkage forces. Infrared spectroscopy has been extensively used for identifying the various functional groups on the catalyst itself, as well as for identifying the adsorbed species and reaction intermediates on the catalyst surface. It can also be used to measure the surface acidity of the catalysts. IR spectroscopy is basically a bulk technique that takes advantage of the surface aspects of the supported metal oxide phases.

In the present study, self-supporting discs were prepared with KBr and catalyst powder by applying pressure. These transparent discs were used for recording FTIR spectra. FTIR spectra were recorded on a Bruker Tensor 27 spectrometer.

2.2.8 Ultraviolet–visible spectroscopy (UV-vis)

Ultraviolet-Visible Spectroscopy is worked based on absorption spectroscopy, and it was explore the difference in light beam to travel through the sample. UV-Vis spectroscopy mainly applied in analytical spectroscopy, and it depends on to absorption ability of UV-Vis light by sample. The UV-Vis spectroscopic instrument contains Avantes-2048 UV-vis

spectrometer and along with deuterium-halogen light source. The UV-Vis spectra were performed with help of optical probe was dipped in the constant stirring reaction vessel and spectral region of 200-1100 nm range and optical distance with 0.4 cm.

2.2.9 Scanning electron microscopy (SEM)

Scanning electron microscopy (SEM) is a useful technique to determine the particle size, shape and morphology of different components of the catalysts. In SEM, an electron beam that is accelerated down the column and passes through a series of lenses that control the diameter of the beam and then focus the beam onto the specimen. An interaction of beam and specimen generates different types of signals that can be detected and processed to produce an image or spectra.

In the present study, SEM measurements were made on JEOL microscope (Model: JSM-6390LV) with beam voltage of 20 kV and 1.38 eV resolution. The gold layer coated on samples to control the conductivity in samples.

2.2.10 Transmission electron microscopy (TEM)

TEM is also useful technique to determine the particle size, shape, composition, distribution and morphology of powdered catalyst samples. TEM measurements were made on a JEM-ARM200F (JEOL) high-resolution electron microscope operated at a voltage of 200 kV; aberration-corrected by a CESCOR (CEOS) for the scanning transmission (STEM) applications. The microscope is equipped with a JED-2300 (JEOL) energy-dispersive x-ray spectrometer (EDXS) that can be used to analyze the chemical composition of catalysts. EDXS imaging the samples were deposited on carbon grid (mesh 300) before taken into microscope.

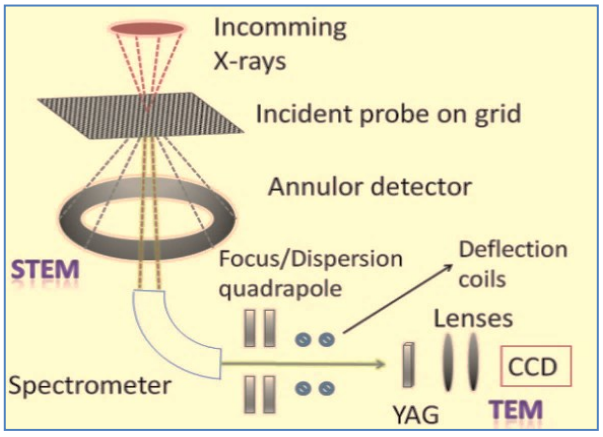

Figure 2.4. Schematic geometry of the electron microscopy

2.3 Experimental set up and catalytic test procedures

The catalytic tests for the hydroxylation of benzene to phenol using N_2O as oxidizing agent were carried out in a continuously operated gas phase set-up using a down flow fixed bed stainless steel reactor. In a typical experiment, 2 g of catalyst (1.0-1.25 mm) diluted with corundum was used. The corundum diluted catalyst (catalyst: corundum = 1: 3 wt/wt) was loaded into the reactor. The solid grains were suspended between two quartz wool plugs in the middle of the reactor. Also the upper and lower portions of the catalyst bed were filled with corundum. The gases such as N_2O (oxidizing agent) and N_2 (as an inert for dilution and for maintaining constant space velocity) supplied were commercially available gases from compressed gas cylinders. The flow rates of these gases were monitored by mass flow controllers. The molar ratio of reactant feed mixture (in general) is C_6H_6: N_2O: N_2 = 1: 1.5: 82.3. The reaction was carried out in the temperature range of 350 to 410 °C and GHSV = 2612 h^{-1}. T-profile along the bed was also taken from time to time. Two thermocouples were positioned one at the center of the catalyst bed to indicate reaction temperature and the other one was attached to furnace through temperature indicator cum controller to monitor the temperature of the reactor. The dosing of benzene to the reactor was done using HPLC pump. Then the reaction temperature was raised to the desired level and the reaction was performed in a continuous manner. The product samples were collected every 30 min and analyzed by off-line gas chromatography (GC-2010 Plus Shimadzu, column (15 m x 0.35 mm x 1.5 µm) using both the detectors, e.g. FID (HP-5 column) for liquid products and TCD (Carbon plot column) for gaseous products. Gaseous products (e.g. CO_x) were collected in glass cylinder. The off-gas volume was measured for each sample and at the same time, the conversion of benzene and the yields of products were also calculated according to the equations given below. Phenol was the desired product and also the major product of the reaction. Additionally, some by-products such as catechol, benzoquinone, hydroquinone, CO_x etc. were also formed to a certain extent some digital images of experimental set up are given in Figure 2.6 while the schematic representation of experimental set up is given in Figure 2.5.

Formulas for calculating conversion of benzene and the yield of phenol:

$$\text{Conversion of benzene (\%)} = \frac{\text{[number of moles of benzene reacted]}}{\text{[number of moles of benzene fed]}} \times 100 \qquad \text{(Eq. 2.5)}$$

$$\text{Yield of phenol (\%)} = \frac{\text{[number of moles of phenol produced]}}{\text{[number of moles of benzene fed]}} \times 100 \qquad \text{(Eq. 2.6)}$$

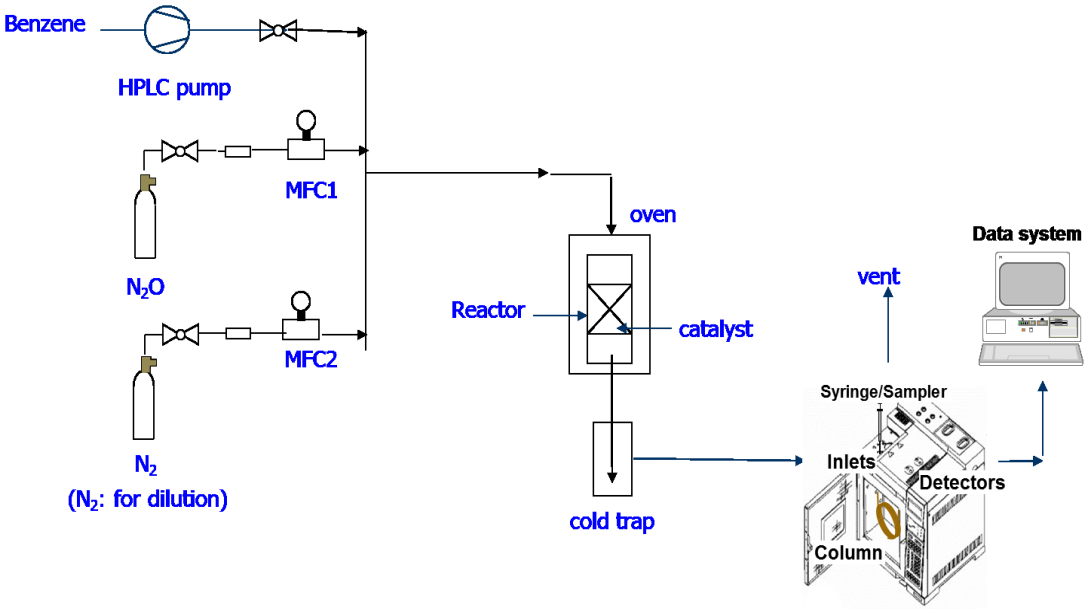

Figure 2.5. Schematic representation of experimental set up

2.3.1 GC calibrations of educts/products

Prior to the real catalytic tests, GC calibrations were performed to quantify both the reactants and products expected from the reaction. This is in fact a usual procedure for estimating the carbon balance and reactant / product concentrations, which in turn is crucial for further calculating the conversion of educts and selectivity and yield data of products. For this purpose, known concentrations of benzene and phenol were weighed in a standard flask having a volume of 50 ml and then diluted with the methanol (as a solvent) up to the mark. Four different concentrations were selected in the same range as that of reaction conditions planned to be applied. A suitable GC analytical method was developed and applied (e.g.

selected conditions of GC program: column temp: 60-200 °C (i.e. 60 °C (1 min hold time), then heating rate 10 K/min to 200 °C (5 min hold time)); injection port (230 °C), Detector temp: 250 °C, split ratio = 40. More details on the GC calibrations are given at the end as an Annexure 1.

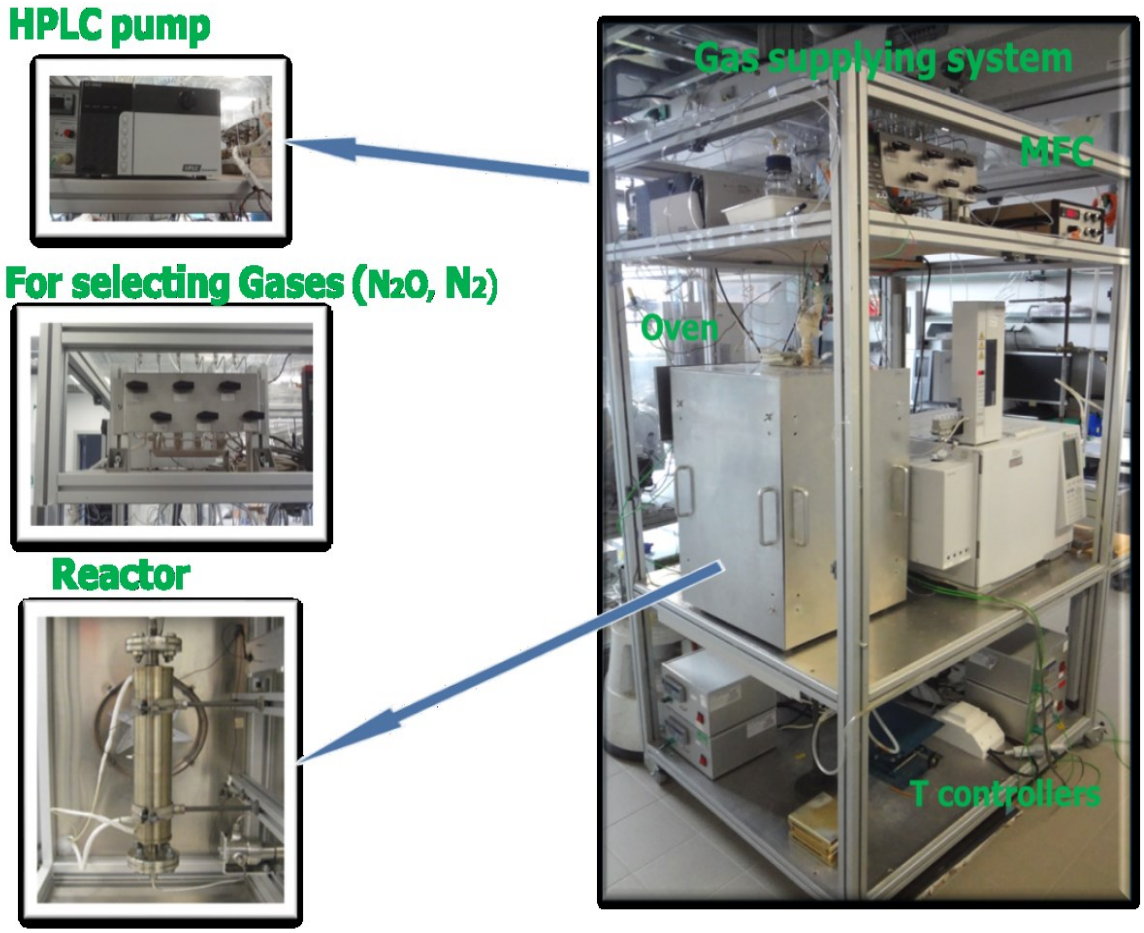

Figure 2.6. Digital image and details of experimental set up

Chapter 3

Benzene hydroxylation over ZSM-5 supported monometallic catalysts

In this chapter, the preparation, characterization and catalytic testing of various monometallic catalysts supported on ZSM-5 material are described. Various characterization techniques such as TGA, ICP, XRD, N_2-adsorption, TPD-NH_3, TPR, FTIR, UV-Vis, and TEM-EDX were applied. Additionally, optimization of key reaction parameters using Fe/ZSM-5 catalyst was carried out to obtain first approximation of the reaction conditions for enhancing the yield of phenol.

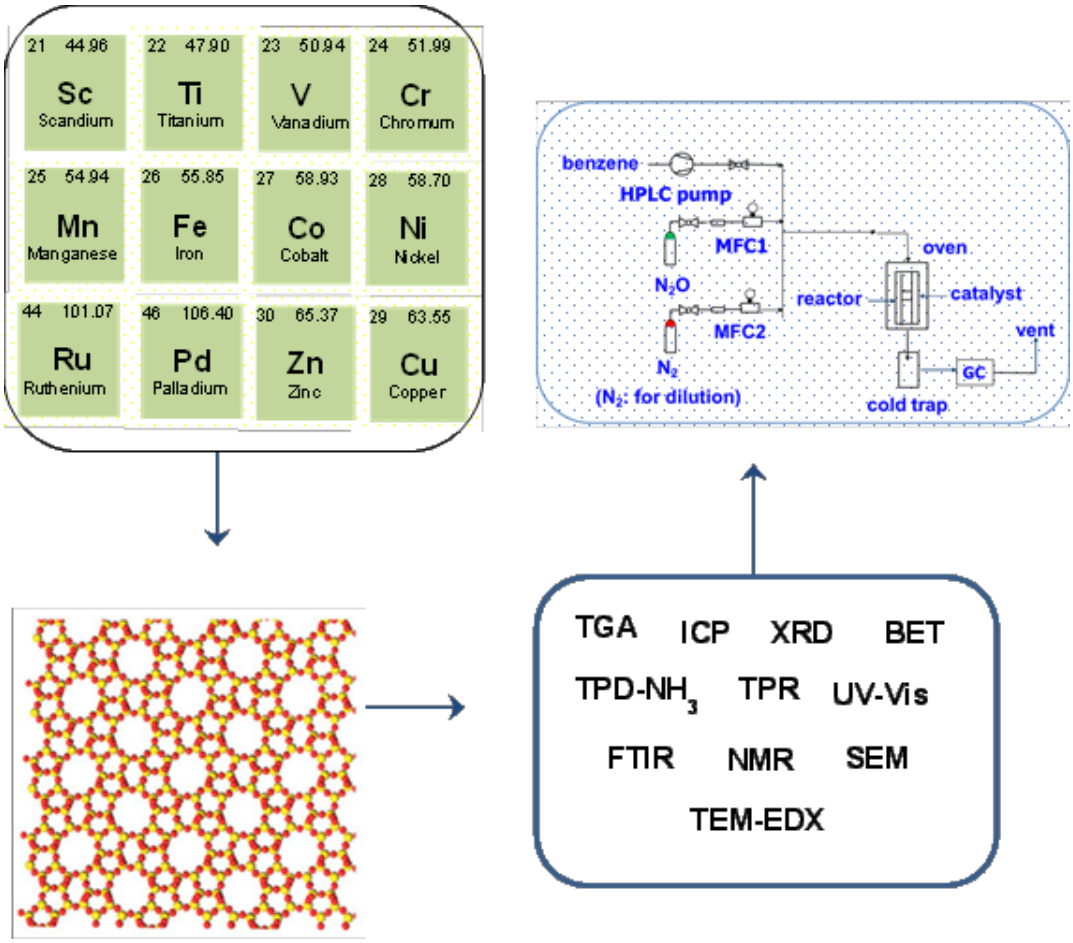

3. Benzene hydroxylation over ZSM-5 supported monometallic catalysts

3.1 Studies on the ZSM-5 supported monometallic catalysts

Direct hydroxylation of benzene to phenol in the gas phase using N_2O as oxidizing agent in the presence of M/ZSM5 zeolite catalysts has been carried out (Scheme 3.1). For the initial catalytic tests, a commercial Fe/ZSM-5 catalyst with Si/Al ratio of 25 was used (BET surface area of 349 m^2/g). These preliminary studies on this Fe/ZSM-5 zeolite catalyst gave some useful hints for further work. At this stage, the effect of various reaction variables such as i) the effect of GHSV, ii) concentration of benzene in the reactant feed mixture, and iii) the effect of reaction temperature was checked.

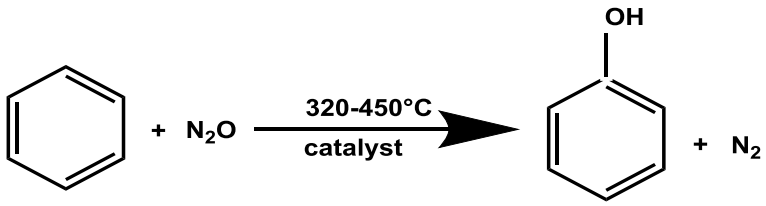

Scheme 3.1. Benzene hydroxylation to phenol using N_2O as oxidizing agent

M/ZSM-5 catalysts with fixed content of transition metal 3 wt%, 2 wt% and 1 wt% were prepared by impregnation method as described below in detail. The properties of the catalysts were characterized by TGA, ICP, XRD, N_2 adsorption, FTIR, TPD, TPR, UV-vis and TEM-EDX techniques. The monometallic supported to ZSM-5 catalyst revealed a good influence on catalytic performance. The catalytic tests for hydroxylation of benzene were carried out at temperature range from 300-500 °C. V and Ti containing solids revealed the superior performance; phenol yield of ca. 11.6 and 10.7 were received, respectively. Furthermore, results revealed that the nature of metal doped has strong influence on the catalytic performance such as BET surface areas, reducible properties and acidity characteristics. Among all catalysts tests V and Ti solid exhibited the superior performance. Catalysts with High reaction temperatures were particularly prone to deactivation.

3.2 Catalyst preparation

Preparation procedure of M/ZSM-5 catalysts (M = metal as shown in Table 3.1) is described below in detail. ZSM-5 powder was used as a support for preparing various monometallic catalysts. In a typical procedure, requisite quantity of suitable metal precursor was dissolved in distilled water. Then the solution of metal precursor was impregnated onto ZSM-5 powder and stirred for 30 min at ambient conditions. Later on, the excess solvent was evaporated on

a hotplate to dryness. Afterwards, the solid obtained was further dried at 110 °C for 12 h in an oven. The content of metal impregnated in all catalysts was kept constant at 1 wt%. Finally, the samples were calcined in air at 500 °C (heating rate of 2 K/min) for 6 h. The composition of such catalysts, type of metal precursor used and calcination conditions are given below in Table 3.1.

Table 3.1. Synthesized catalysts and used precursor compounds

No.	Catalyst	Metal precursors	Calcination (°C/h/air)
1	Sc/ZSM-5	$Sc(NO_3)_3•H_2O$	500/6
2	Ti/ZSM -5	$(NH_4)_2TiO(C_2O_4)_2•H_2O$	500/6
3	V/ZSM-5	VCl_3	500/6
4	Cr/ZSM-5	$CrCl_3•6H_2O$	500/6
5	Mn/ZSM-5	$MnCl_2$	500/6
6	Fe/ZSM-5	$FeCl_3•6H_2O$	500/6
7	Co/ZSM-5	$CoCl_2•6H_2O$	500/6
8	Ni/ZSM-5	$NiCl_2•6H_2O$	500/6
9	Cu/ZSM-5	$CuCl_2•2H_2O$	500/6
10	Zn/ZSM-5	$ZnCl_2$	500/6
11	Ru/ZSM-5	$RuCl_3$	500/6
12	Pd/ZSM-5	$PdCl_2$	500/6

3.3 Characterization of ZSM-5 supported monometallic catalysts

3.3.1 Thermogravimetric analysis

3.3.1.1 ZSM-5 supported monometallic Fe, Ti, V and Sc catalysts

TGA/DTG are helpful to find out the thermal stability and phase transformation temperatures of the solid materials to obtain desired active phase with good catalytic properties. TGA/DTG analysis curves of the M/ZSM-5 (M = Fe, Ti, V, Sc) catalysts are given Figure 3.1. It is obvious that weight loss in all these samples occurs in two stages. The first and major weight loss occurred in every case below 300 °C, which can be attributed to the desorption of adsorbed water, and dehydroxylation of the catalyst samples. Depending upon the nature of metal incorporated, the weight loss is varied in the range from 6 to 7% below 300 °C. The second and gradual weight loss occurred in the range of 300-500 °C is due to phase

transformation of metal precursors into metal oxide phase due to the thermal treatment in air [101-102]. In view of the low amount of metallic components (1 wt%) impregnated, the second weight loss is occurring to a smaller extent (< 2%). No considerable weight loss beyond 500 °C is noticed. Based on TG results, a calcination temperature of 500 °C is fixed for all catalysts.

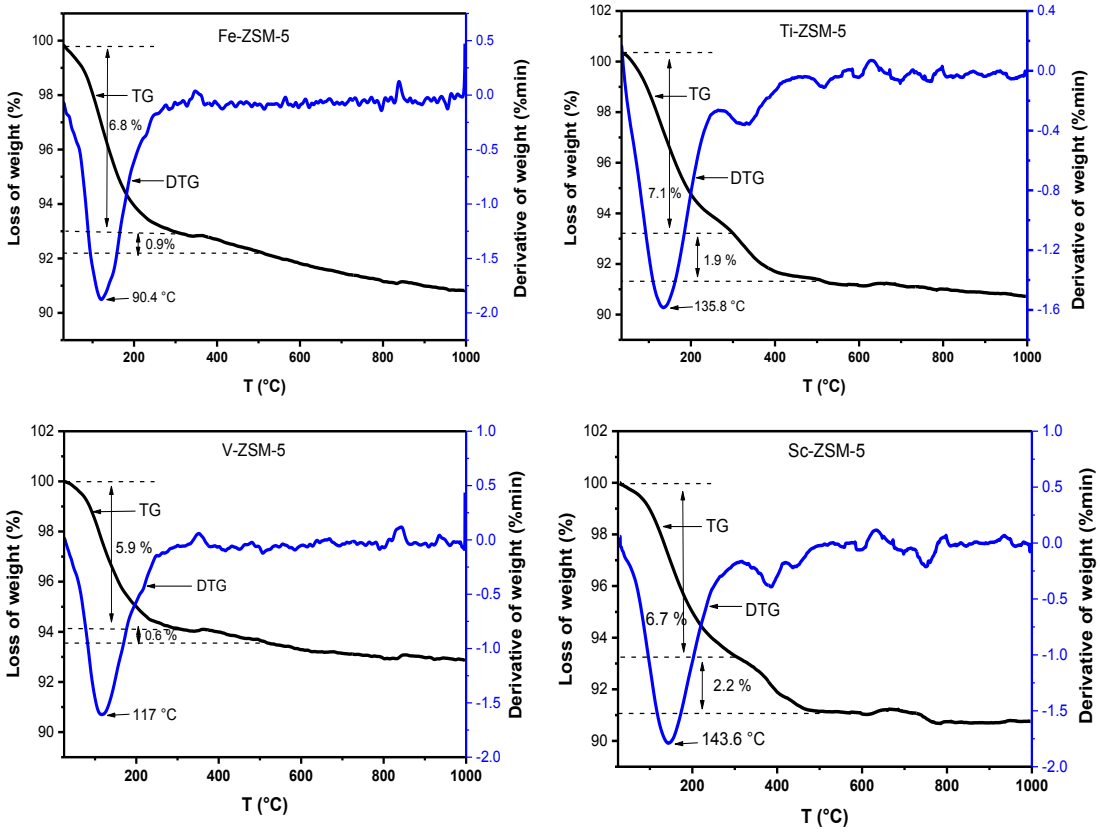

Figure 3.1. TGA-DTG curves of ZSM-5 supported monometallic Fe, Ti, V and Sc catalysts

3.3.1.2 ZSM-5 supported monometallic Co, Ni, Cu and Zn catalysts

TG-DTG curves of ZSM-5 supported Co, Ni, Cu and Zn based catalysts are given in Figure 3.2. Below 300 °C, the catalysts exhibited a weight loss in the range from 5 to 8%. As explained above, this loss in weight can be assigned to the removal of water contents, dehydroxylation of catalyst's surface and also partly due to decomposition of metal precursors [103-105]. The shoulder peak observed in derivative thermogravimetric (DTG) shows the temperatures at which weight loss takes place for ZSM-5 supported Co, Ni, Cu and Zn based catalysts. Actually, such weight loss took place at 103.2, 129.5, 126.5 and

121.6 °C respectively. The second weight loss occurred between 300 to 500 °C is low (< 1%), which is somewhat similar to the one shown above in Figure 3.2. Based on the TG analysis, a calcination temperature of 500 °C in air was fixed for the catalyst samples.

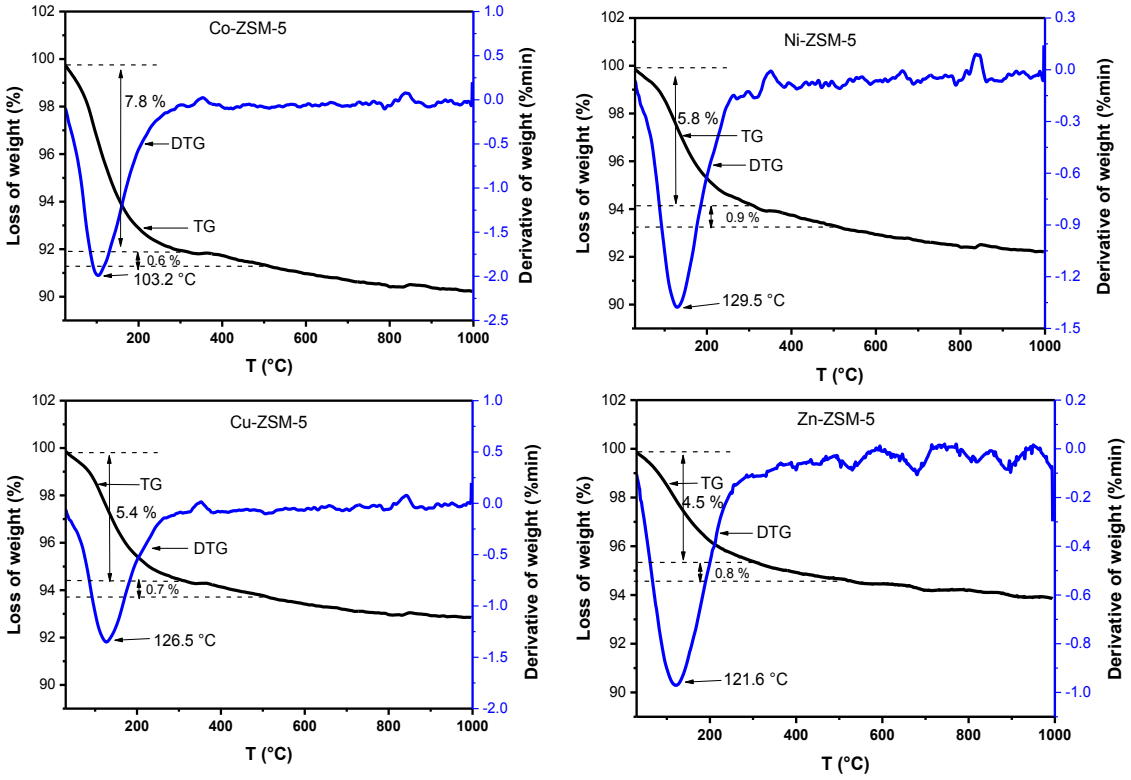

Figure 3.2. TG-DTG curves of monometallic Co, Ni, Cu and Zn supported on ZSM-5 catalysts

3.3.2 Textural properties and catalyst composition

The elemental analysis, BET-Surface areas and total pore volume results of M/ZSM-5 catalysts are presented in Table 3.2. The metal contents estimated from ICP are observed to vary in the range from 0.8 to 1.1 of the M/ZSM-5 solids. Furthermore, the contents of M/ZSM-5 estimated from ICP are in good agreement with those of nominal values (1 wt%). The BET-surface area and pore volume of this catalyst samples determined from N_2 adsorption (Table 3.2) are found to depend upon the nature of metal doped. As a result, the surface areas and pore volumes of the catalysts are found to vary over a range from 353 to 394 m^2/g and 0.312 to 0.349 cm^3/g, respectively. Among all, Cu/ZSM-5 solid exhibited the high surface area while

Mn/ZSM-5 sample displayed the low surface area. Moreover, all these samples also contain micropores. Metals can be on diffusing interior channels or on the exterior surface of the ZSM-5 catalyst. Hence, the surface areas and porous volume of support ZSM-5 decrease in the same manner because of mesoporous is blocked by slot of channel of support or interior the pore as oxide aggregates. It is generally beneficial catalytic components to have high surface area. Furthermore, diffusional impedance might be a trouble due to the slot of channel is too small.

Table 3.2. The physical characteristics of M/ZSM-5 catalysts

No.	Catalyst	Metal content (wt%) ICP	BET-SA m^2g	Total pore volume cm^3/g
1.	HZSM-5	0.00	388.2	0.311
2.	Sc/ZSM-5	0.91	386.4	0.342
3.	Ti/ZSM-5	1.03	386.6	0.332
4.	V/ZSM-5	0.84	379.9	0.336
5.	Cr/ZSM-5	0.85	372.6	0.342
6.	Mn/ZSM-5	0.81	353.3	0.327
7.	Fe/ZSM-5	0.88	387.3	0.346
8.	Co/ZSM-5	0.87	380.5	0.331
9.	Ni/ZSM-5	0.99	377.0	0.336
10.	Cu/ZSM-5	0.96	394.0	0.349
11.	Zn/ZSM-5	1.11	361.8	0.312
12.	Ru/ZSM-5	0.89	388.9	0.340
13.	Pd/ZSM-5	1.09	382.6	0.340

* Nominal content of metal impregnated in all catalysts was kept constant at 1 wt%.

3.3.3 Pore-size distribution of ZSM-5 supported metal oxide catalysts

3.3.3.1 ZSM-5 supported Zn, Cu, Ni and Co catalysts

The pore size distribution of ZSM-5 supported Zn, Cu, Ni and Co catalysts is shown Figure 3.3. Barrett, Joyner, and Halenda (BJH) method was applied using desorption branch of isotherm. It can be seen that all catalysts exhibited bimodal pore size distribution. The first one and the major pore volume distribution appeared in the range of 50 to 100 Å with a dominant pore diameter of around 85 Å. It has been reported that pores can be divided into

three categories based on their size i.e. microporous (<2 nm), mesoporous (2-50 nm) and macroporous (>50 nm) [106-108]. The second pore volume distribution appeared at 100 to 170 Å. The major contribution towards total pore volume of the catalysts arises from the first one. The results in Figure 3.3 shows that all ZSM-5 supported Zn, Cu, Ni and Co based catalysts are macroporous samples. It is also observed that when 1 wt% of the metal is doped onto pure ZSM-5 support, the pore size is slightly shifted towards lower pore diameter range.

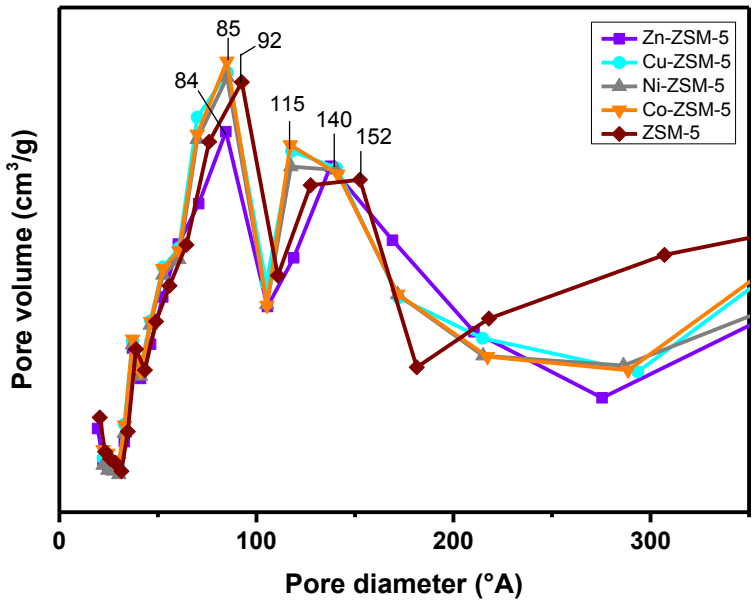

Figure 3.3. Pore size distribution for ZSM-5 supported Zn, Cu, Ni and Co based catalysts

3.3.3.2 ZSM-5 supported Mn, Cr, V and Ti catalysts

In Figure 3.4 displays the pore size distribution of ZSM-5 supported Mn, Cr, V and Ti catalysts. It is obvious that all catalysts exhibited same pore size distribution trend as that of ZSM-5 supported Mn, Cr, V and Ti based catalysts. All catalysts consisted of macropores having peaks at 85, 92, 86, 117,119 and 152 nm. Mn, Cr and V based catalyst supported on ZSM-5 showed more pore volume as compared to parent catalysts. Doping of metals even in small amount totally changed the pore size distribution patterns. Therefore, adding metal in support caused decrease in the intensity of pore located at 85, 86 and 92 nm while the pores were totally vanished located at 152 nm. In the contras, parent ZSM-5 solid is slightly less than the ZSM-5 supported Mn, Cr, V and Ti catalysts see Table 3.2.

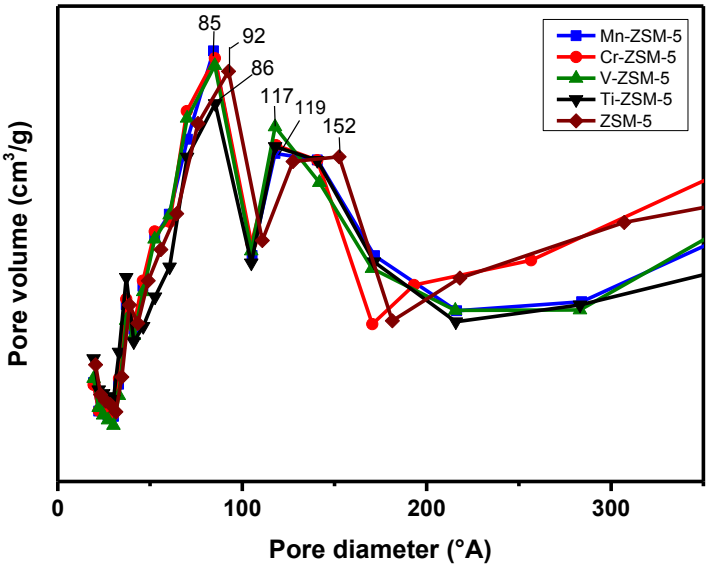

Figure 3.4. Pore size distribution for ZSM-5 supported Mn, Cr, V and Ti based catalysts

3.3.3.3 ZSM-5 supported Sc and Pd catalysts

Pore-size distribution curves of ZSM-5 supported Sc, and Pd based catalysts obtained from desorption branch of N_2 adsorption measurements are given in Figure 3.5. The pore size distribution of these samples revealed mainly two regions of pore volume distributions in the range of 50 to 100 Å and 100 to 180 Å, respectively. The first being the dominant one and contributes to the major proportion of total pore volume. The dominant pore diameters of these distributions are 85 and 140 Å. This pore volume is more or similar to the previously discussed samples.

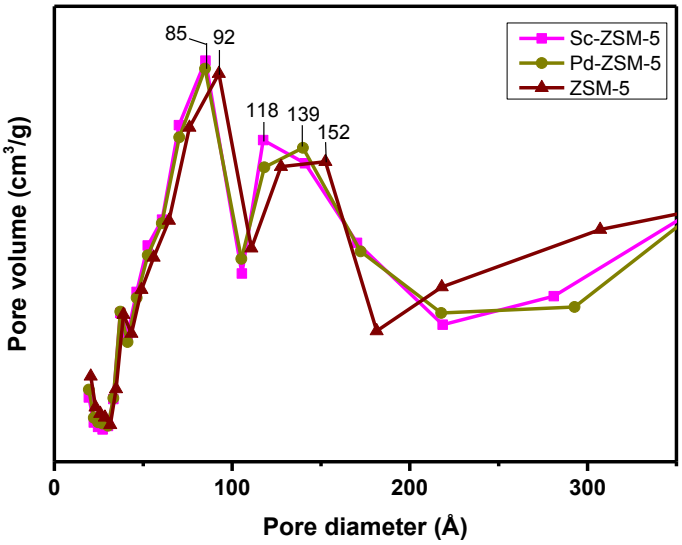

Figure 3.5. Pore size distribution for ZSM-5 supported Sc, and Pd based catalysts

3.3.4 X-ray diffraction

3.3.4.1 ZSM-5 supported Co, Ni, Cu and Zn catalysts

Phase identification is one of the important aspects of heterogeneous catalysis. Different types of phases contribute in a different way towards the catalytic performance of the catalysts in a reaction. In order to assess the different forms of phases present in ZSM-5 supported Co, Ni, Cu and Zn based catalysts, XRD analysis was performed and obtained patterns are shown in the Figure 3.6. It can be seen that all the catalysts showed similar diffraction patterns dictating the presence of only support (i.e. ZSM-5) reflections. In other words, no reflections corresponding to impregnated metals (Co, Ni, Cu, and Zn) or their corresponding metal oxides could be seen. Presence of only reflections for support material indicate that all metals i.e. Co, Ni, Cu and Zn are probably uniformly distributed and another possible reason for the absence of doped metal reflections might be due to low concentration of metal (1 wt%). More likely, the samples seem to be X-ray amorphous in nature. However, no loss of active components could be found either during synthesis or under calcination conditions, which is also evidenced from ICP measurements.

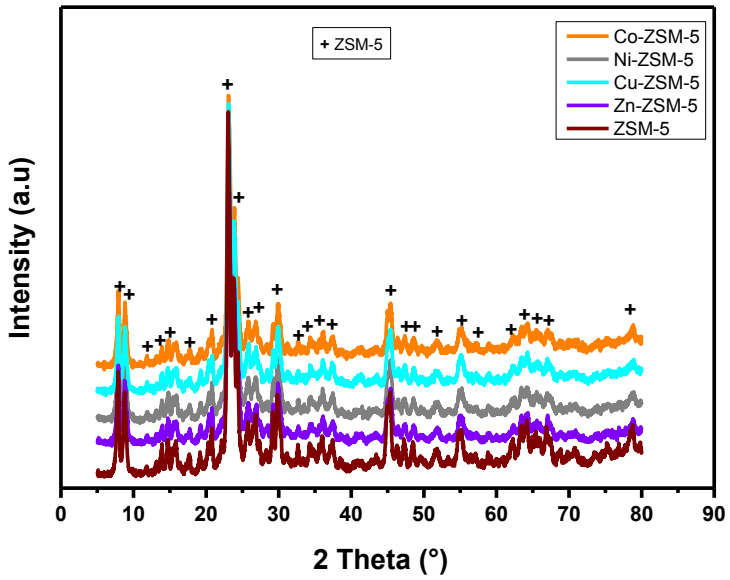

Figure 3.6. XRD patterns of ZSM-5 supported Co, Ni, Cu and Zn catalysts

3.3.4.2 ZSM-5 supported Mn, Cr, V and Ti catalysts

X-ray diffraction patterns for ZSM-5 supported Mn, Cr, V and Ti catalysts are presented in Figure 3.7. For better comparison, the XRD pattern of pure support (ZSM-5) is also shown in the figure. As mentioned above, the metal doping is very low in concentration (for instance 1 wt%), which might be below the detection limit of XRD due to probable formation of small crystallites and thus no metal or metal oxide reflections could be seen in the XRD patterns as shown in Figure 3.7. A minimum crystallite size of 5 nm might be available to be detected by XRD. In our catalysts, crystallite is more likely less than the 5 nm, which is the detection limit of powder XRD technique. On the contrary, diffraction peaks of pure ZSM-5 in the whole range of 2Θ (5-80°) are appeared, which indicates that the pure ZSM-5 support is a crystalline sample, The absence of XRD reflections corresponding to doped metals points to the amorphous nature of the doped metals/metal oxide phases. This is undeniably due to low concentration of metal contents (1 wt%) doped. However, the metal contents estimated from ICP analysis are in good agreement with those of nominal values. This result suggests that the metals doped are certainly present in the framework but could not be seen from XRD probably due to the small crystallite size of metals doped. All the crystalline reflections appeared in the XRD patterns belong to the parent ZSM-5 sample. Hence this XRD analysis

is not really suitable technique for the analysis of the present samples. However, ICP is more reliable to know the actual contents of metals in the final catalysts.

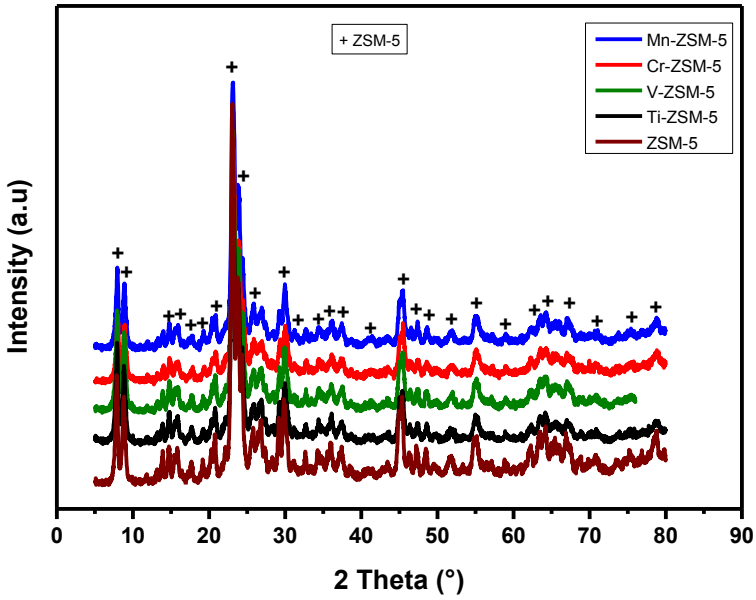

Figure 3.7. XRD patterns of ZSM-5 supported Mn, Cr, V and Ti catalysts

3.3.4.3 ZSM-5 supported Ru, Sc, Pd and Fe catalysts

Figure 3.8 depicts the XRD patterns looking similar to the patterns shown above. Also demonstrates that all the samples are crystalline in nature. However, the crystalline XRD reflections belong to mainly to pure ZSM-5 support. As observed earlier, no XRD reflection corresponding to either MOx or metal phases could be seen in any of the samples. This is again due to low metal contents (Ru, Sc, Pd, Fe) impregnated onto the support (i.e. 1 wt% each). Therefore it is more likely that these metals components are present in the catalysts in X-ray amorphous form. However, ICP analysis clearly supports the presence of these metallic components within the expected range. It can be inferred from the diffraction patterns that it is difficult to identify the crystalline phases formed corresponding to impregnated metals. Therefore, one has to look for other suitable characterization techniques to gain deeper insights on the nature metal oxide phases present in these samples.

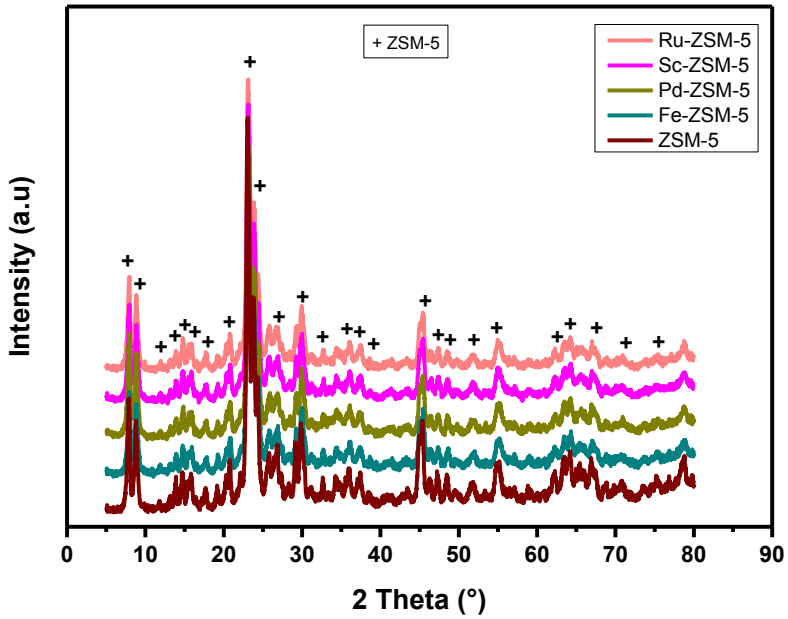

Figure. 3.8. XRD pattern of ZSM-5 supported Ru, Sc, Pd, Fe catalysts

3.3.5 Fourier transform infrared spectroscopy

3.3.5.1 ZSM-5 supported Mn, Cr, V and Ti catalysts

In order to assess the structure and functional groups associated with the catalytic material, one of the useful vibrational spectrocopy i.e. fourier transform infrared spectroscopy is utilized. FTIR spectra of Mn, Cr, V and Ti based ZSM-5 supported catalysts are shown in Figure 3.9 and it can be seen that all the catalysts exhibited almost similar spectra. The band at around 792 cm^{-1} could be attributed to the symmetric stretching and T-O bending vibration of the interior linkages, It might be slight vibration. The shift of the streching Si-O-Si vibration take plase when the change content of sample such as Si ,Al or Mn, Cr, V and Ti low wight metal atom to high wight. The transmittance bands at 1072 and 1220 cm^{-1} might be assigned to the internal asymmetric stretching vibrations of SiO_4, AlO_4 tetrahedron as well as pore opening interior vibrations. [109-112]. The wavenumber regions at 1072 might be assigned to Si-O stretching of ZSM-5 framework. Metals introduced in the ZSM-5 structure showed slight variation. In generally the strong and weak bands exhibited the shift of stretching vibration $Si–O–M^+$ [113-115]. Eventually, the allocation of the bands depends on nature of metals present in ZSM-5 support. ZSM-5 parameters such as crystal size Si/Al ratio and acidity play important role for asymmetric stretching vibration. [116].

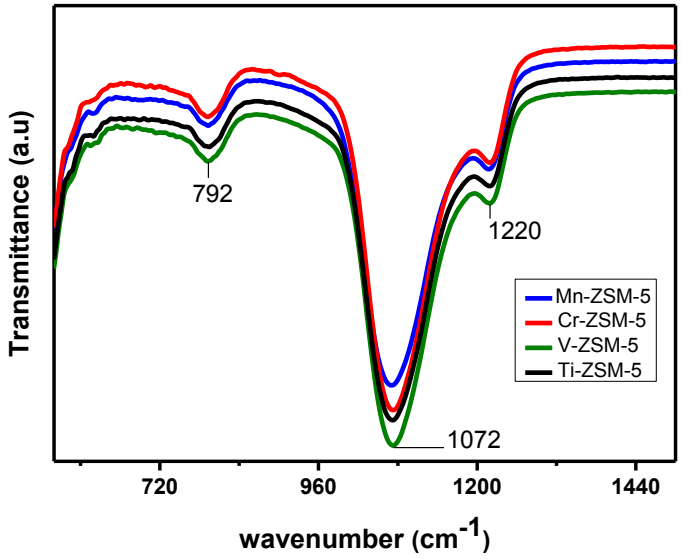

Figure. 3.9. FTIR spectra of ZSM-5 supported Mn, Cr, V and Ti based catalysts

3.3.6 Temperature programmed desorption of ammonia

3.3.6.1 ZSM-5 supported Zn, Cu, Ni and Co catalysts

Temperature Programmed Desorption (TPD) is a useful technique to know the acid-base characteristics of the solid heterogeneous catalysts. NH_3 is used as a probe molecule to estimate the total acidity of the catalysts. Depending upon probe gas, catalyst surface's acidity/basicity, the strength and/or number of acidic/basic sites can be evaluated. In this case, ammonia (NH_3) gas is employed as probe molecule [117-118]. Since NH_3 is basic in nature, it is anticipated to adsorb more easily on the acidic sites. The strength of acidic sites, ordered as weak and strong, was evaluated based on NH_3 desorption peak for instance acidic sites associated with the temperature of < 300 °C and > 300 °C are taken as weak and strong sites, respectively. Figure 3.10 shows TPD-NH_3 profiles of ZSM-5 supported Zn, Cu, Ni and Co based catalysts. For better comparison, pure ZSM-5 support is also included in the figure. It can be seen that all catalysts exhibited only one distinct peak at a temperature < 300 °C except Ni and Co catalysts which also showed one low intensity peak at a temperature of >300 °C. Moreover, Cu/ZSM-5 catalyst presented distinct peak at around 207 °C with relatively low intensity, Ni and Co based catalysts had almost similar peak maxima at around 212 °C while Zn/ZSM-5 catalyst showed desorption peak at 229 °C. It can be inferred from the intensity of low temperature peaks that Cu/ZSM-5 possess less number of acid sites and Zn/ZSM-5 contains more acid sites [119-122]. Furthermore shift of temperature from 207

°C, in case of Cu based catalyst, to 229 °C for Zn based catalyst dictates that later catalyst had more acidity in weak zone of acid sites. Conversly, Ni and Co based catalysts exhibited one more peak with low intensity that correspond to strong acid sites (i.e. peak at around 401 °C). Overall both these catalysts exhibit high acidity than other two catalysts. Pure ZSM-5 support also exhibits these two desorption peaks corresponding to both weak and strong acidic sites. The NH_3 uptakes and the TPD profiles of these catalysts are illustrated in Table 3.3 The amount of NH_3 desorbed of these samples are found to depend on the nature of metal doped and varied in the range from 902 to 924 µmol/g.

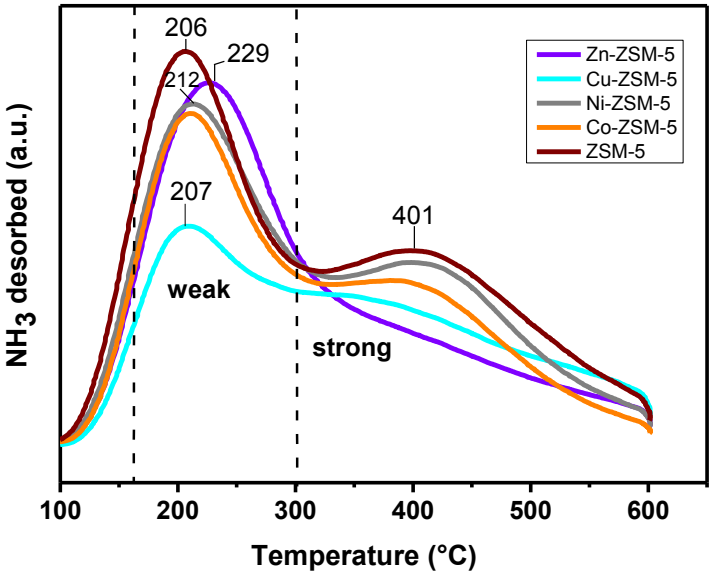

Figure 3.10. TPD-NH_3 profiles of ZSM-5 supported Zn, Cu, Ni and Co catalysts

Table 3.3 Amount of NH_3 desorbed (µmol/g) of various ZSM-5 supported catalysts

No.	Catalyst	Amount of NH_3 desorbed (µmol/g)
1.	ZSM-5	924.3
2.	Zn/ZSM-5	916.8
3.	Cu/ZSM-5	902.4
4.	Ni/ZSM-5	913.7
5.	Co/ZSM-5	910.1

3.3.6.2 ZSM-5 supported Mn, Cr, V and Ti catalysts

In Figure 3.11 depicts the ammonia desorption profiles as a function of temperature to assess the behavior of Mn, Cr, V and Ti based ZSM-5 supported catalysts against probe ammonia gas. Among all, Cr-doped exhibit higher acidity while the V/ZSM-5 shows the low acidity. In Figure.3.11 also demonstrates the presence of both weak and strong acidic sites in all the catalysts. The first type of acid sites with weak acid strength is getting desorbed relatively at low temperature for instance around 211 °C in case of Cr/ZSM-5 catalyst. The second type of acidic sites with somewhat higher acid strength is getting desorbed at higher temperatures at 400 °C. It is obvious from desorption profiles that each catalyst exhibted one distinct peak with peak maxima at 211 °C and a hump at 400 °C. These two peak maxima can be claasified, based on temperature, into two types i.e., low temperature peak can be assigned to weak acidic sites while high temperature peaks can be associated with strong acidic sites. Since all catalysts showed almost similar peak maxima at low and high temperature, the acidic strength can be distinguished based on quantity of ammonia desorbed as a function of temperature for each catalyst. For instance, Cr/ZSM-5 catalyst exhibited more number of acidic sites at both low and high temperature range while V based catalyst showed lower in both types of acidic sites [123-124].

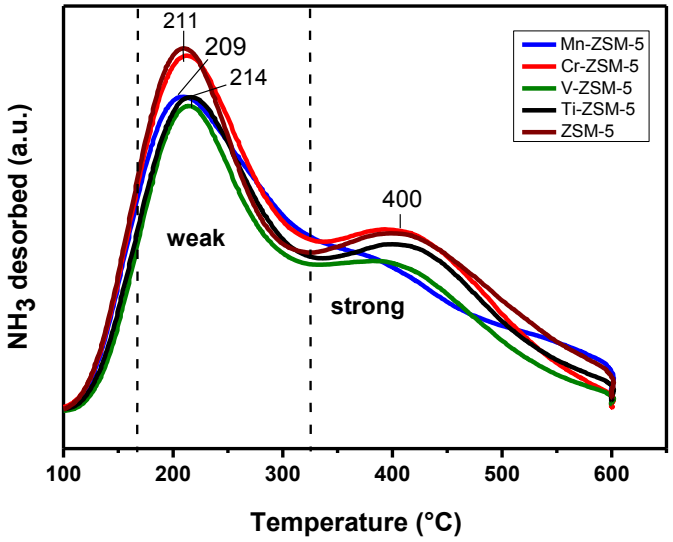

Figure 3.11. TPD-NH_3 profiles of ZSM-5 supported Mn, Cr, V and Ti based catalysts

If we compare the concentration of these two types of acidic sites, the weak acid sites appear to be major in proportion compared to stronger acidic sites. It is evident from Table

3.4 that the amount of NH_3 desorbed depends upon the type of metal doped into ZSM-5 support material. In other words, the acidity characteristics are different from metal to other metal.

Table 3.4. Amount of NH_3 desorbed (µmol/g) from various ZSM-5 supported catalysts

No.	Catalyst	Amount of NH_3 desorbed (µmol/g)
1.	ZSM-5	924.3
2.	Ti/ZSM-5	841.8
3.	V/ZSM-5	788.5
4.	Cr/ZSM-5	802.7
5.	Mn/ZSM-5	906.3

3.3.7 Temperature programmed reduction

It has been reported in several research articles in the literature that the active species in the reduced metal at the catalyst surface as well as metal-support interaction are important factors affecting catalytic performance in heterogeneous catalysis. Temperature programmed reduction (TPR) is a convenient technique to assess the number of reducible species. Moreover, the relative order of energy bonds existing between the reducible element/species and its surrounding environment can be estimated as well. Generally, more stable element needs higher reduction temperature to be reduced completely. Therefore, TPR experiments are carried out to investigate the reducibility as well as the interaction between active metal and support. TPR profiles for ZSM-5 supported Mn, Ti, Cr and V based catalysts are shown in Figure 3.12. Mn based ZSM-5 supported catalyst exhibited just a shoulder at 381 °C, which means the catalyst has low reducibility with low number of reducible species in terms of manganese oxide which are having weak interaction with the support and thus no distinct reduction peak is observed in case of Mn based catalyst. Probably MnO_x is present as Mn^{+2}, which may not be further reduced to metal under the conditions applied and hence no reduction peak appeared in the TPR profile. This shoulder can be assigned to the reduction of isolated CrO species reduction of Cr^{+3} to Cr^{+2}. It can be seen from reduction profiles in Figure 3.12 that Cr, Ti and V based ZSM-5 supported catalyst showed one distinct reduction peak having maxima at 381, 509 and 548 °C for Cr^{+2}, Ti^{+4} and V^{+4} containing catalysts, respectively. Since Cr based ZSM-5 supported catalyst showed peak maxima at lower

temperature which means that the catalyst contains more number of reducible species having weak interaction with the support and readily available for reduction. Moreover this peak can be assigned to the reduction of either chromium oxide species weakly interacted with ZSM-5 or the reduction of Cr(III) to Cr(II). CrOx species interaction in the ZSM-5 support is not highly dispersed or weak. Isolated CrOx particles species are existent on the ZSM-5 support. The high temperature reduction peaks for Ti and V based catalysts show that these catalysts contain species which need more temperature to be reduced and thus they are fully attached to the support dictating more metal-support interaction. VOx and TiOx species are highly scattered and may have strong intreraction with the support. The highly scattered TiOx and VOx species are accountable for the higher activity for Ti and V supported ZSM-5 [125-128]. TPR reduction peak having maxima at 509 °C in case of Ti based catalyst can be ascribed to the reduction of Ti^{+4} to Ti^{+3} species having strong interaction with the support while reduction peak at 548 °C for V based catalyst can be attributed to the reduction of strongly interacted vanadium oxide species V^{+5} to V^{+4} with ZSM-5. Therefore, it can be concluded that Mn and Cr based catalysts contain less metal-support interaction as compared to Ti and V based catalysts which are reduced at higher temperatures showing strong metal-support interaction. Eventually, it is obvious that the reduction behavior of the catalysts is considerably different. The reducible properties of these catalysts are strongly dependent upon the nature of metal doped.

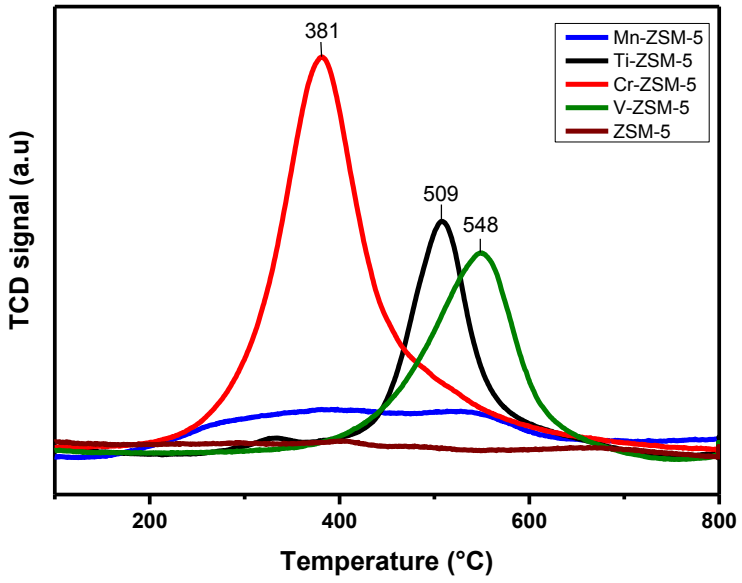

Figure 3.12. TPR profiles of ZSM-5 supported Cu, Ni, Cr and V based catalysts

3.3.8 Ultraviolet visible spectroscopy

3.3.8.1 ZSM-5 supported Mn, Cr, V and Ti catalysts

First of all, the Ultraviolet-Visible Spectroscopy is good technique to get information about chemical bonds, coordination and oxidation degree. Figure 3.13 illustrates the UV-vis spectra for ZSM-5 supported Mn, Cr, V and Ti based catalysts. It is obvious from the results that each catalyst exhibited absorption bands at different wavelengths. Apparently, Mn based catalyst did not show any significant absorption band that can be assigned to the d-d charge transfer band in manganese oxide [129-131]. Cr based catalyst supported on ZSM-5 showed different absorption bands at 274 and 369 nm. These bands correspond to presence of Cr^{+3} in chromium oxide (274 nm) and chromium oxide clusters (369 nm). In Vanadium based catalyst supported on ZSM-5, location of charge transfer band depends upon the symmetry of vanadium and oxygen atoms. The absorption band at 258 nm can be ascribed to low energy charge transfer of tetrahedral oxygen to central vanadium ion and the band at 396 nm can be attributed to charge transfer of vanadium oxide species dispersed over catalyst surface. Titanium, being isolated, tetrahedral coordinated showed an absorption band at 248 nm [132-133].

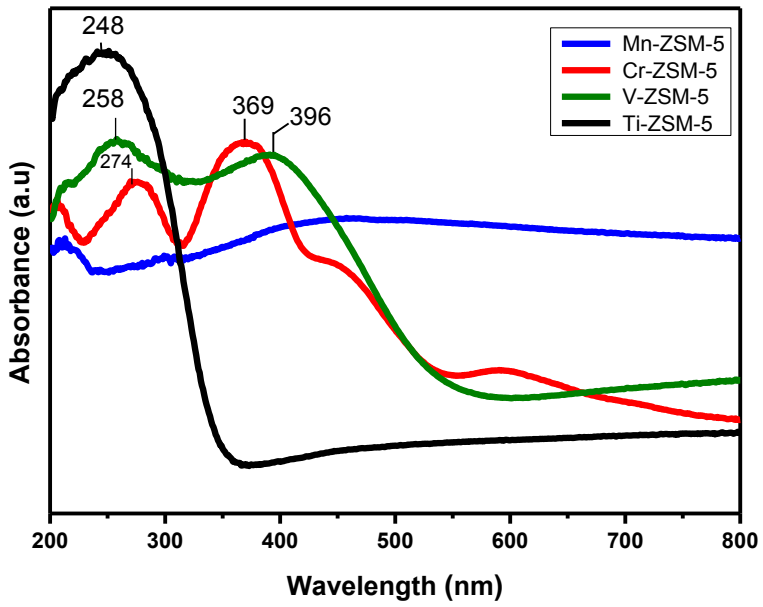

Figure 3.13. UV-Vis spectra of ZSM-5 supported Mn, Cr, V and Ti based catalysts

3.3.8.2 ZSM-5 supported Zn, Cu, Ni and Co catalysts

ZSM-5 supported Co, Cu, Ni and Zn catalysts are depicted in Figure 3.14. In the range 260-800 nm the absence of the d-d band is expected for Co^{+2}, Cu^{+2}, Ni^{+2} and Zn^{+2} ions in the spectrum of catalysts due to the absence of paramagnetic ions. On the other hand, bands at 272, 429 and 582 nm refer to oxygen-tetrahedral for Co^{+2} charge-transfer (CT) transitions t2→ (d) e and t1 →(d) e [134]. The results showed that no significant absorption peak was observed for both Zn and Ni based catalysts due to deformed tetrahedral species. The only peak at 339 nm for Cu based ZSM-5 supported catalyst can be assigned to Cu^{+2} having interaction with oxygen atoms of zeolite structure. Moreover, absorption peak at 272 nm, in case of Co supported on ZSM-5 catalyst, can be ascribed to zeolite structural electronic transitions as well as Co^{+2} sitting inside zeolite channel. The peaks in the absorption range of 400-600 nm can be attributed to oxides of cobalt [135]. Therefore, not any peak of Co, Cu, Ni and Zn in XRD analysis could be observed due to the reason that the metal is probably located inside the catalyst and form nano crystallites of below 5 nm size, which is the detection limit of XRD.

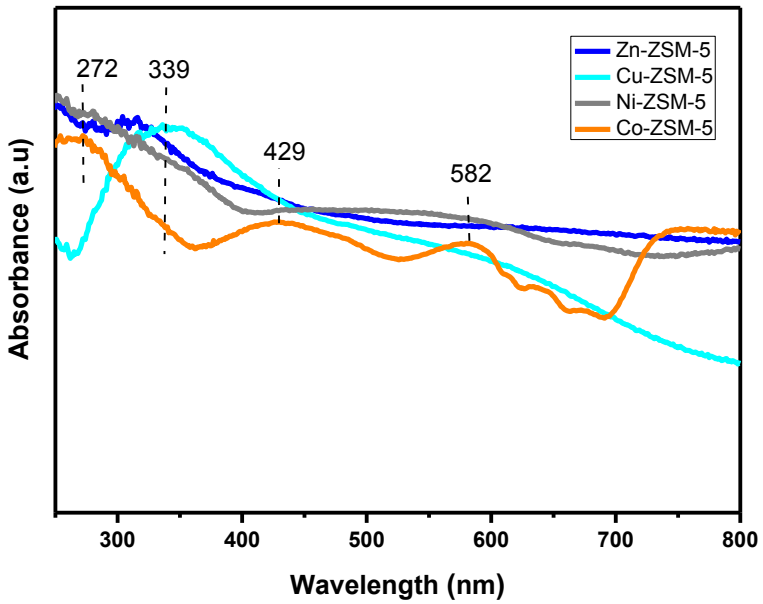

Figure 3.14. UV-Vis spectra of ZSM-5 supported Zn, Cu, Ni and Co catalysts

3.3.9 Transmission electron microscopy and Energy dispersive X-ray spectroscopy

Transmission electron microscopy (TEM) is a powerful tool to know the morphology, particle size, and size distribution. In order to assess some of the most important parameters affecting catalytic activity in heterogeneous catalysis, including active metal particle size, shape and distribution over support and morphology of the catalyst TEM is used. In addition, Energy Dispersive X-ray spectroscopy (EDX) was applied to get knowledge on elemental composition of studied spots.

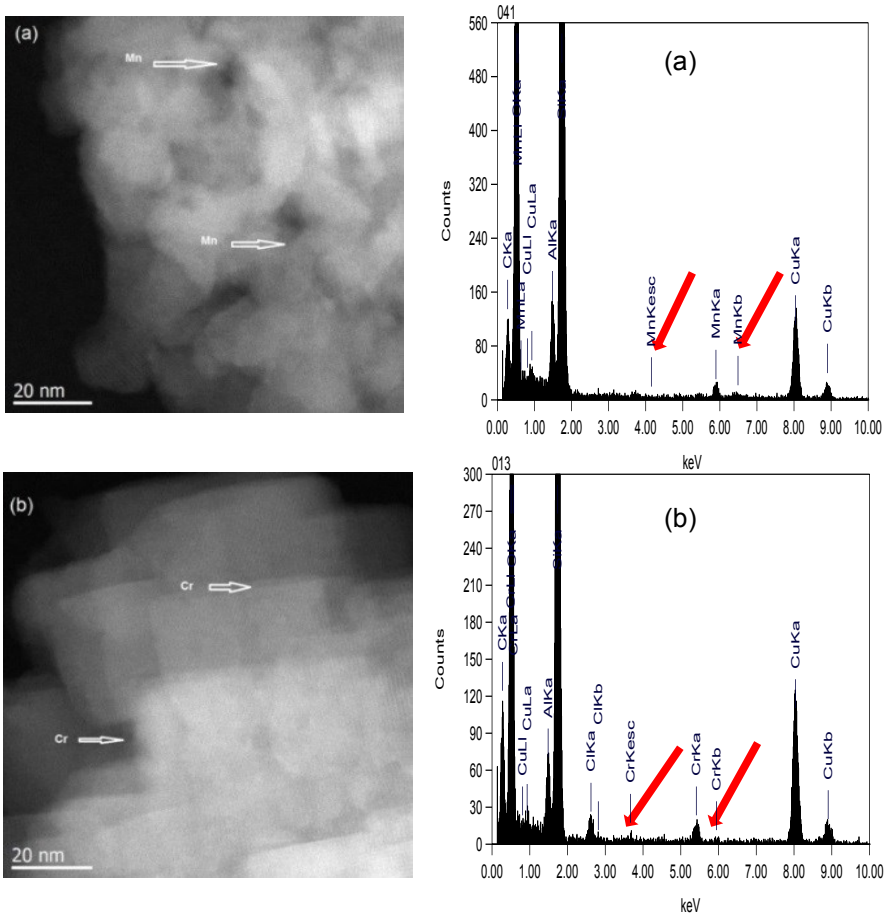

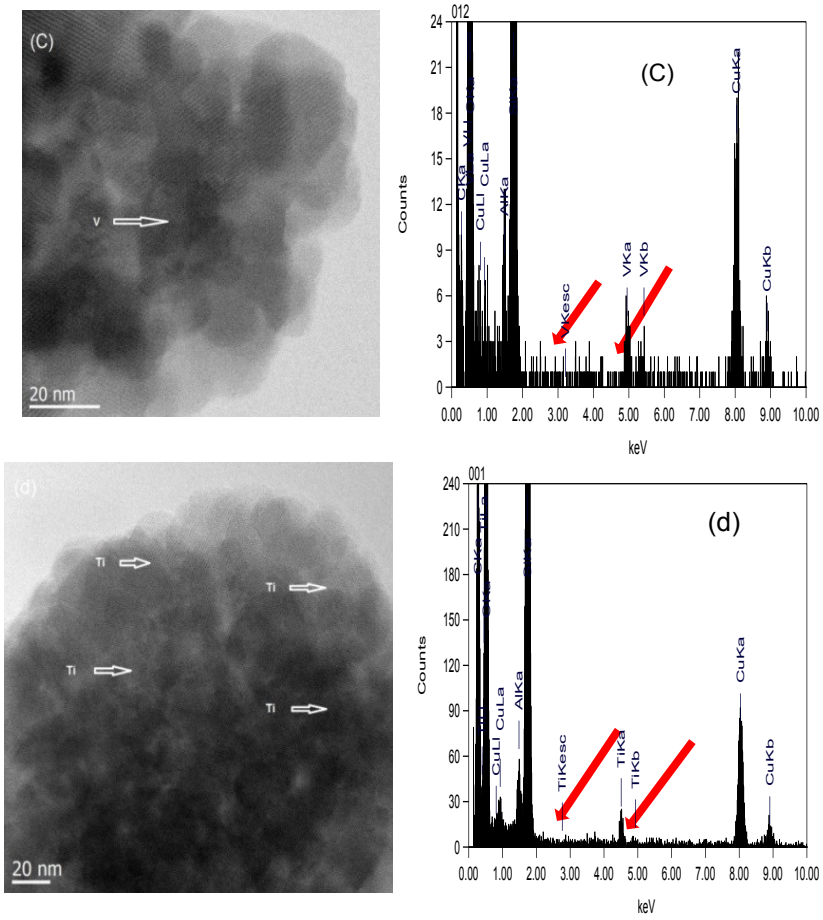

Figure 3.15. TEM images and EDX results of different catalysts of different catalysts: (a) Mn/ZSM-5, (b) Cr/ZSM-5, (c) V/ZSM-5, (d) Ti/ZSM-5

It is evident from Figure 3.15 that distinguished morphology corresponding to the doped metal could be seen in all images. However, it is observed that the metals doped are present in all these images. The oxide particles are indicated by white arrows. It is obvious from Figure 3.15 that ZSM-5 supported Mn, Cr, V and Ti catalysts could not show a clearly distinct morphology and distribution due to very low loading of active metal (1 wt%) also possibly due to incorporation of metals into the micro channels of zeolite structure or possibly destruction by electron-beam irradiation [136-138]. The size of particles of metal oxide play important role in activity and selectivity. Eventually, nature of metal revealed a significant effect on the distribution such as (Mn, Cr, V and Ti). Moreover, an EDX spectrum confirms the low contents of each metal as shown in the Figure 3.15. Doped metals are clear and can be seen

from EDX analysis. EDX) is generally used for the elemental analysis, which clearly revealed the presence of the metal doped in the ZSM-5 supported catalysts.

3.4 Catalytic results

3.4.1 General catalytic test conditions

ZSM-5 solid was used as support for preparing catalysts. The quantity of transition metals impregnated was 1 wt%. All catalysts were dried and calcined in a furnace at 500 °C at a heating rate of 2 K/min and held for 6 h under air atmosphere. Catalytic tests were carried out in a fixed bed stainless steel tubular reactor in the temperature range of 320 to 450 °C. N_2O was used as an oxidant and the catalytic tests were performed under varying reaction conditions. The reactor was filled with 2.0 g (as initial step for optimization of reaction) of catalyst particles (1-1.25 mm fraction) that were diluted with an equivalent weight of quartz beads of the same size to achieve isothermal operation. The reactant feed mixture was then introduced into the reactor and the reaction was performed, at a residence time of 1.4 sec at varying gas hourly space velocities 2612 h^{-1}. Liquid products were collected for every half-an-hour in an ice cooled trap and analyzed by off line GC equipped with FID, while gaseous products were detected by TCD.The reactant feed mixture was then introduced into the reactor and the reaction was performed, at a residence time of 1.4 sec. The benzene hydroxylation using nitrous oxide as an oxidant was carried out using different catalysts comprising various translation metals (each 1 wt%). The conversion of benzene and the yield of phenol obtained over these catalysts are shown in different figures. The phenol yield is the number of moles of phenol produced per mole of benzene. It is observed that the yields vary from 1.6 to 11.6%. Coking of catalyst seems to be an important problem of this reaction. Moreover, gas phase hydroxylation also leads to the formation of various other by-products such as catechol, bisphenol, 1,4-benzoquinone and total oxidation to CO and CO_2 too. The best selectivity of phenol with improved performance was obtained at a reaction temperature of 410 °C.

3.4.2 Optimization of reaction conditions

3.4.2.1 Effect of reaction temperature on the catalytic performance

Effect of reaction temperature on the conversion of benzene and the selectivity of phenol over 3 wt% Fe/ZSM-5 catalyst as initial test is presented in Figure 3.16. It is clear from the figure that the temperature has a promotional effect on the conversion of benzene but an adverse effect on the selectivity of phenol. The conversion of benzene is observed to increase from ca. 1% to over 7% with rise in temperature from 290 to 390 °C and then decreased with further increase in reaction temperature to 430 °C. Such decrease of conversion at high temperatures (430 °C) might be due to possible catalyst deactivation. Some additional hints on the deactivation process were also noticed from the change of color of the catalyst during the course of the reaction; for instance the red color of fresh catalyst is turned to black in the spent sample. On the other hand, the selectivity of phenol is maintained between > 80 to ca. 100% up to a temperature of 330 °C and then decreased continuously with further increase in reaction temperature to 430 °C, as expected. On the whole, the best selectivity of phenol is obtained at a temperature of 330 °C. The carbon balance, which indicates the quality of product analysis, is found to be good and vary in the range from 96 to 100%.

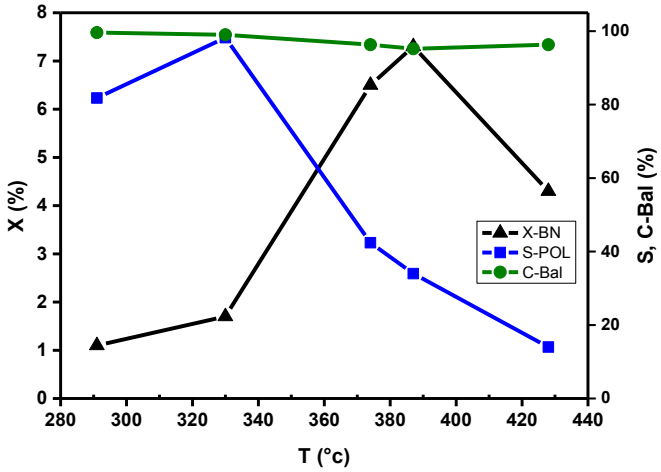

Figure 3.16. Effect of reaction temperature on the activity/selectivity of 3% Fe/ZSM-5 catalyst

(Reaction conditions: catalyst weight = 0.5 g; dilution: cat: glass beads = 1: 3 (wt/wt); Mole ratio of BN: N_2O: N_2 = 1: 0.5: 15; T = 330 °C; τ = 1.8 s; GHSV: 2006 h^{-1}; benzene: 5 mmol/h)

3.4.2.2 Effect of benzene to N_2O mole ratio on the catalytic activity and selectivity

Figure 3.17 demonstrates the influence of benzene/N_2O mole ratio on the catalytic performance of 3% Fe/ZSM-5 catalyst. It can be seen that the conversion of benzene is increased from about 2 to 3.5% with rise in the concentration of N_2O in the reactant feed mixture. However, the selectivity of phenol is enhanced only up to a benzene/N_2O mole ratio of 1: 1.6 beyond which the selectivity of phenol is observed to decrease. Based on this observation, benzene/N_2O mole ratio of 1: 1.6 appears to be optimum for future catalytic tests using various other catalyst compositions. The carbon balance is also found to be high in every case.

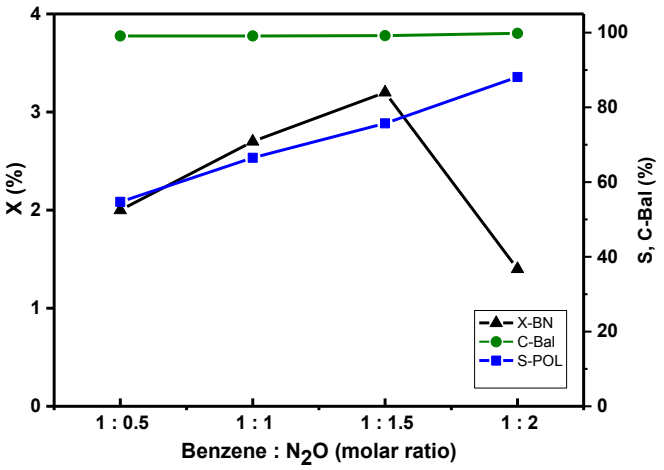

Figure 3.17. Effect of benzene: N2O mole ratio on the activity/selectivity of 3% Fe/ZSM-5 catalyst

(Reaction conditions: catalyst weight = 0.5 g; dilution: cat: glass beads = 1: 3 (wt/wt); T = 330 °C; τ = 1.8 s; GHSV: 2006 h^{-1}; benzene: 5 mmol/h)

3.4.2.3 Effect of benzene feed rate on the catalytic performance

Effect of benzene feed rate on the conversion of benzene and the selectivity of phenol is depicted in Figure 3.18. It can be seen that an increase in benzene concentration in the reactant feed mixture caused a decrease in the conversion of benzene, as expected. The conversion is decreased slightly from 3.5% to 1.5% with rise in its feed from 7 to 25 mmol/h. usually; one expects a decreased conversion with rise in the concentration of benzene in the feed due to its increased partial pressure. As a result, the adsorption of N_2O is affected to a considerable extent by the enhanced partial pressure of benzene in the reactant feed

mixture. At the same, the selectivity of phenol is enhanced from ca. 60% to close to 100%. Again the carbon balance is found to be maintained high and remained almost close 100%.

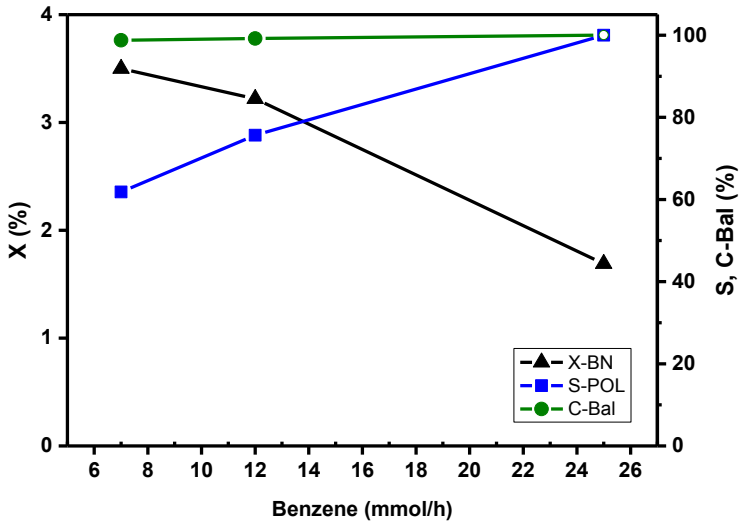

Figure 3.18. Effect of benzene feed rate on the activity/selectivity of 3 wt% Fe/ZSM-5 catalyst

(Reaction conditions: catalyst weight = 0.5 g; dilution: cat: glass beads = 1: 3 (wt/wt); T = 330 °C; τ = 1.8 s; GHSV: 2006 h^{-1})

3.4.2.4 Effect of GHSV on the catalytic performance

Figure 3.19 illustrates the influence of gas hourly space velocity (GHSV) on the catalytic performance of 3% Fe/ZSM-5 sample. It can be seen that the conversion of benzene is decreased with increase in GHSV from 1660 to 2006 h^{-1}, while the selectivity is enhanced from ca. 75 to 100 %. Surprisingly, the conversion is increased again at high GHSV, which is difficult to explain and needs further experiments to clarify this aspect. The carbon balance is observed to be close to 100 % in every case. From these studies, it appears that the GHSV of 2006 h^{-1} seems to be optimum over 3% Fe/ZSM-5 catalyst.

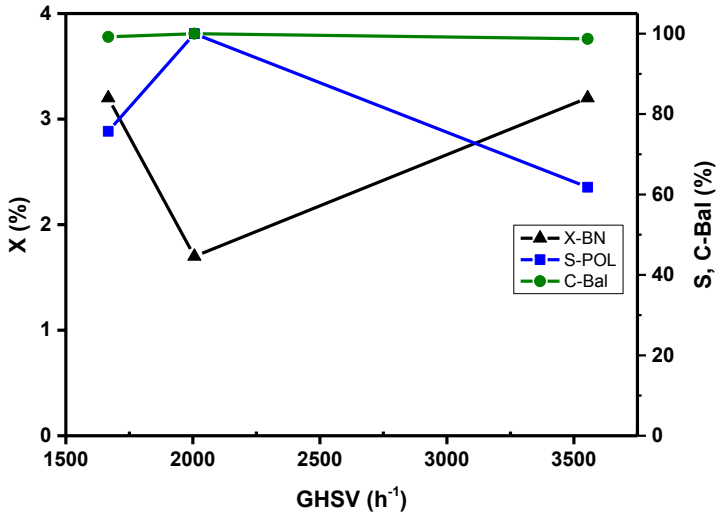

Figure 3.19 Effect of space velocity on the activity/selectivity of 3% Fe/ZSM-5 catalyst (Reaction conditions: catalyst weight = 0.5 g; T = 330 °C; mole ratio of BN: N_2O: N_2 = 1: 0.5: 15; τ = 1 to 2.1 s; benzene: 5 mmol/h)

3.4.2.5 Effect of Fe loading in Fe/ZSM-5 on the catalytic performance

This study was devoted to check the influence of Fe contents on ZSM-5 support. Three different loadings of Fe were used such as 1 wt%, 2 wt% and 3 wt%. The catalytic results obtained by varying the contents of Fe are shown in Figure.3.20. It is obvious from the figure that both the conversion of benzene and the yield of phenol were decreased considerably with increase in loading. The conversion of benzene decreased from 21.5. to 7.8% while the yield of phenol decreased from 8.8 to 4.9%, respectively. Among all, 1 wt% Fe was found to be optimum for achieving improved performance.

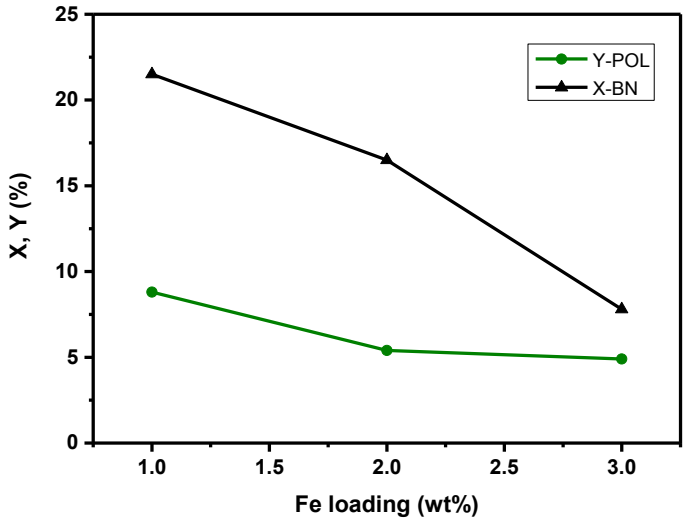

Figure 3.20. Dependence of X, Y on Fe loading of Fe/ZSM-5 catalyst
(Reaction conditions: catalyst weight = 0.5 g; T = 410 °C; mole ratio of BN: N_2O: N_2 = 1: 1.5: 82.3; τ = 1.8 s; benzene: 5 mmol/h)

3.4.3 Catalytic tests

3.4.3.1 Impact of V, Ti and Sc doping on the catalytic performance

It is evident from Figure. 3.21 that the nature of metal oxide has shown a clear influence on the catalytic performance. As expected, the pure ZSM-5 support has exhibited relatively poor performance compared to others. Pure ZSM-5 gave the lowest yield of phenol (about 1.6%) Results revealed that the yield of phenol obtained strongly depends upon the type of metal impregnated onto ZSM-5. V/ZSM-5 catalyst has displayed the best performance giving acceptably good selectivity of phenol (50%) at a benzene conversion of 24%. The remaining two catalysts such as Ti/ZSM-5 and Sc/ZSM-5 displays moderate conversions with a phenol yield of about 9%, and 7%, respectively. Of all the catalysts applied, V/ZSM-5 has shown the superior performance with acceptably high yield of phenol (Y = 12%). Ti-ZSM-5 is the second best catalyst with high selectivity (> 50%) but marginally low conversion compared to the best V/ZSM-5 catalyst. Even though, the yields of phenol achieved from these catalysts are not that high, they are not that bad compared to literature reports. Based on the performance of these catalysts, it was also thought to combine both the 1st and 2nd best metals such as V and Ti with similar amount and prepare a new catalyst containing both these metals using again ZSM-5 support. These results will however be discussed in a separate section focusing on bimetallic.

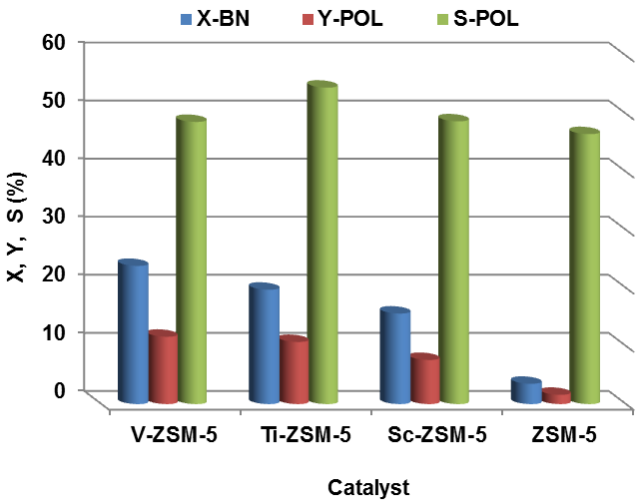

Figure 3.21. Effect of nature of metal on the benzene conversion and phenol yield at 410 °C (Reaction conditions: catalyst weight = 2 g; T = 410 °C; mole ratio of BN: N_2O: N_2 = 1: 1.5: 82.3; total flow: 12.8 l/h; τ = 1.8 s)

3.4.3.2 Impact of Co, Mn, and Cr doping on the catalytic performance

It is evident from Figure 3.22 that the Cr/ZSM-5 revealed the highest yield of phenol about 9.3% compared to other catalysts. However, this yield is low compared to earlier V/ZSM-5 catalyst (see Figure 3.21). For better comparison, the catalytic performance of pure ZSM-5 sample is also included in this Figure. As discussed earlier, the pure ZSM-5 solid displayed poor performance and hence the lowest percentage yield of phenol about 1.6%. The yield obtained on the remaining two catalysts such as Co/ZSM-5 and Mn/ZSM-5 represents moderate values with a percentage yield of phenol about 6% in each case. The conversion of benzene obtained on Mn/ZSM-5 and Cr/ZSM-5 catalysts is the highest which is close to 20%. However, Co/ZSM-5 catalyst showed somewhat low conversion of benzene (ca. 16%) compared to the above solids. The yields of phenol achieved from these catalysts are not that high. Three Coordination forms for Co/ZSM-5 catalyst namely Co-*α*, Co-*β*, and Co-*γ* are present inside the ZSM-5 channel [139]. The acidity of these catalysts has relationship with catalytic activity.

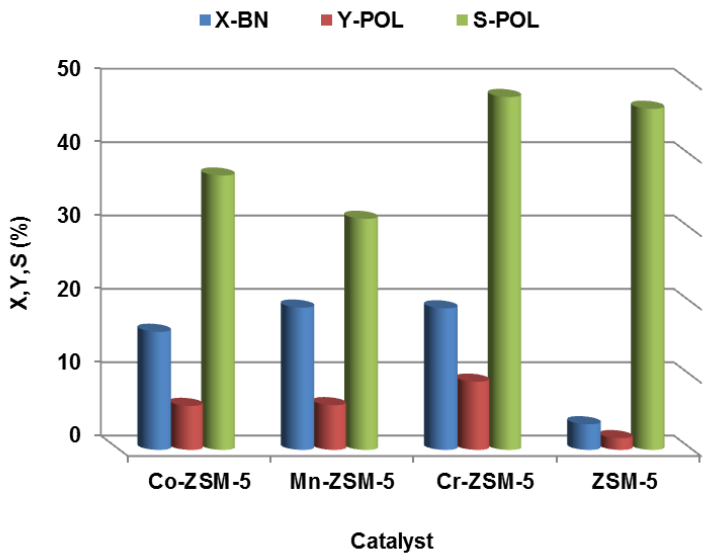

Figure 3.22. Effect of nature of metal on the benzene conversion and phenol yield at 410 °C (Reaction conditions: catalyst weight = 2 g; T = 410 °C; mole ratio of BN: N_2O: N_2 = 1: 1.5: 82.3; total flow: 12.8 l/h; τ = 1.8 s)

3.4.3.3 Impact of Ni, Cu, and Zn doping on the catalytic performance

Figure 3.23 illustrate the catalytic performance of M/ZSM-5 (M = Ni, Cu, Zn) catalysts tested at 410 °C. It is evident from the figure that the yield of phenol obtained in this series is the highest on Zn doped catalyst compared to all others. Among them, Cu-doping gave the lowest yield. Zn/ZSM-5 exhibit acceptably good yield of nearly 9% at a benzene conversion of ca. 20%. As mentioned above, pure ZSM-5 support has exhibited relatively poor performance compared to the three different metals doped onto it. The remaining proportion (i.e. the missing gap between the benzene conversion and phenol yield) is from the formation of different by-products such as catechol, 1,4-benzoquinone, CO, CO_2 etc. Moreover, the catalysts are observed to deactivate gradually with time due to coking. Results showed that the nature of transition metal has considerable influence on the catalytic performance. Among the three different transition metals used, Zn displayed the best performance of this series giving ca. 9% yield of phenol. The Brønsted acid site of HZSM-5 plays a key role in catalytic activity for an increase in the yield of phenol. The differences in catalytic activity for Ni, Cu, and Zn-containing catalysts can be referred to different coordination of metals and varying activities of cations doped [140]. Other important factors that can play a crucial role on catalytic activity are oxygen partial charge, electro negativity and radius of cations doped.

Therefore, cation radius of Zn^{+2} is bigger and it is also more electronegative than others. As a result, it seems to exhibit better performance compared to other two metals (Ni, Cu) of this series.

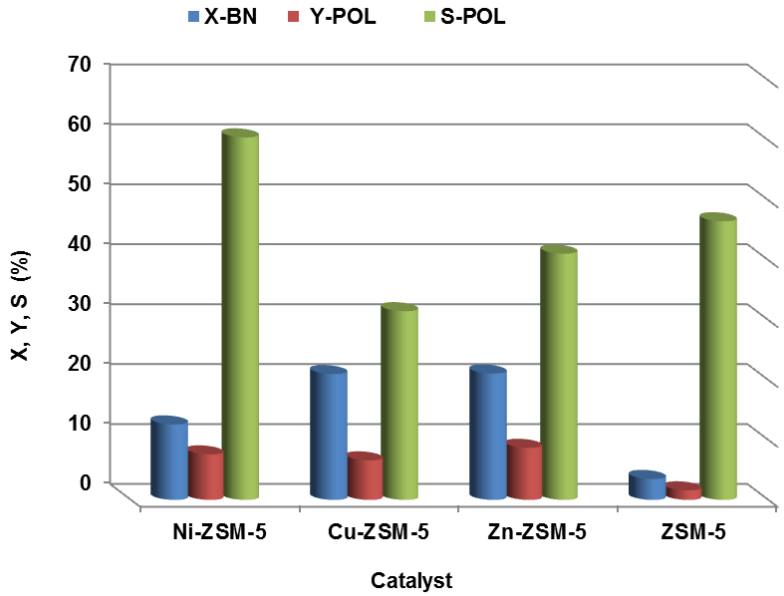

Figure 3.23. Effect of nature of metal on the benzene conversion and phenol yield at 410 °C (Reaction conditions: catalyst weight = 2 g; T = 410 °C; mole ratio of BN: N_2O: N_2 = 1: 1.5: 82.3; total flow: 12.8 l/h; τ = 1.8 s)

3.4.3.4 Impact of Pd, Ru and Fe doping on the catalytic performance

The catalytic performance of Pd, Ru, and Fe-doped ZSM-5 catalysts is compared in Figure 3.24.Here also the conversion of benzene and yield of phenol obtained over pure ZSM-5 solid is compared. In this series of three catalysts (Pd, Ru, Fe), Pd/ZSM-5 exhibit relatively high yield of phenol ca. 6.2%. The remaining two catalysts Ru/ZSM-5 and Fe/ZSM-5 also showed comparable yields of phenol (Ca. 6%) as that Pd/ZSM-5 catalyst. However, there is a clear difference in the conversion of benzene obtained over these three catalysts. Pd/ZSM-5 revealed the highest conversion (>30%) and low selectivity of phenol, while Fe/ZSM- showed low conversion (ca. 10%) and high selectivity of phenol close to 50%.

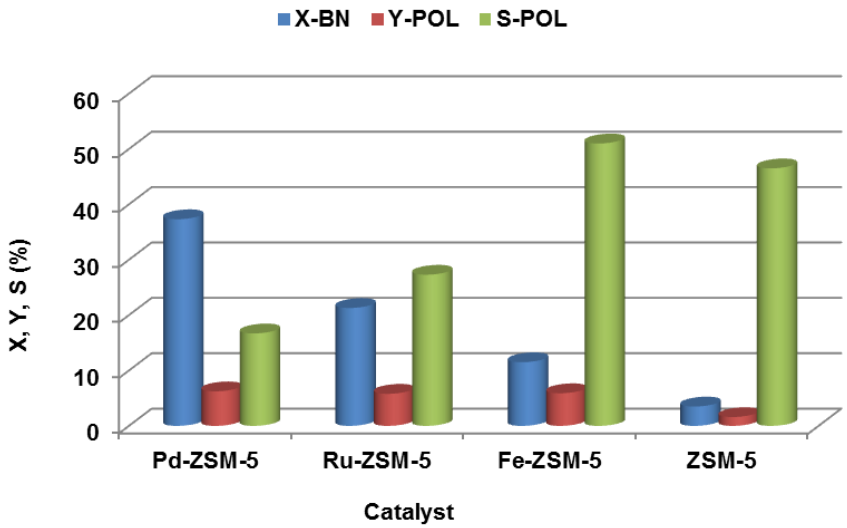

Figure 3.24. Effect of nature of metal on the benzene conversion and phenol yield at 410 °C (Reaction conditions: catalyst weight = 2 g; T = 410 °C; mole ratio of BN: N_2O: N_2 = 1: 1.5: 82.3; total flow: 12.8 l/h; τ = 1.8 s)

3.5 Summary and conclusions

Catalytic tests using various M/ZSM-5 solids have been carried out towards the direct conversion of benzene to phenol using N_2O as an oxidant. Furthermore, the basic characterisation of all these catalysts was also performed by various techniques such as BET-SA, TGA, XRD, FTIR, TPR, TPD, TEM etc.

- TGA-DTG profiles of ZSM-5 supported Co, Ni, Cu and Zn containing catalysts revealed two stages of weight loss due to removal of moisture and dehydroxylation while the second weight loss above 300 °C is due to transformation of precursor phase into active metal oxide phase. Similar trend of thermal stability and moisture evaporation was also observed for other catalysts of this study, e.g. Fe, Ti, V and Sc catalysts supported on ZSM-5 sample.

- XRD patterns of ZSM-5 supported Ni, Co, Cu and Zn based catalysts exhibited diffraction patterns of support material only. Similar results were obtained for Mn, Cr, V, Ti, Ru, Sc, Pd and Fe based ZSM-5 supported catalysts. Moreover, no crystalline reflection corresponding to doped metal was detected. All the catalysts samples seem to be X-ray amorphous due to low metal loading (1 wt%). However, only reflections corresponding to pure ZSM-5 support material could be seen.

- Nature of metal doped has strong influence on the BET surface areas, reducible properties, acidity characteristics and thereby the catalytic performance as well.
- Textural properties i.e. pore size distribution of ZSM-5 supported Zn, Cu, Ni and Co based catalysts showed bi-modal pore volume distributions with the dominant pore diameter at 85 and 110 nm, respectively.
- FTIR spectra of Mn, Cr, V, and Ti based ZSM-5 supported catalysts showed the presence of symmetric stretching of external linkages, pore opening external vibrations and O–H bending vibrations.
- TPD-NH_3 results of ZSM-5 supported Ni, Co, Cu and Zn based catalysts showed two peaks i.e., one at temperature of < 300 °C and other at temperature of > 300 °C depicting weak and strong acidic sites. In a similar way, Mn, Cr, V and Ti based ZSM-5 supported catalysts also showed similar peaks and distribution of acidic sites.
- TPR profiles of Mn, Ti, Cr and V based catalysts supported on ZSM-5 presented that Cr/ZSM-5 catalyst is easily reducible compared to other catalysts of this series.
- UV-Vis spectra of Mn, Cr, V and Ti based ZSM-5 supported catalysts showed the presence of Cr^{+3}, low energy charge transfer of tetrahedral oxygen to central vanadium ion, tetrahedral coordination of titanium. In case of Zn, Cu, Ni and Co based catalysts supported on ZSM-5, interactions of Cu^{+2} and Co^{+2} with zeolite was observed as well. V-Ti based bimetallic catalysts supported on different support materials showed isolated titanium atoms in octahedral-coordinated titanium species.
- TEM-EDX results of Mn, Cr, V and Ti based catalysts supported on ZSM-5 showed metal particles and these metal contents were confirmed through EDX.
- The pure ZSM-5 support exhibited poor performance, as expected, but if transition metals were introduced, the catalytic activity is enhanced significantly over the whole range of temperature. A variety of metals were doped onto ZSM-5 support, e.g. M/ZSM-5 (where M = Sc, Ti, V, Cr, Mn, Fe, Co, Ni, Cu, Zn, Ru and Pd).
- Concentration of metal on ZSM-5 support strongly affects the selectivity of phenol and benzene conversion.

- 1 wt% metal loading on ZSM-5 was found to be suitable value for improved yield of phenol and benzene conversion.
- V/ZSM-5 has shown the best performance among twelve different metals doped followed by Fe.
- From this study, a yield of phenol close to 11.6% could be achieved over V/ZSM-5 catalyst
- Deactivation of catalyst with time is observed and such deactivation is due to coke deposition during the course of the reaction.

Chapter 4

Effect of second metal addition to V/ZSM-5 on benzene hydroxylation

In this chapter the preparation, characterization and catalytic results obtained from the impact of second metal addition to V/ZSM-5 catalyst such as titanium, chromium, manganese, iron, nickel and zinc are described. These catalysts have been characterized by various techniques such as XRD, ICP, BET surface area, and NH_3-TPD.

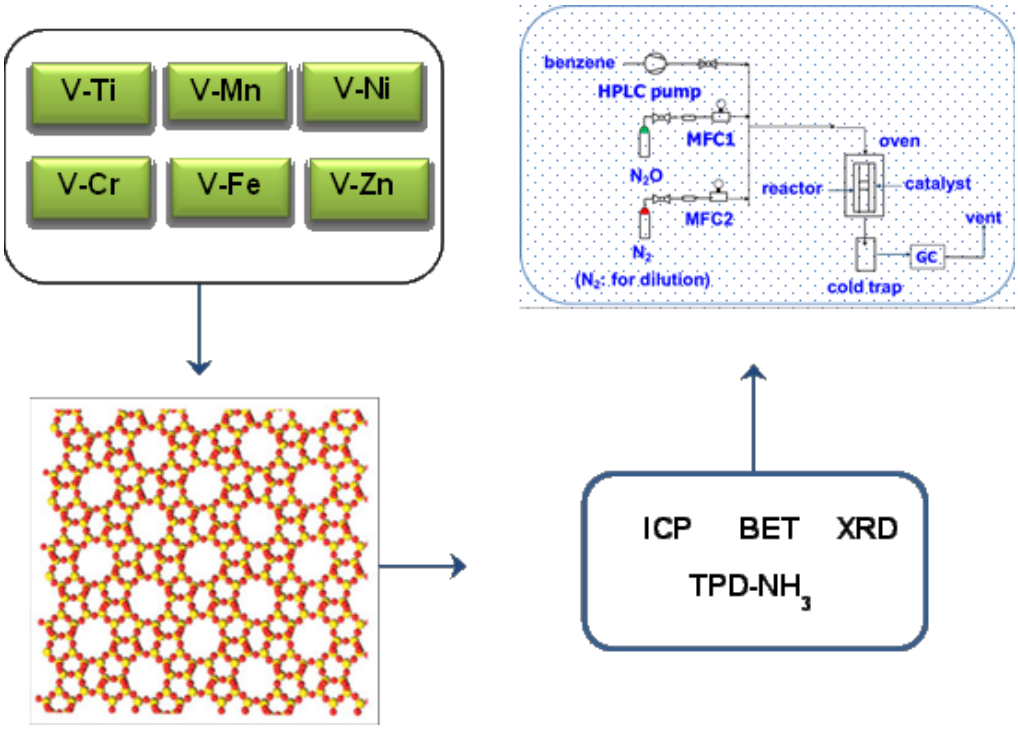

4. Effect of second metal addition to V/ZSM-5 on benzene hydroxylation

4.1 Studies on the ZSM-5 supported bimetallic catalysts

In chapter 3, the catalytic properties of various monometallic catalysts supported on ZSM-5 were investigated. It was found out that V/ZSM-5 was the best active and selective catalyst. Based on this result, it is proposed to prepare bimetallic catalysts by the addition of a second metal to V/ZSM-5. With such idea of exploring the potential of different bimetallic compositions, a variety of catalyst compositions (keeping vanadium content constant in every case) was prepared, characterized and tested. The bimetallic catalysts such as V-Ti/ZSM-5, V-Cr/ZSM-5, V-Mn/ZSM-5, V-Fe/ZSM-5, V-Ni/ZSM-5 and V-Zn/ZSM-5 were prepared by impregnation method again. Catalysts were calcined at 500 °C in air for 6 h. All these catalysts revealed considerably good catalytic performance with reasonably high conversion of benzene at high yields of phenol. The parent ZSM-5 support and bimetallic catalysts were characterized by, ICP, XRD, N_2 adsorption, and TPD-NH_3, techniques. The catalytic tests towards one step hydroxylation of benzene to phenol using by nitrous oxide was carried out in gas phase using fixed bed tubular reactor in the temperature range of 320-450 °C.

4.2 Catalyst preparation

Preparation method of the present bi-metallic catalysts is described below in detail (see Table 4.1). ZSM-5 was used as a support for the present study and the catalysts were prepared by impregnation method. In a typical procedure, requisite quantity of suitable metal precursor was dissolved in distilled water. Then the aqueous solutions of two metal precursors such as (V-Ti, V-Cr, V-Mn, V-Fe, V-Ni and V-Zn) were impregnated onto ZSM-5 powder and stirred for 30 min at ambient conditions. Then, the excess solvent was evaporated on a hotplate to dryness. Afterwards, the solid obtained was further dried at 110 °C for 12 h in an oven. Finally, the samples were calcined in air at 500 °C (heating rate of 2 K/min) for 6 h. The composition of such catalyst, type of metal precursors used and calcination conditions are given below in Table 4.1.

4.3 Characterization of bimetallic V-M/ZSM-5 catalysts

4.3.1 Textural properties and catalyst composition

The metal contents (V-Ti, V-Cr, V-Mn, V-Fe, V-Ni and V-Zn) determined by ICP-OES method are shown in Table 4.2. Parent HZSM-5 is having Si\Al mole ratio of 25. The BET-surface areas and metal content of these catalyst samples are determined by N_2 adsorption (Table 4.2). Elemental analysis and BET-Surface areas results of bimetallic catalysts are compiled

in Table 4.2. The nominal contents of metals impregnated are in good agreement with those of the values determined by ICP. It is also noteworthy that the surface areas depend upon the nature of metal impregnated. There is no big deference between the surface areas of parent ZSM-5 and the V-Ti/ZSM-5 catalyst. On the whole, the surface areas of the catalysts are found to vary in the range from 364 to 388 m^2/g.

Table 4.1. Composition of catalyst, type of metal precursors and calcination conditions

No.	Catalyst	Metal precursors	Calcination (°C/h/air)
1.	V-Ti/ZSM-5	VCl_3: $(NH_4)_2TiO(C_2O_4)_2 \bullet H_2O$	500/6
2.	V-Cr/ZSM-5	VCl_3: $(NH_4)_2TiO(C_2O_4)_2 \bullet H_2O$	500/6
3.	V-Mn/ZSM-5	VCl_3: $(NH_4)_2TiO(C_2O_4)_2 \bullet H_2O$	500/6
4.	V-Fe/ZSM-5	VCl_3: $(NH_4)_2TiO(C_2O_4)_2 \bullet H_2O$	500/6
5.	V-Ni/ZSM-5	VCl_3: $(NH_4)_2TiO(C_2O_4)_2 \bullet H_2O$	500/6
6.	V-Zn/ZSM-5	VCl_3: $(NH_4)_2TiO(C_2O_4)_2 \bullet H_2O$	500/6

* The content of metals impregnated was kept constant at 0.25wt% for each metal.

Table 4.2. The physical characteristics of the bimetallic and pure ZSM-5 catalysts

No.	Catalyst	Metal content* V & M (wt%) ICP	BET-SA (m^2g)
1.	V-Ti/ZSM-5	0.21 & 0.27	379.9
2.	V-Cr/ZSM-5	0.23 & 0.29	377.1
3.	V-Mn/ZSM-5	0.25 & 0.26	375.3
4.	V-Fe/ZSM-5	0.29 & 0.22	380.9
5.	V-Ni/ZSM-5	0.24 & 0.21	370.8
6.	V-Zn/ZSM-5	0.28 & 0.26	364.5
7.	HZSM-5	0.0	388.2

* Nominal contents of bimetallic are 0.25 wt% for each

4.3.2 XRD patterns

In order to estimate the different forms of phases existing in ZSM-5 supported (V-Ti, V-Cr, V-Mn, V-Fe, V-Ni and V-Zn) based catalysts, X-ray diffraction analysis was carried out and the obtained patterns are presented in Figure 4.1. It can be seen that all the bimetallic catalysts revealed similar diffraction patterns that corresponds to only support (ZSM-5) reflections. Moreover, no reflections corresponding to metal oxides doped could be seen, due to the presence of low concentration of metals doped (0.25 wt%) All the catalyst samples appear to be X-ray amorphous. However, the crystalline XRD reflections of only parent ZSM-5 support could be seen from the Figure 4.1.

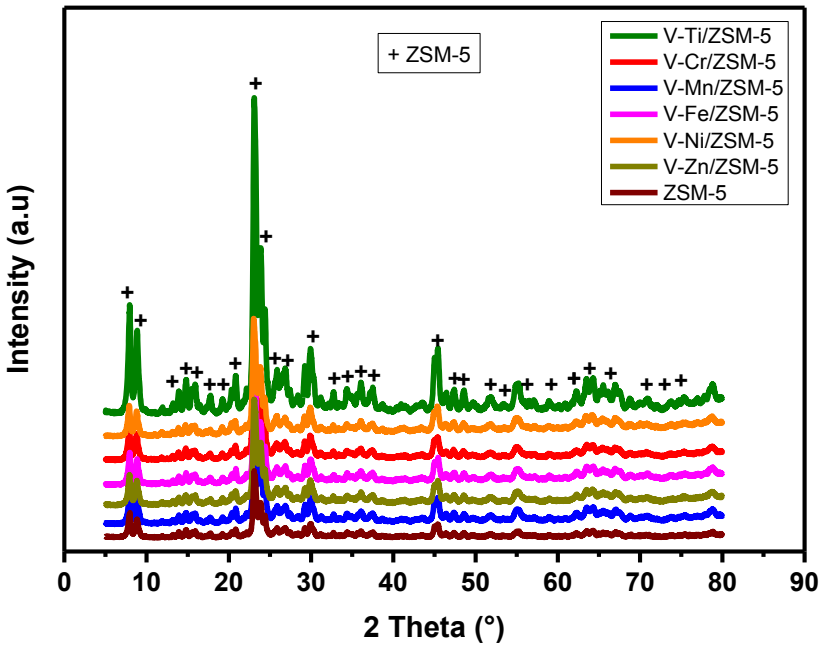

Figure. 4.1. XRD patterns of pure ZSM-5 and bimetallic catalysts

4.3.3 Temperature programmed desorption of ammonia profiles

The ammonia desorption profiles of pure ZSM-5 and bimetalic catalysts such as (V-Ti/ZSM-5, V-Cr/ZSM-5, V-Mn/ZSM-5, V-Fe/ZSM-5, V-Ni/ZSM-5 and V-Zn/ZSM-5) are depicted in Figure 4.2. NH_3 as a probe molecule assess the total acidity of the catalysts. It is evident from the figure that V-Ti/ZSM-5 catalyst and HZSM-5 support revealed higher acidity (related to high intensity of the peaks) while the other bimetallic solids exhibit relatively low acidity. All these bimetallic catalysts possess both types of acidic sites with varying strengths and the strength of the acidic sites depend upon the type of metal (s) doped onto ZSM-5 support.

The strong acidic sites appear in the temperature range from 310 to 450 °C while the weak acidic sites appear at around 200 °C. These two peaks can be claasified, based on the desorption temperature of NH_3 [141-142]. It is also evident from the NH_3-desorption profile that the two samples such as pure ZSM-5 and V-Ti/ZSM-5 exhibted one intense peak with peak maxima at 201-211 °C and a hump at 405 °C. Eventually, the NH_3 uptakes of theses catalysts are varied in the range from 842 to 924.3 µmol/g (Table 4.3).

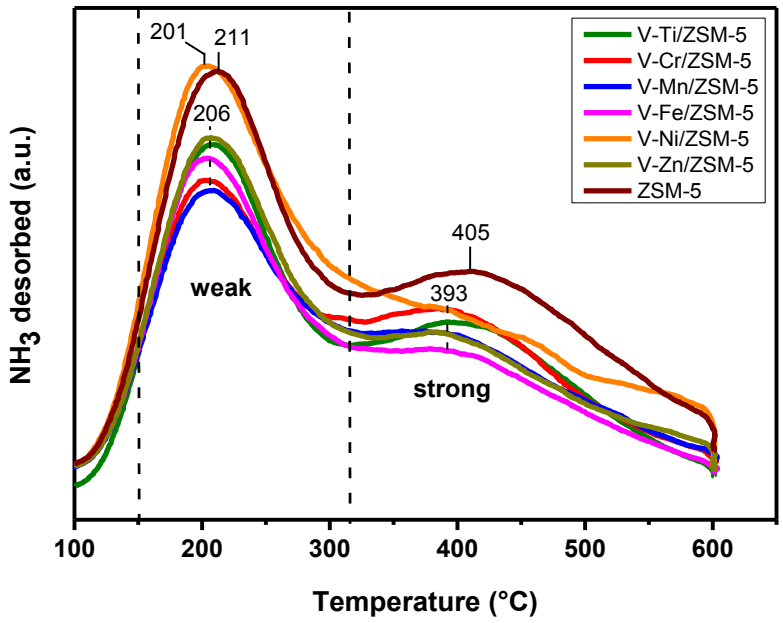

Figure. 4.2. NH_3-TPD profiles for parent ZSM-5 and bimetallic catalysts

Table 4.3. Amount of NH_3 desorbed (µmol/g) of various ZSM-5 supported bimetallic catalysts

No.	Catalyst	Amount of NH_3 desorbed (µmol/g)
1.	V-Ti/ZSM-5	893.0
2.	V-Cr/ZSM-5V	842.3
3.	V-Mn/ZSM	884.4
4.	V-Fe/ZSM-5	857.7
5.	V-Ni/ZSM-5	863.9
6.	V-Zn/ZSM-5	847.2
7.	HZSM-5	924.3

4.4 Catalytic results

4.4.1 Effect of V,Ti loading in 0.25V-0.25Ti/ZSM-5 catalyst on the performance

The influence of Vanadium and Titanium contents in V-Ti/ZSM-5 catalyst were explored. For this study, three different concentrations of V and Ti such as V: Ti = 0.25: 0.25 wt%, 0.5: 0.5 wt% and 1.0: 1.0 wt% were chosen. Figure 4.3 illustrates that the contents of V and Ti have shown considerable influence on the conversion of benzene and the yield of phenol. The conversion of benzene slightly decreased from 26.3 to 28.0% while the yield of phenol decreased from 16.4 to 12.0%, respectively. Eventually, a V: Ti concentration of 0.25: 0.25 wt% has revealed the best performance compared to other contents investigated.

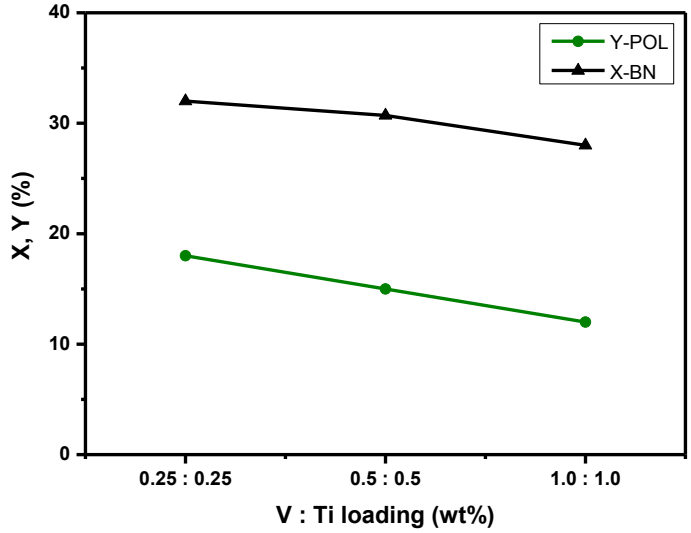

Figure 4.3. Dependence of X, and Y on V and Ti loading of V-Ti/ZSM-5 catalyst
(Reaction conditions: catalyst weight = 2 g; T = 410 °C; mole ratio of BN: N_2O: N_2 = 1: 1.5: 82.3; total flow: 12.8 l/h; benzene: 5 mmol/h; τ = 1.4 s)

4.4.2 Catalytic results of V-Fe, V-Ni, V-Zn bimetallic catalysts

It is clear from Figure 4.4 that metal oxide doped plays a vital role on the activity and selectivity of the catalysts. Parent ZSM-5 support has revealed comparatively poor performance compared to all other catalysts. Parent ZSM-5 has given the lowest yield of phenol (about 1.6%) at benzene conversion of < 5%. Results revealed that the yield of phenol obtained strongly depends upon the type of metal impregnated onto ZSM-5. Among them, V-Fe/ZSM-5 catalyst has exhibited the best performance giving reasonably good selectivity of phenol (ca. 35%) at a benzene conversion of 31%. The remaining two catalysts

such as V-Ni/ZSM-5 and V-Zn/ZSM-5 showed moderate benzene conversions (< 31%) with a phenol yield of about 8.0%, and ca.11%, respectively. The properties of metals such as radius of cations doped electronegativity and acidity are some of the key performance indicators that are responsible for the enhanced activity and stability of catalysts. The missing products for instance the gap between phenol yield and benzene conversion is due to the formation of various other by-products such as CO, CO_2 etc. These compounds in turn cause the deactivation of the catalysts. Therefore, deactivation of catalyst is essentially a problem during the reaction. On the other hand, the acidity of the catalyst plays a crucial role on catalytic activity which is increasing the yield of phenol. As expected, increasing the reaction temperature leads to increased conversion of benzene. Overall, the results exhibit that bimetallic catalysts have significantly affected the catalytic performance.

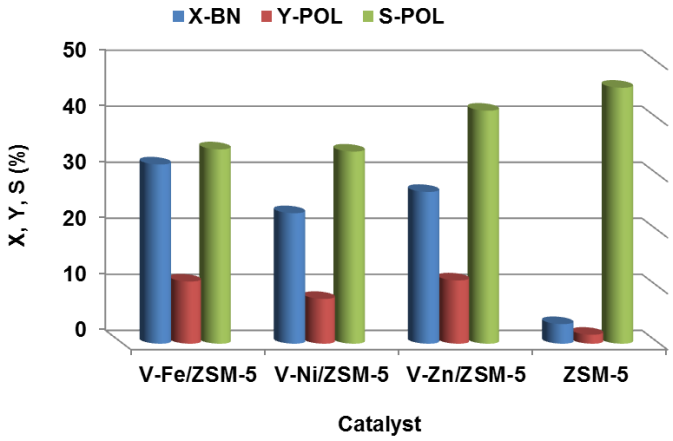

Figure 4.4. Effect of 2nd metallic component on the benzene conversion and phenol yield (Reaction conditions: catalyst weight = 2 g; T = 410 °C; mole ratio of BN: N_2O: N_2 = 1: 1.5: 82.3; total flow: 12.8 l/h; τ = 1.8 s)

4.4.3 ZSM-5 supported V-Ti, V-Cr, V-Mn bimetallic catalysts

In Figure 4.5 illustrates the catalytic performance of V-M/ZSM-5 (M = Fe, Ni and Zn) catalysts tested at 410 °C: It is clear from the figure that the yield of phenol obtained is the highest on V-Ti/ZSM-5 compared to others. The remaining two catalysts such as V-Cr/ZSM-5 and V-Mn/ZSM-5 showed somewhat low benzene conversion but comparable yield of phenol, i.e. about ca.12% and 9% respectively. As expected, the parent ZSM-5 solid exhibited the poor performance and hence the lowest yield of phenol (i.e. 1.6%). Of all the catalysts applied, V-Ti/ZSM-5 has revealed improved catalytic performance with respect to the yield of phenol (Y

= 16.4%). Among the three, V-Cr/ZSM-5 is the second best catalyst with slightly less phenol yield (ca.12%).

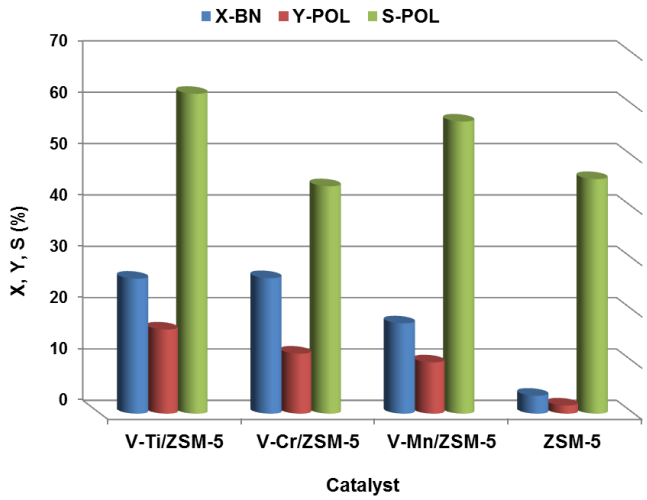

Figure 4.5. Effect of 2nd metallic component on the benzene conversion and phenol yield (Reaction conditions: catalyst weight = 2 g; T = 410 °C; mole ratio of BN: N_2O: N_2 = 1: 1.5: 82.3; total flow: 12.8 l/h; τ = 1.8 s)

4.5 Conclusions

The idea of doping 2nd metal and examining their catalytic potential was quite successful. Results have shown that the nature of 2nd metallic component revealed considerable influence on the catalytic performance. For this purpose, six different metals such as (V-Ti, V-Cr, V-Mn, V-Fe, V-Ni and V-Zn) with similar amount as vanadium (the best monometallic catalyst from the earlier results) were proposed. The catalysts were prepared in a similar manner as earlier. Among all, vanadium and titanium were observed to be the best two active components. As a result, the yield of phenol improved from 11.6% (on the best monometallic V/ZSM-5 catalyst) to 16.4% on the V-Ti/ZSM-5 bimetallic catalyst, optimized through the present study. All these catalysts were characterized by various techniques. XRD analysis revealed that no crystalline XRD reflections corresponding to any of the metals doped could be noticed in any of samples. Probable reason for the absence of crystalline reflections corresponding to doped metallic components is due to presence of small amount of metal (0.25 wt% each) in these bimetallic catalysts. As a result, the crystallite size of these metals is probably less than 5 nm, which is the detection limit of powder XRD technique. In

NH_3–TPD, the catalysts exhibited both weak and strong acidic sites. Among them, V-Ti/ZSM-5 catalyst has higher acidity than other catalysts. The parent ZSM-5 support showed poor performance, as expected. Eventually, among different catalyst applied, V-Ti/ZSM-5 has exhibited the best catalytic performance that can be attributed to acidic as well reducible properties of V, Ti metals doped. The variation in catalytic activity for bimetallic catalyst might be attributed to size of cations and coordination of metals. Deactivation of catalyst is noticed due to coke deposition on the surface of the catalyst. In view of the best performance of V-Ti/ZSM-5 bimetallic catalyst, it will be further discussed in the next chapter. Attempts were also made to optimize the right composition of this particular catalyst and at the same time the optimization of reaction conditions using this catalyst might be further helpful in improving the yield of the phenol.

Chapter 5

Benzene hydroxylation over bimetallic V-Ti/ZSM-5 catalyst

In this chapter the preparation, characterization and catalytic testing of V-Ti/ZSM-5 catalyst is described. Optimization of reaction conditions using V-Ti/ZSM-5 catalyst was also performed to obtain good results for enhanced phenol production from benzene using nitrous oxide as an oxidant. The V-Ti/ZSM-5 material has been characterized by various techniques such as TGA, ICP, N_2-adsorption, XRD, TPD-NH_3, and TEM-EDX. Such results were also discussed in this chapter.

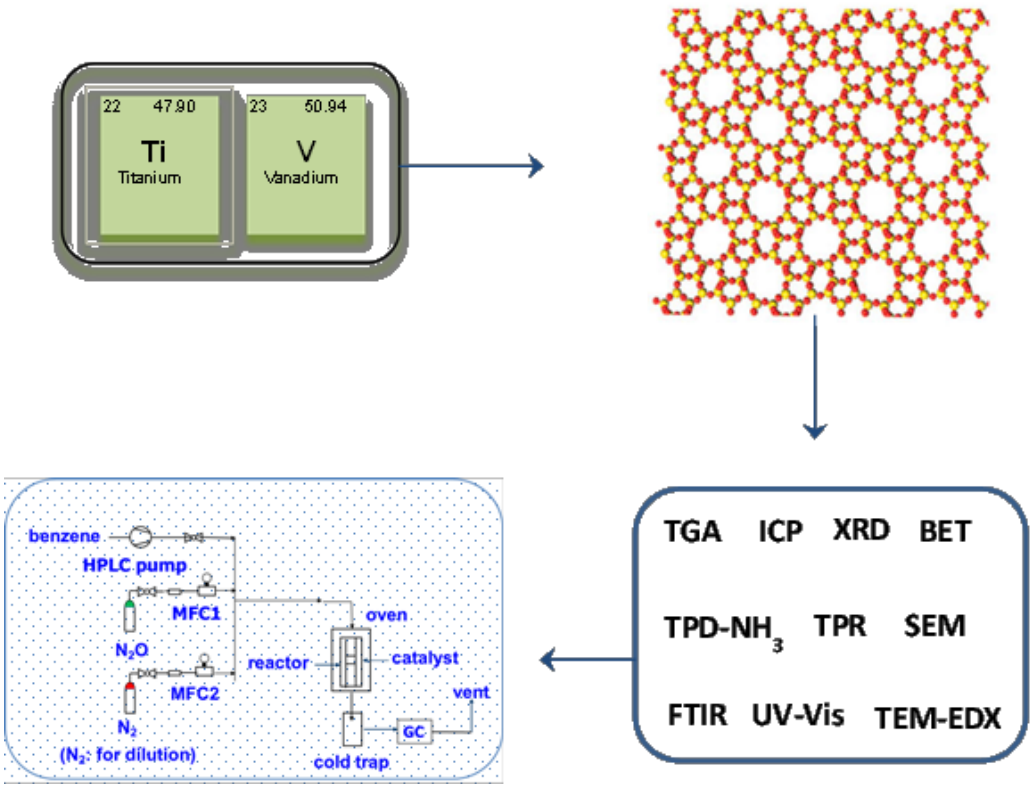

5. Benzene hydroxylation over bimetallic V-Ti/ZSM-5 catalyst

5.1 Studies on the ZSM-5 supported bimetallic V-Ti/ZSM-5 catalyst

Chapter 3 dealt with monometallic ZSM-5 catalyst and it was found out that vanadium and titanium were the best two active components. Based on those results on mono-metallic catalysts, it is proposed to combine the best two metals (V, Ti) as bimetallic two-component catalyst system supported on ZSM-5. Such results were described in this chapter 4 and such catalyst composition represents a simple system exhibiting considerably good catalytic performance. ZSM-5 was modified with vanadium and titanium by impregnation and such doped V-Ti/ZSM-5 solid was calcined in the range of temperature from 500-700 °C. This catalyst showed the best performance with significantly high yields of phenol at relatively high conversion of benzene. The pure ZSM-5 support and V-Ti/ZSM-5 catalysts were characterized by TGA, ICP, XRD, N_2 adsorption, TPD, TPR, SEM and TEM-EDX techniques. In addition, three different Si/Al ratios in the range of 25, 240, and 400 were selected for optimization purpose. Production of phenol from benzene using N_2O as an oxidizing agent was performed in gas phase using tubular reactor in the temperature range of 320-450 °C. Catalytic tests using V-Ti/ZSM-5 solid revealed amazing performance. In this study, the influence of all possible reaction variables was examined. For instance, i) the effect of calcination temperature, ii) the influence of Si/Ai ratio of ZSM-5 material, iii) the effect of reaction temperature, iv) the effect of GHSV, v) the impact of benzene feed rate, vi) the effect of benzene to nitrous oxide mole ratio on the catalytic activity and selectivity were explored. It should be noted that high reaction temperatures of >440 °C lead to rapid deactivation of the catalyst.

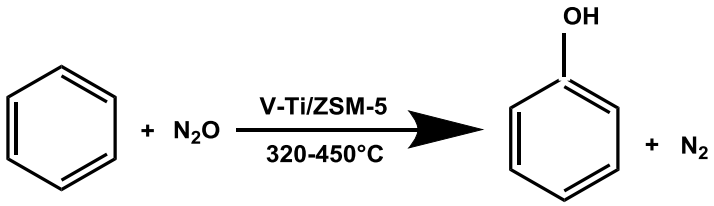

Scheme 5.1. Benzene hydroxylation to phenol using N_2O as an oxidizing agent

5.2. Catalyst preparation

Preparation method of V-Ti/ZSM-5 catalysts as shown in Table 5.1 is described below in detail. ZSM-5 powder (Si/Al ratio = 25) was used as a support for preparing various bimetallic catalysts by means of impregnation method. In a typical procedure, requisite quantity of

suitable metal precursor was dissolved in distilled water. Then the aqueous solutions of vanadium and titanium precursors were impregnated onto ZSM-5 powder and stirred for 30 min at ambient conditions. Then, the excess solvent was evaporated on a hotplate to dryness. Afterwards, the solid obtained was further dried at 110 °C for 12 h in an oven. Finally, the samples were calcined in air at 500 °C (heating rate of 2 K/min) for 6 h. The content of metals impregnated was kept constant at 0.25 wt% for each metal (i.e. V and Ti). The composition of such catalyst, type of metal precursors used and calcination conditions are given below in Table 5.1.

Table 5.1. Metal precursor sources, calcination conditions and metal contents of V-Ti/ZSM-5 catalyst

No.	Catalyst	Metal precursors	Calcination (°C/h/air)	Metal content
1	V-Ti/ZSM-5	Ti: $(NH_4)_2TiO(C_2O_4)_2 \bullet H_2O$ V: VCl_3	500/6	V = 0.25 wt% Ti = 0.25 wt%

5.3 Characterization of bimetallic V-Ti/ZSM-5 catalyst

5.3.1 Thermogravimetric analysis

In order to study the transformation temperatures and thermal stability of solid materials, thermogravimetric (TG) analysis and Derivative Thermo Gravimetry (DTG) were performed on V-Ti/ZSM-5 catalysts and these results are given in Figure 5.1. V-Ti/ZSM-5 showed a weight loss of 5.7% in the first stage. It is evident from the figure that the weight loss in the sample takes place in two stages. The first is related to desorption of adsorbed water, dehydroxylation of surface and party due to decomposition of metal precursors and their conversion to their corresponding oxides and all these changes occur below 300 °C. As a result, the major weight loss is occurring below 300 °C. Absence of weight could be allocated to the elimination water from the surface due to decay of metal precursors [143]. The second stage weight loss occurs in the range of 300-500 °C, which is due to conversion of residual metal precursors into oxides. Such weight loss is low because of low amount of active metal loadings (only 0.5 wt% together) used. As expected, no considerable weight loss is observed beyond 500 °C. The shoulder peak observed in derivative thermogravimetric shows the temperature (i.e. 130.7 °C) at which the weight loss takes place for ZSM-5 supported V and

Ti catalysts. Based on the results of this investigation, a calcination temperature of 500 °C in air is fixed for V-Ti/ZSM-5 catalyst.

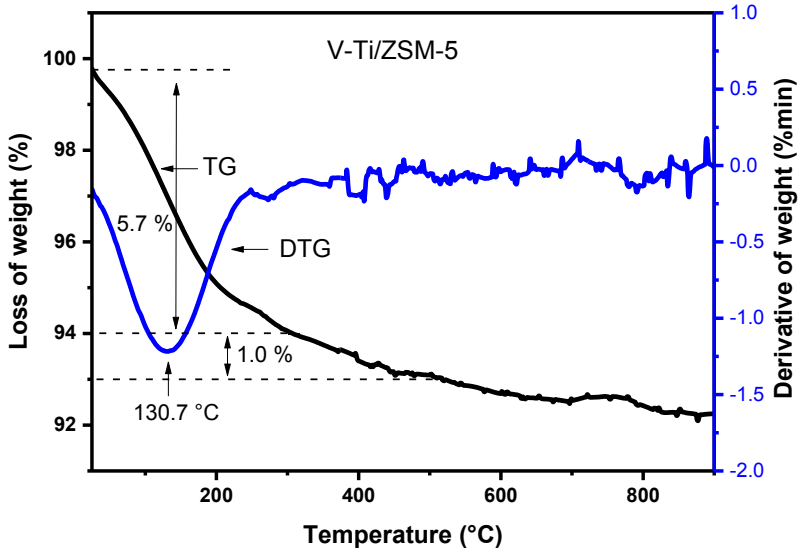

Figure 5.1. TGA-DTG curves of bimetallic V-Ti supported on ZSM-5 catalyst

5.3.2 Textural properties and catalyst composition

BET-Surface areas, elemental analysis and total pore volume results of V-Ti/ZSM-5 catalysts are compiled in Table 5.2. The metal content (V, and Ti) determined by Inductively Coupled Plasma Optical Emission Spectroscopy (ICP-OES) are also shown in the same table. Parent zeolite used is HZSM-5 having Si\Al molar ratio of 25. The BET-surface areas and pore volumes of this catalyst samples are determined by N_2 adsorption (Table 5.2). It is noteworthy that there is no big deference between the surface area of parent ZSM-5 and the V-Ti/ZSM-5 catalyst.

Table 5.2. Physical characteristics of pure ZSM-5 and V-Ti/ZSM-5 catalysts

No.	Catalyst	Metal content* (wt%) ICP	BET-SA (m^2g)	Total pore volume (cm^3/g)
1.	HZSM-5	0.00	388.2	0.311
2.	V-Ti/ZSM-5	0.21-0.27	379.9	0.331

* Nominal contents of V and Ti are 0.25 wt% each

5.3.3 Pore-Size distribution of pure ZSM-5 and V-Ti/ ZSM-5 samples

Barrett, Joyner, and Halenda (BJH) method was applied to estimate the pore size distribution of these two samples using desorption branch of the isotherm.

Pore size distribution curve of the pure ZSM-5 sample exhibits bi-modal distribution with the dominant pore diameter of 92 and 153 nm, respectively (Figure 5.2.). However, doping of V and Ti even in small amounts completely changed the pore size distribution patterns. Consequently, incorporation of V and Ti caused dramatic decrease in the intensity of pore located at 92 nm while the pores located at 153 nm were completely vanished. Moreover, some new pores with the dominant pore diameter of 207 nm were generated in V-Ti/ZSM-5 sample. In other words, the pore size distribution of pure ZSM-5 solid is considerably shifted to higher pore diameter range by the doping of V and Ti metals into ZSM-5 sample. In addition, it is noticed the total pore volume for parent HZSM-5 support is slightly less than the ZSM-5 supported V and Ti catalyst (Table 5.1).

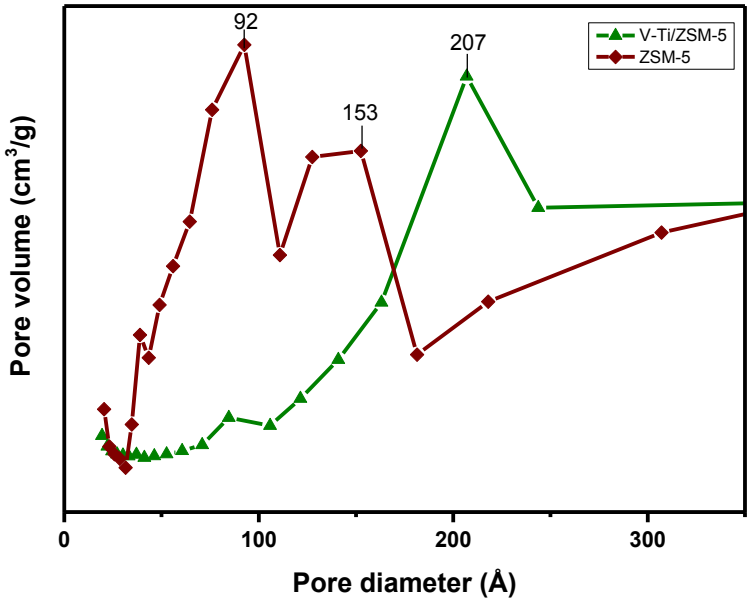

Figure 5.2. Pore size distribution for pure ZSM-5 and V-Ti/ZSM-5 catalysts

5.3.4 X-ray diffraction

The X-ray diffraction (XRD) pattern V-Ti/ZSM-5 catalyst is portrayed in Figure 5.3. For comparison, the XRD pattern of parent ZSM-5 is also presented in the same figure. Vanadium and Titanium metals are present in very low concentration (0.25 wt% for each) and hence the crystallite size of these metals is more likely less than 5 nm, which is below

the detection limit of powder XRD. Therefore, no metal or metal oxide reflections could be seen in the XRD pattern, which is again due to formation of small crystallites and low concentration of metal content (0.25 wt% for V and Ti). However, our ICP results suggest that these two metals (V and Ti) undoubtedly exist in the framework. Moreover, all the crystalline reflections belong to ZSM-5 support could be clearly seen (Figure 5.3). Therefore, it appears that the catalysts are X-ray amorphous in nature. It is well-known that ICP is more accurate method to determine the metal contents existing in these catalysts.

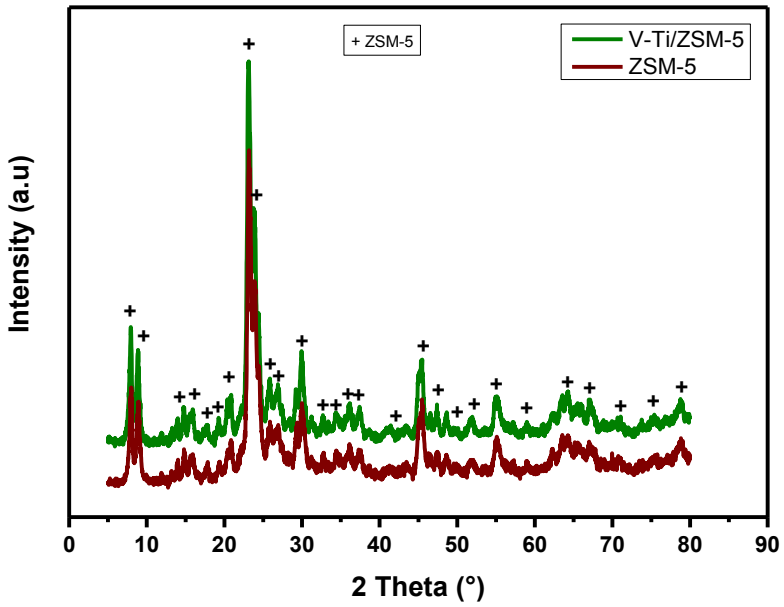

Figure 5.3. XRD patterns of pure ZSM-5 and V-Ti/ZSM-5 catalysts

5.3.5 Temperature programmed desorption of ammonia

Figure 5.4. shows the ammonia desorption profiles of pure ZSM-5 and V-Ti/ZSM-5 catalysts as a function of temperature. Ammonia as a probe molecule estimates the total acidity of the catalysts. It is clear from the figure that pure V-Ti/ZSM-5 supoort exhibits higher acidity whiles the vanadium and titanium doped solid shows the low acidity. The first peak appeared at around 200 °C corresponding to weak acidic sites that are getting desorbed relatively at low temperate of 200 °C. The second and weak peak appeared at 405 °C is related to stronger acidic sites. These two peaks can be claasified, based on temperature of desorption It is also evident from the NH_3-desorption profile that the two samples exhibted one intense peak with peak maxima at 202-211 °C and a hump at ca. 405 °C increasing of Si/Al ratio

leads to decrease with the acid sites of ZSM-5 [144].The ammonia uptakes of HZSM-5 and V-Ti/ZSM-5 samples are compiled in Table 4.3.

Table 5.3. Amount of NH_3 desorbed (μmol/g) of ZSM-5 supported bimetallic V-Ti/ZSM-5 catalysts

No.	Catalyst	Amount of NH_3 desorbed (μmol/g)
1.	V-Ti/ZSM-5	893.0
2.	HZSM-5	924.3

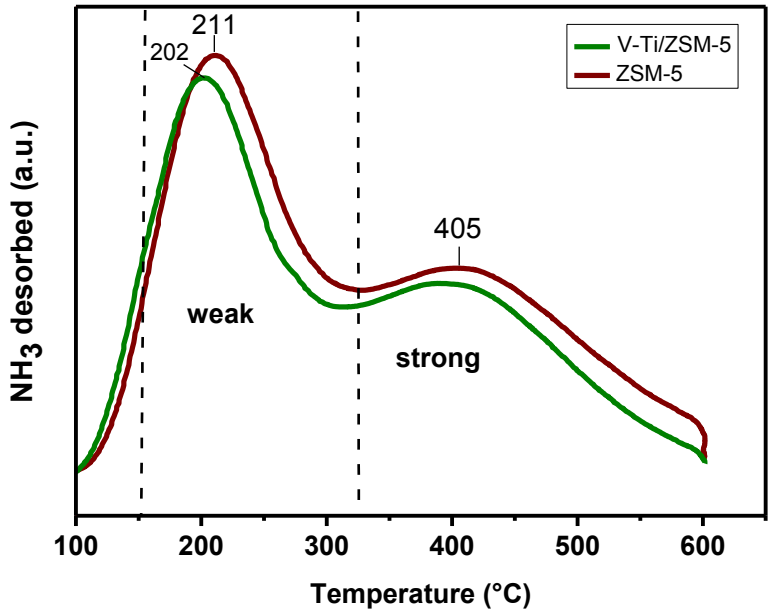

Figure 5.4. NH_3-TPD profiles for pure ZSM-5 and V-Ti/ZSM-5 catalysts

5.3.6 Transmission Electron Microscopy and Energy dispersive X-ray spectroscopy

TEM is powerful technique to determine the shape, size and distribution of particles over support and overall morphology of the catalyst. It is evident from Figure 5.5 that the presence of Ti and V could be seen in the electron micrograph of V-Ti/ZSM-5 sample. However, clearly distinguishable morphology of the sample could not be observed. At the same time, it is also difficult to determine the size of VOx and TiOx particles and their distribution, which is certainly due to presence of very small loadings of active metals (0.25 wt%V and 0.25 wt%Ti)

in the catalyst sample. Moreover, an EDX spectrum also confirms the presence of V and Ti in low amounts (see Figure 5.5). The locations of metals are indicated by white arrows in electron micrograph and with red arrows in EDX spectrum.

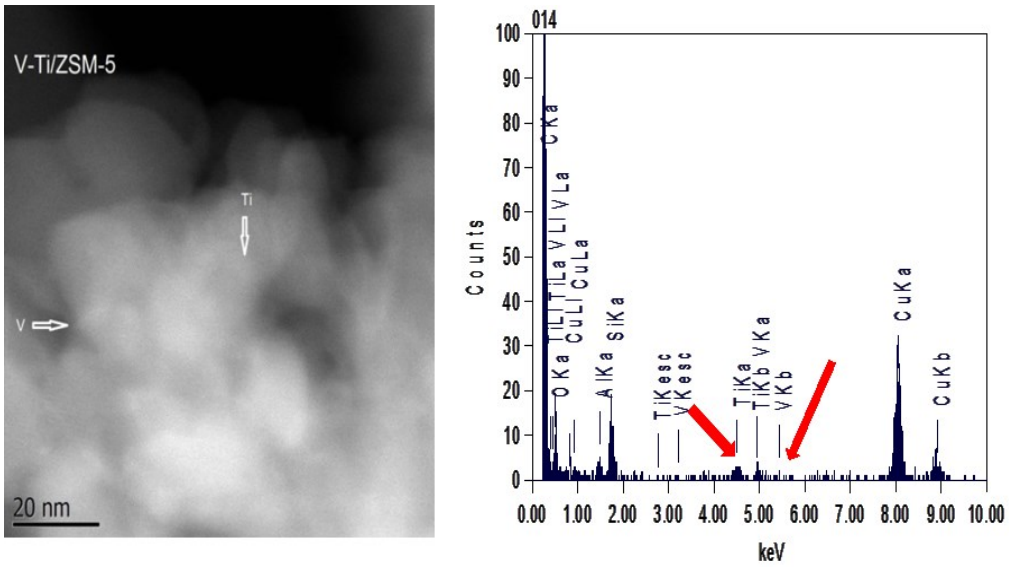

Figure 5.5. TEM image and EDX spectra of V-Ti/ZSM-5 catalyst

5.4. Catalytic tests

V-Ti/ZSM-5 catalyst with (Si/Al = 25) were selected as an efficient catalyst for benzene to phenol. Catalytic tests were carried out in a fixed bed stainless steel tubular reactor in the temperature range from 300 to 440 °C. The catalytic tests were carried out under varying reaction conditions using nitrous oxide as an oxidizing agent. Liquid products were collected for every half-an-hour in an ice-cooled trap and analyzed by off-line GC equipped with FID, while gaseous products were detected by TCD.

5.4.1 Optimization of reaction conditions

5.4.1.1 Influence of calcination temperature on the catalytic activity of V-Ti/ZSM-5

Effect of calcination temperature on the conversion of benzene and yield of phenol was explored using V-Ti/ZSM-5 catalyst. As mentioned earlier, this particular catalyst is selected due to its superior performance compared to others tested so far. This V-Ti/ZSM-5 catalyst has been subjected to three different calcination temperatures such as 500, 600 and 700 °C under identical calcination conditions except temperature variation. It is quite evident from Figure 5.6 the calcination temperature has shown considerable influence on the catalytic

performance. It is also apparent from Figure 5.6 both the conversion of benzene and the yield of phenol are observed to decrease with increase in calcination temperature from 500 to 700 °C. The conversion of benzene was decreased from 26.3 to 22.5% while the yield of phenol was decreased from 16.4 to 14.8%. Therefore it is clear that a calcination temperature of 500 °C has given the best performance. Based on these results, a calcination temperature of 500 °C is considered to be an optimum and hence such temperature is further used in subsequent runs, where all catalysts are calcined at this temperature. The inferior catalytic performance of other two catalysts calcined at higher temperature (600 and 700 °C) might be due to forming of different active phase, varying crystallinity of VO_x and TiO_x species and also probably due to decreasing surface areas on the other hand. Deactivation of samples calcined at 500 to 700 °C might be due to various concentration of active site which leads to decrease of oxidative activity [145-146].

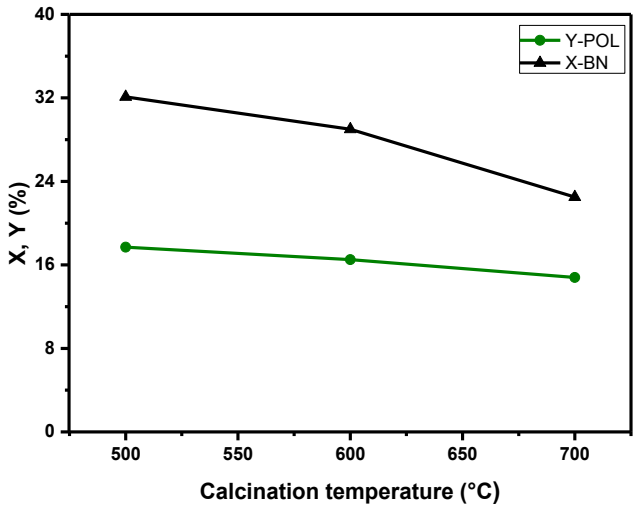

Figure 5.6. Effect of calcination temperature on X, Y over 0.25V-0.25Ti/ZSM-5 catalyst (Reaction conditions: catalyst weight = 2 g; T = 410 °C; mole ratio of BN: N_2O: N_2 = 1: 1.5: 82.3; benzene: 5 mmol/h; τ = 1.4 s)

5.4.1.2 Impact of Si/Al ratio of ZSM-5 in V-Ti/ZSM-5 catalyst

After catalytic testing on optimization of the calcination temperature, the subsequent focus was laid on exploring the influence of Si/Al ratio of ZSM-5 support on the catalytic properties of V-Ti/ZSM-5 catalyst. For this study, three different ZSM-5 supports with varying Si/Al ratios (25, 240, and 400) were selected. It is obvious from Figure 5.7 that the conversion of

benzene increased first with increase in Si/Al ratio from 25 to 240 and then decreased considerably with further increase in Si/Al ratio to 400. On the other hand, the yield of phenol has been observed to decrease continuously from 16.4 to 7.9% with rise in Si/Al ratio from 25 to 400. Among the three ratios applied, a Si/Al ratio of 25 seems to be optimum for obtaining higher conversion of benzene (26.3%) and higher yield of phenol (16.4%) under the conditions applied.

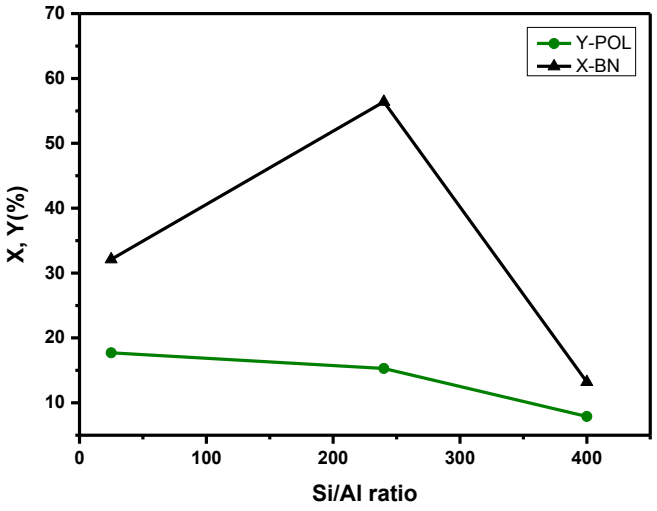

Figure 5.7. Influence of Si/Al ratio of ZSM-5 on X, Y over 0.25V-0.25Ti/ZSM-5 catalyst (Reaction conditions: catalyst weight = 2 g; T = 410 °C; mole ratio of BN: N_2O: N_2 = 1: 1.5: 82.3; benzene: 5 mmol/h; τ = 1.4 s)

5.4.1.3 Effect of reaction temperature on the catalytic performance of V-Ti/ZSM-5

Influence of reaction temperature on the conversion of benzene and the yield of phenol is portrayed in Figure 5.8. The reaction was carried out in the temperature range from 320 to 440 °C under the reaction conditions described in the figure caption. It is apparent from the figure that both the conversion of benzene and yield of phenol increased up to a reaction temperature of 410 °C and then decreased with further increase in temperature. The conversion is increased initially from 4.1 to 26.3% (at 410 °C) and then decreased to 24.2% (at 440 °C). On the whole, a reaction temperature of 410 °C seems to be optimum and hence all the catalytic tests were carried at this particular reaction temperature. Normally, one expects an increase in the conversion with rise in temperature, but surprisingly the opposite trend is observed here. The more probable reason for such decrease in conversion with increase in temperature could be due to the possible deactivation.

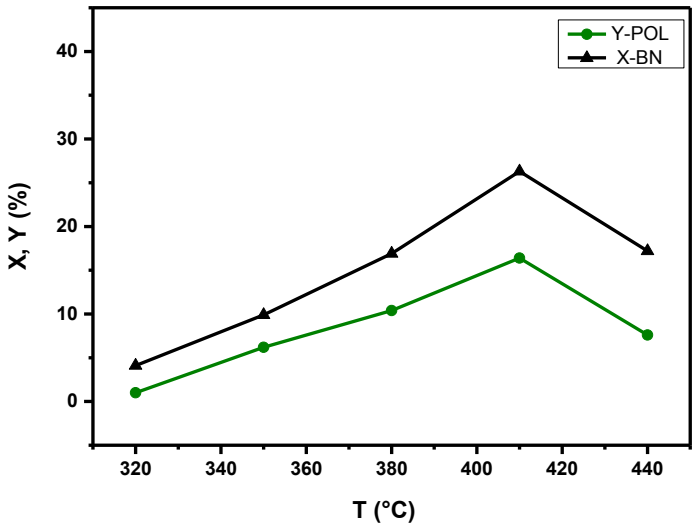

Figure 5.8. Impact of reaction temperature on the X, Y over 0.25V-0.25Ti/ZSM-5 catalyst (Reaction conditions: catalyst weight = 2 g; mole ratio of BN: N_2O: N_2 = 1: 1.5: 82.3; benzene: 5 mmol/h; τ = 1.4 s)

5.4.1.4 Effect of GHSV on the catalytic performance of V-Ti/ZSM-5 catalyst

The effect of Gas Hourly Space Velocity (GHSV) on the catalytic performance of V-Ti/ZSM-5 catalyst was also explored. The results are presented in Figure 5.9.

As expected, the conversion of benzene was observed to decrease from 26.3 to 13.8% with increase in space velocity from 2612 to 10667 h^{-1}. This is simply due to decreased contact time from 0.7 to 1.4 sec. In a similar way, the yield of phenol was also found to decrease from 16.4 to 8.5%. Of all the three space velocities investigated, a GHSV of 2612 h^{-1} was found to be optimum in terms of enhanced yield of phenol.

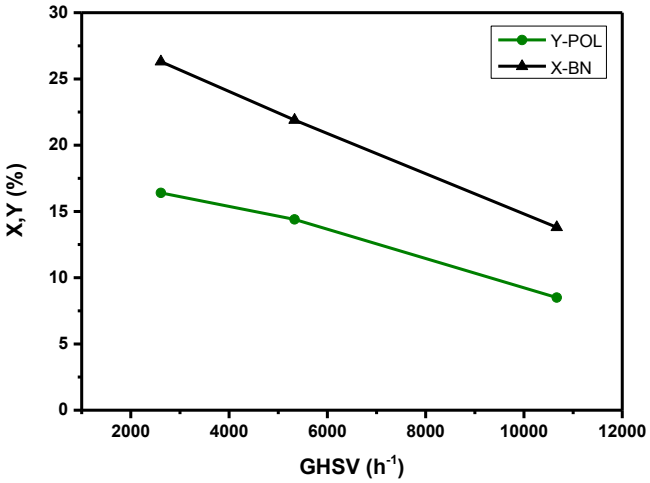

Figure 5.9. Effect of GHSV on the catalytic performance of V-Ti/ZSM-5 catalyst
(Reaction conditions: catalyst weight = 2 g; T = 410 °C; mole ratio of BN: N_2O: N_2 = 1: 1.5: 82.3; benzene: 5 mmol/h; τ = 0.7 to 1.4 s)

5.4.1.5 Effect of benzene feed rate on the catalytic performance V-Ti/ZSM-5 catalyst

Effect of benzene feed rate on the conversion of benzene and the yield of phenol is presented in Figure 5.10.

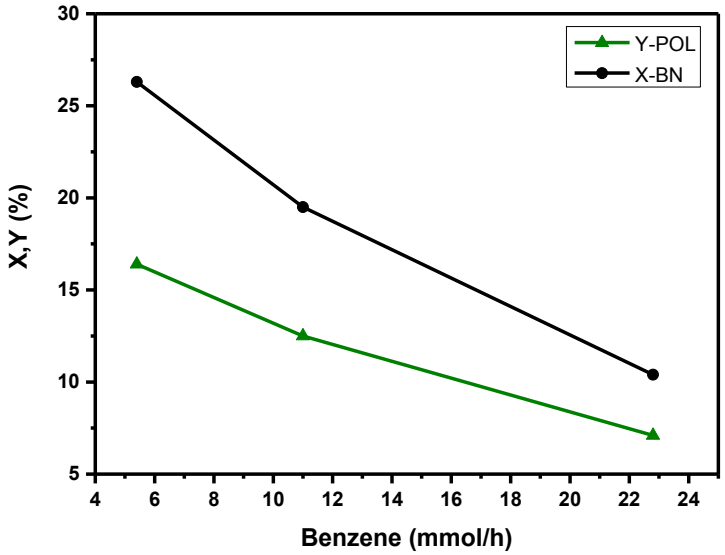

Figure 5.10. Effect of benzene feed rate on the conversion of benzene and yield of phenol over 0.25V-0.25Ti/ZSM-5 catalyst
(Reaction conditions: catalyst weight = 2 g; T = 410 °C; mole ratio of BN: N_2O: N_2 = 1: 1.5: 82.3; benzene: 5 to 23 mmol/h; τ = 1.4 s)

Increase in benzene concentration in the reactant feed mixture caused a decrease in the conversion of benzene. The conversion is decreased from 26.3% to 10.4% with rise in its feed rate from 5 to 23 mmol/h. Usually, an increase in the concentration of benzene feed rate causes a decrease in the conversion of benzene due to its increased partial pressure of benzene, and decreased the adsorption of nitrous oxide. As a result, the conversion of benzene is expected to decrease to a considerable extent. Consequently, the yield of phenol decreased from 16.4% to 7.1% with increased benzene feed rate from 5 to 23 mmol/h.

5.4.1.6 Effect of N_2O molar portion on the catalytic activity of V-Ti/ZSM-5 catalyst

The effect of benzene/nitrous oxide mole ratio on the catalytic performance of V-Ti/ZSM-5 catalyst was described in Figure 5.11. The conversion of benzene is increased from about 15.0% to 28.1% with rise in the concentration of N_2O in the reactant feed mixture. However, the yield of phenol is enhanced only up to a benzene/N_2O mole ratio of 1: 1.5 beyond which the conversion of benzene is observed to decrease. Based on this result, benzene/N_2O mole ratio of 1: 1.5 appears to be optimum for hydroxylation of benzene to phenol.

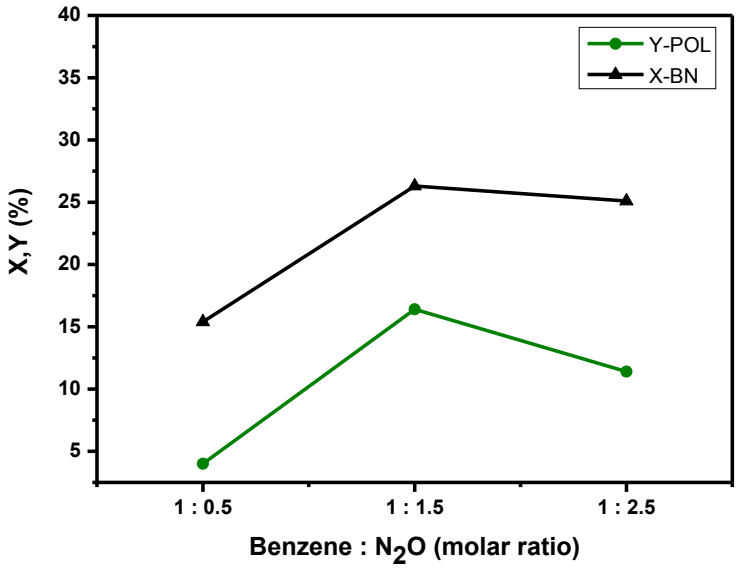

Figure 5.11. Effect of benzene N_2O on the conversion of benzene and yield of phenol over 0.25V-0.25Ti/ZSM-5 catalyst
(Reaction conditions: catalyst weight = 2 g; T = 410 °C; mole ratio of BN: N_2O: N_2 = 1: 0.5-2.5: 82.3; benzene: 5 mmol/h)

5.5 Conclusions

Results revealed that the calcination temperature, contents of metallic components (V and Ti) of V-Ti/ZSM-5 catalyst has shown clear influence on the catalytic performance. A calcination temperature of 500 °C is found to be optimum in obtaining improved catalytic properties and leads to formation of metal species complexes. On the other hand, high temperature at 700 °C leads to diminution in Brønsted acidity. Parent ZSM-5 matrix of Si/Al ratio of 25 modified with Vanadium and Titanium is highly active and comparatively stable catalyst for hydroxylation benzene to phenol. The optimum contents of V and Ti are observed to be 0.25 wt% each. No crystalline XRD reflections corresponding to both VO_x and TiO_x species could be observed in the bimetallic V-Ti/ZSM-5 catalyst. This fact suggests that the metallic components incorporated into ZSM-5 matrix appear to be X-ray amorphous. Increasing concentration of these metals or strength of acidic sites in V-Ti modified ZSM-5 considerably affects the catalytic activity and also the selectivity. TEM results of this catalyst showed no clearly distinguishable morphology for the metal particles incorporated, which is more likely due to low contents of metals doped. On the whole, 26.3% conversion of benzene with 16.4% yield of phenol could be successfully achieved over V-Ti/ZSM-5 catalyst. Even though the results achieved so far from the catalytic tests were excellent, they provided many useful hints on identifying the crucial parameters and also to monitor the useful reaction variables for enhancing the yield of phenol. Coking of catalyst seems to be an important problem of this reaction, which still needs to be investigated further.

Chapter 6
Effect of support nature on the performance of bimetallic V-Ti/zeolite catalyst

This chapter deals with the catalytic results related to the effect of zeolite support. Various zeolite supports used for this study are ZSM-5, Ga-ZSM-5, USY, BEA and Mordenite. These catalytic tests were performed using the potential catalyst composition (V-Ti) identified so far. Additionally, optimization of reaction conditions using V-Ti/Ga-ZSM-5 catalyst was also carried out. Among all, Ga-ZSM-5 was found to be the best in support and hence V-Ti/Ga-ZSM-5 was the best catalyst terms of benzene conversion and phenol yield. Moreover, the results of catalyst characterization methods such as TGA, ICP, BET, XRD, TPD-NH_3, TPR and SEM are discussed.

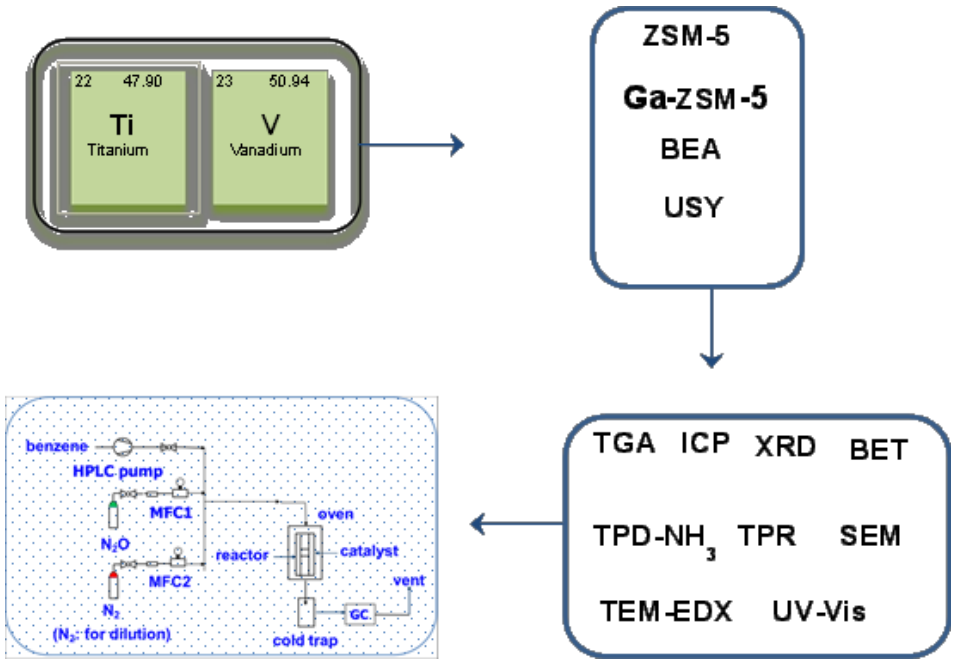

6. Effect of support nature on the performance of bimetallic V-Ti/zeolite catalysts

6.1 Studies on different parent supported bimetallic catalysts

This chapter focuses on the application of different zeolite supports such as ZSM-5, Ga-ZSM-5, USY and BEA for one step benzene conversion to phenol using nitrous oxide as an oxidizing agent. Suitable precursors of vanadium and titanium were incorporated into the zeolite framework by impregnation method and then these catalysts were calcined at 500 °C in air. The best catalyst with improved yield of phenol was found to be V-Ti/Ga-ZSM-5 solid. All Catalysts were characterized by TGA, ICP, XRD, N_2 adsorption, TPR, TPD and SEM techniques. Furthermore, the influence of reaction variables such as i) the effect of calcination temperature, ii) comparison of coke deposits in the spent bimetallic V-Ti catalysts on various supports, iii) the effect of GHSV were investigated.

6.2 Catalyst preparation

The catalysts were prepared according to the procedure given below. The commercial ZSM-5, Ga-ZSM-5, USY, BEA and Mordenite powders were used as supports for preparing the present V-Ti bimetallic catalysts. In a typical procedure, requisite quantity of suitable metal precursor was dissolved in distilled water. Then the aqueous solutions of metal precursors were impregnated on to (ZSM-5, Ga-ZSM-5, USY and BEA powder) and stirred for 30 min at ambient conditions. Later on, the excess solvent was evaporated on a hotplate to dryness. Afterwards, the solid thus obtained was further dried at 110 °C for 12 h in an oven. Finally, the samples were calcined in air at 500 °C (at a heating rate of 2 K/min) for 6 h. The content of metals impregnated was kept constant (i.e. 0.25 wt% V and 0.25 wt% Ti). Catalyst composition, type of metal precursors and calcination conditions are given in Table 6.1.

Table 6.1. Metal precursor sources and calcination conditions of zeolite

No.	Catalyst*	Metal precursors	Calcination (°C/h/air)
1	V-Ti/ZSM-5	VCl_3; $(NH_4)_2TiO(C_2O_4)_2 \bullet H_2O$	500/6
2	V-Ti/Ga-ZSM-5	VCl_3; $(NH_4)_2TiO(C_2O_4)_2 \bullet H_2O$	500/6
3	V-Ti/BEA	VCl_3; $(NH_4)_2TiO(C_2O_4)_2 \bullet H_2O$	500/6
4	V-Ti/USY	VCl_3; $(NH_4)_2TiO(C_2O_4)_2 \bullet H_2O$	500/6
5	V-Ti/Mordenite	VCl_3; $(NH_4)_2TiO(C_2O_4)_2 \bullet H_2O$	500/6

* V and Ti contents are 0.25 wt% V and 0.25 wt% Ti

6.3 Characterization of zeolite supported V-Ti catalysts

6.3.1 Thermogravimetric analysis

Thermogravimetric analysis and Derivative Thermo Gravimetry (DTG) were carried out on bimetallic V-Ti catalysts supported on various zeolites and the results are given in Figure 6.1.

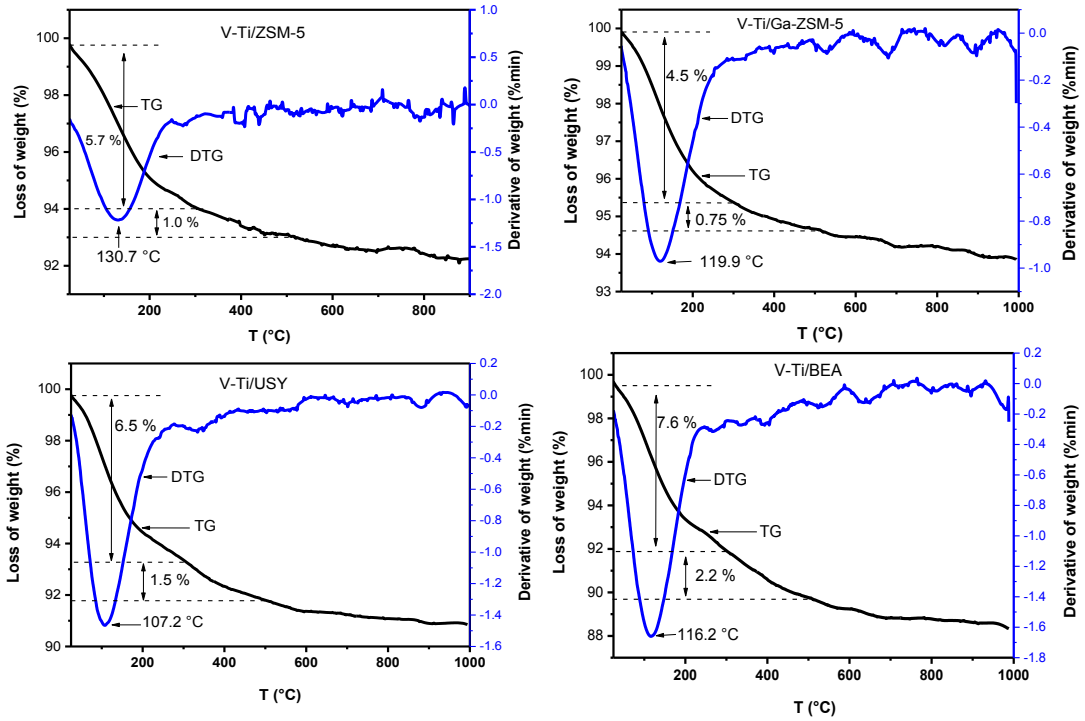

Figure 6.1. TG-DTG curves of bimetallic V-Ti catalysts on various supports

It is evident from the figure that the weight loss in all these samples occurs in two stages. The first weight loss is commonly occurring below 300 °C, which is due to removal of adsorbed water, dehydroxylation of surface, and also partly due to decomposition of metal precursors. The second weight loss is occurring to a smaller extent due to transformation of metal precursor into active metal oxide phase. Such low weight loss is more likely due to low amounts of metals (i.e. 0.25 wt% each) doped into zeolite framework. The second stage weight loss gradually continued until 500 °C which is illustrated in the figure. Interestingly the weight loss occurred beyond 500 °C is almost negligible. It appears that the nature and concentration of active metal loading plays a role on weight loss as a function of temperature [147-148]. The second weight loss recorded for V-Ti/USY sample is ca. 7% while V-Ti/BEA sample is somewhat higher (ca. 8%) than the other two solids such as V-Ti/ZSM-5 and V-

Ti/Ga-ZSM-5 (5.7, 4.5% weight loss), respectively. On the whole, the weight loss observed in all the samples is varied in the range from 4 to 8%. Based on the TG analysis results, a calcination temperature of 500 °C in air was fixed for the present catalyst samples. V-Ti/ZSM-5 has the highest temperature compared to the other catalysts. As expected, V-Ti-USY has lower acidity than other catalyst.

6.3.2 BET-surface areas and pore volumes

The surface areas and pore volumes of supported V-Ti catalysts are shown in Table 6.2. It is evident that the surface areas are found to depend strongly on the nature of support used. On the whole, these values are varied in the range from 363 to ca. 748 m^2/g. The pore volumes are also observed to depend on the type of support applied. Depending upon the type of catalyst, the total pore volumes are changed from 0.360 to 0.855 cm^3/g, respectively. Among them, V-Ti/USY showed relatively higher surface area and also higher micropore volume. Surface areas, micropore volumes, metal contents and total pore volumes of supported V-Ti catalysts were compiled in Table 6.2.

Table 6.2. Surface area, micropore volume, metal contents and total pore volumes of supported V-Ti catalysts

Sample	V-Ti content* (wt%) ICP	S_{BET} (m^2/g)	Micropore volume(cm^3/g)	Total pore volume (cm^3/g)
V-Ti/ZSM-5	0.21-0.27	379.9	0.127	0.431
V-Ti/Ga-ZSM-5	0.26-0.25	363.2	0.128	0.360
V-Ti/Beta	0.40-0.30	567.3	0.182	0.855
V-Ti/USY	0.25-0.37	747.7	0.290	0.460

*Nominal contents of V and Ti are 0.25wt% each

6.3.3 X-ray diffraction

Figure.6.2 demonstrates that all the samples are crystalline in nature. However, all the crystalline reflections observed belong fundamentally to their parent supports. As mentioned above in Table 6.2, the content of metal doped is very low in concentration, and hence most likely small crystallites might be formed. As a result, no XRD reflections corresponding to either VOx or TiOx species could be seen in any of the samples (Figure 6.2). This is again due to the fact that the actual metal contents (V, Ti) impregnated onto the supports are

considerably low (i.e. 0.25 wt% each). Therefore it is more likely that these V or Ti components are present in the catalysts in X-ray amorphous form and hence they are below the detection limit of XRD technique. In our catalysts, crystallite is more likely less than the 5 nm, which is the detection limit of powder XRD technique. However, ICP analysis clearly supports the presence of these metallic components within the expected range.

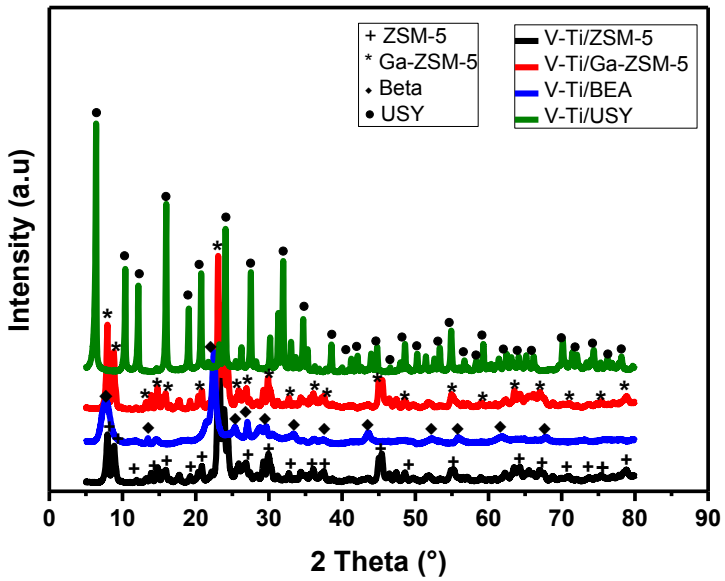

Figure 6.2. XRD patterns of bimetallic V-Ti catalysts on various supports

6.3.4 TPR profiles of bimetallic V-Ti catalysts on various supports

The TPR profiles of the present supported V-Ti catalysts are illustrated in Figure. 6.3. The nature of support (e.g. ZSM-5, Ga-ZSM-5, USY, and BEA) has shown strong influence on the reducible properties of the catalysts. It is expected that the reducibility of the catalyst is one of the essential factors that can strongly affect the catalytic performance. It can be seen from reduction profiles (Figure 6.3) that all catalysts exhibit only one reduction peak but with varying intensity. At the same time, reduction temperature of the peak is found to depend upon the nature of support applied. Such peak reduction temperature varied in the range from 503 to 531 °C. Among all, V-Ti/Ga-ZSM-5 catalyst revealed peak maxima at relatively lower temperature (ie. 503 °C) with high intensity of such reduction peak compared to others.This peak can be attributed to the reduction of V^{+5} to V^{+4} [149-150]. In view of this, enhanced performance is expected from this solid. Catalytic results also proved this assumption. The reduction peaks appeared in all these catalysts in the temperature range of

503 to 531 °C is more probably due to reduction of V^{+5} to V^{+4}. Among the four, the V-Ti/Beta exhibits the reduction peak at higher temperature while the V-Ti/Ga-ZSM-5 at low temperature. In other words, the VOx species are easily reducible on V-Ti/Ga-ZSM-5 sample compared to others. Table 6.3 compares the H_2 uptakes obtained from TPR analysis of these four catalysts.

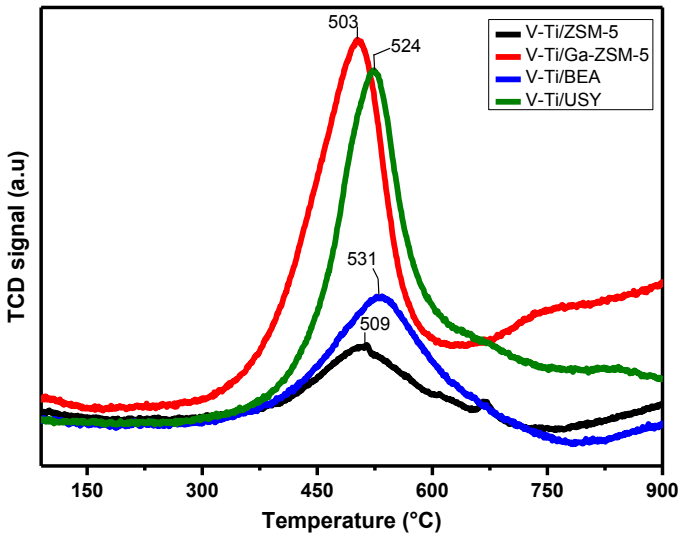

Figure 6.3. H_2-TPR profiles of bimetallic V-Ti catalysts on various supports

Table 6.3 H_2-uptakes (TPR) of V-Ti catalysts supported on various zeolites

No.	catalyst	H_2 uptake (μmol/g)
1	V-Ti/ZSM-5	39.6
2	V-Ti/Ga-ZSM-5	165.0
3	V-Ti/BEA	46.8
4	V-Ti/USY	161.2

6.3.5 Temperature programmed desorption of ammonia

Temperature Programmed Desorption (TPD) studies using ammonia as a probe molecule is used to estimate the total acidity of the present catalysts. The ammonia (NH_3) gas is utilized as probe molecule [151-152]. The TPD profiles of supported V-Ti bimetallic catalysts are

shown in Figure 6.4. It is evident that all the catalysts contain acidic sites in different proportions and with varying strengths. Mainly these solids possess weak (~ 200 °C) and strong (310-450 °C) acidic sites. Among them, V-Ti/ZSM-5 and V-Ti/Beta showed intense desorption peaks in the temperature range of 204 to 209 °C indicating high concentration of weak acidic sites. Overall both these catalysts revealed relatively high acidity. V-Ti/USY showed the lowest acidity compared to others. The acidic characteristics of V-Ti/Ga-ZSM-5 are in the middle and possess both the weak and strong acidic sites more or less in equal proportion. Probably this might be another reason for its enhanced catalytic performance compared to other catalysts of this series. The NH_3 uptakes of these samples are compiled in Table 6.4 and these values are found to depend on the type of support used. On the whole, the NH_3 uptakes are varied in the range from 415 to 940 (µmol/g).

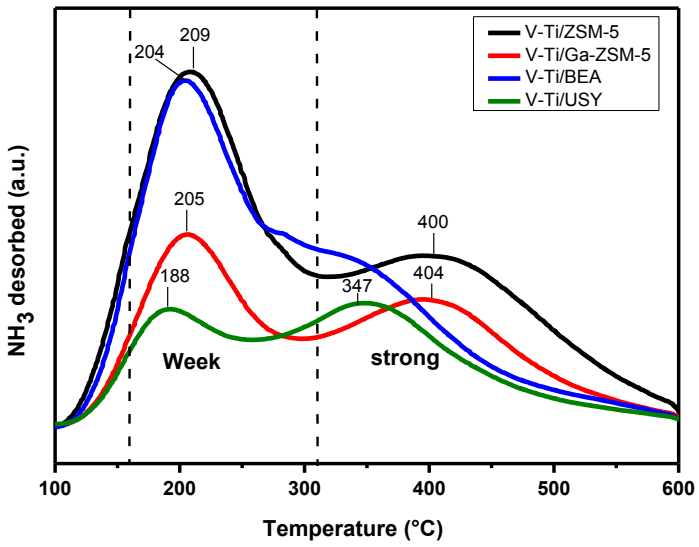

Figure 6.4. TPD-NH_3 profiles of bimetallic V-Ti catalysts on various supports

Table 6.4. Amount of NH_3 desorbed (µmol/g) of supported V-Ti catalysts

No.	catalyst	Amount of NH_3 desorbed (µmol/g)
1	V-Ti/ZSM-5	940.0
2	V-Ti/Ga-ZSM-5	524.8
3	V-Ti/BEA	778.5
4	V-Ti/USY	415.5

6.3.6 Scanning electron microscopy

The surface morphological analysis of as-prepared catalysts was carried out using scanning electron microscope (SEM). SEM images of V-Ti based catalyst supported on ZSM-5, Ga-ZSM-5, BEA and USY with the same enlargement are shown in Figure 6.5. The micrographs revealed morphology, cube-like crystals and conglomerate particles. Indeed the particle size distribution of active metals in all catalysts is not uniform shape. It can be seen from Figure 6.5 that V-Ti/ZSM-5 catalyst showed agglomerated particles as compared to homogeneous disintegrated small particles and unsmooth surface as in case of V-Ti/Ga-ZSM-5 catalyst. On the contrary, the ensembles of small particles joined together for V-Ti/Beta catalyst while V-Ti/USY sample exhibited homogeneous catalyst particles with zeolite crystals densely packed with each other. Moreover, USY supported V-Ti based catalyst comprised large catalyst particles ranging from nano to micro scale. V-Ti/USY catalyst is more obvious, smooth surface, and distinct rather than others.

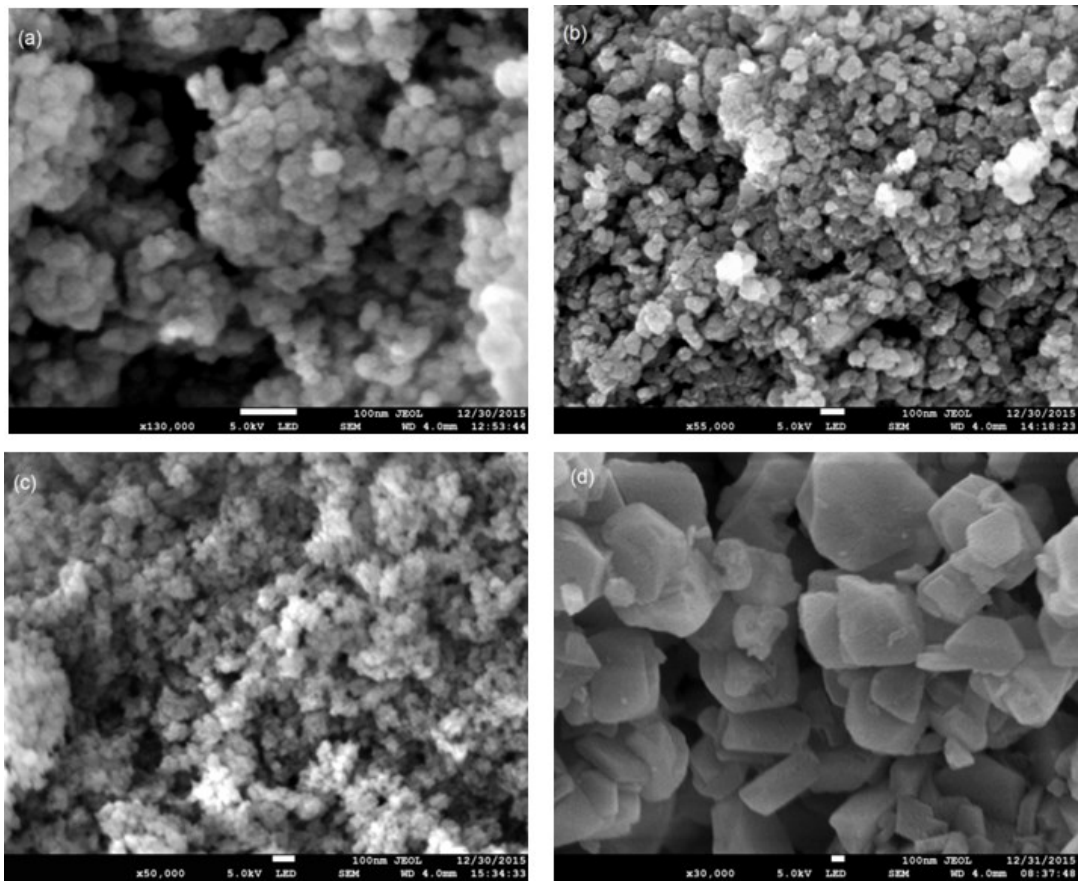

Figure 6.5. SEM images (a) V-Ti\ZSM-5 (b) V-Ti\Ga-ZSM-5 (C) V-Ti\BEA (d) V-Ti\USY

6.4. Catalytic results

6.4.1 Optimization of reaction conditions for direct conversion of benzene to phenol

6.4.1.1 Effect of support on the catalytic performance of bimetallic V-Ti catalysts

Even though considerably high yield of phenol close to 17% was achieved over V-Ti/ZSM-5 catalyst, there might be still an ample scope for further improvement in the yield of phenol. With such objective of finding potential catalyst composition, the effect of support in subsequent runs was explored. For this purpose, five different supports were selected. Figure 6.6 demonstrates that the nature of support has clear influence on the catalytic performance. Despite similar contents of V and Ti, the catalysts revealed remarkable differences in their activity and selectivity behavior. Among five different supports applied, Ga-ZSM-5 supported catalyst has shown the best performance giving 33.6% conversion of benzene with a 27.2% yield of phenol. This accounts to a phenol selectivity of ca. 81%. To our knowledge, this is the best yield reported so far. The second best catalyst of the series is V-Ti/ZSM-5, which gave a benzene conversion of 26.3% and a phenol yield of ~17%. Among all, Mordenite supported catalyst is found to be almost inactive (X-BN < 1%). The order of catalytic performance of these five supported samples is given below: V-Ti/Ga-ZSM-5 > V-Ti/ZSM-5 > V-Ti/Beta > V-Ti/USY >

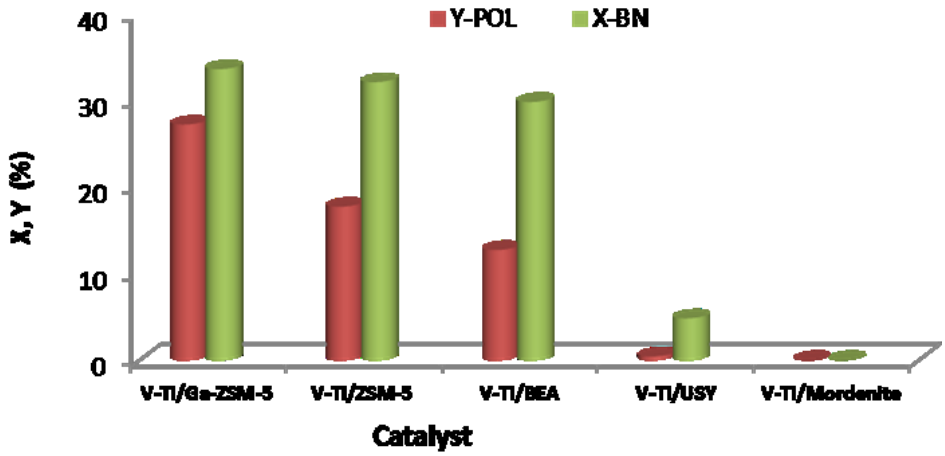

Figure 6.6. Influence of support on the catalytic properties of V-Ti catalysts

(Reaction conditions: catalyst weight = 2 g; T = 410 °C; mole ratio of BN: N_2O: N_2 = 1: 0.5-2.5: 82.3; total flow: 12.8 l/h; τ = 1.4 s; benzene: 5 mmol/h)

6.4.1.2 Effect of reaction temperature on the catalytic performance of V-Ti/Ga-ZSM-5

Marked influence of reaction temperature on the conversion of benzene and the yield of phenol is portrayed in Figure. 6.7. The reaction was carried out in the temperature range from 380 to 460 °C under the reaction conditions described in the figure caption. It is apparent from the figure that both the conversion of benzene and yield of phenol increased up to a reaction temperature of 410 °C and then decreased with further increase in temperature. The conversion is increased initially from 16.4 to 33.6% (at 410 °C) and then decreased to 27.1% (at 460 °C). On the whole, a reaction temperature of 410 °C seems to be optimum and hence all the catalytic tests were carried at this particular reaction temperature. Normally, one expects an increase in the conversion with rise in temperature, but surprisingly the opposite trend is observed here. The more probable reason for such decrease in conversion with temperature could be the possible deactivation. It is also known that high reaction temperature promotes deactivation process. The analysis of carbon deposits (by C H N S) in the spent catalysts also supports this view such results are discussed below in a separate section.

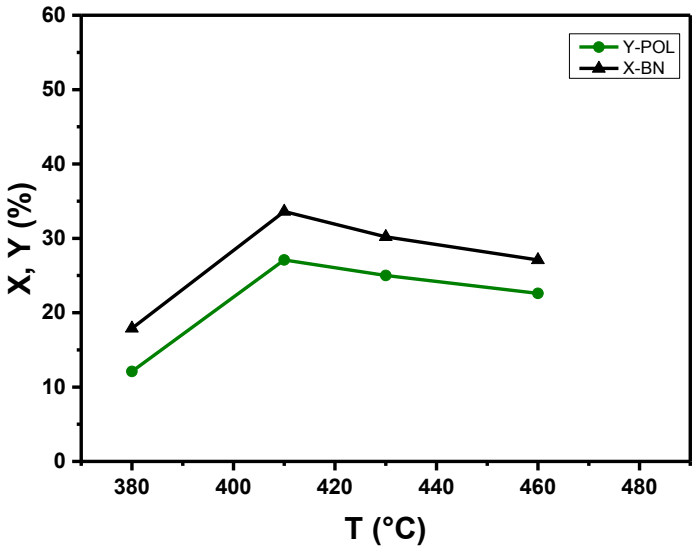

Figure 6.7. Impact of reaction temperature on the X, Y over V-Ti/Ga-ZSM-5 catalyst

(Reaction conditions: catalyst weight = 2 g; T = 380-460 °C; mole ratio of BN: N_2O: N_2 = 1: 1.5: 82.3; total flow: 12.8 l/h; τ = 1.4 s; benzene: 5 mmol/h)

6.4.1.3 Effect of GHSV on the catalytic performance of V-Ti/Ga-ZSM-5

The effect of Gas Hourly Space Velocity (GHSV) on the catalytic performance of V-Ti/Ga-ZSM-5 catalyst was also explored. The results on the influence of GHSV are presented in Figure. 6.8. As expected, the conversion of benzene was observed to decrease from 33.6 to 27.2% with increase in space velocity from 2667 to 5333 h^{-1}. This is simply due to decreased contact time from 0.7 to 1.4 sec. In a similar way, the yield of phenol was also found to decrease from 14.4 to 27.2%. Of all the three space velocities investigated, a GHSV of 2667 h^{-1} was found to be optimum in terms of enhanced yield of phenol.

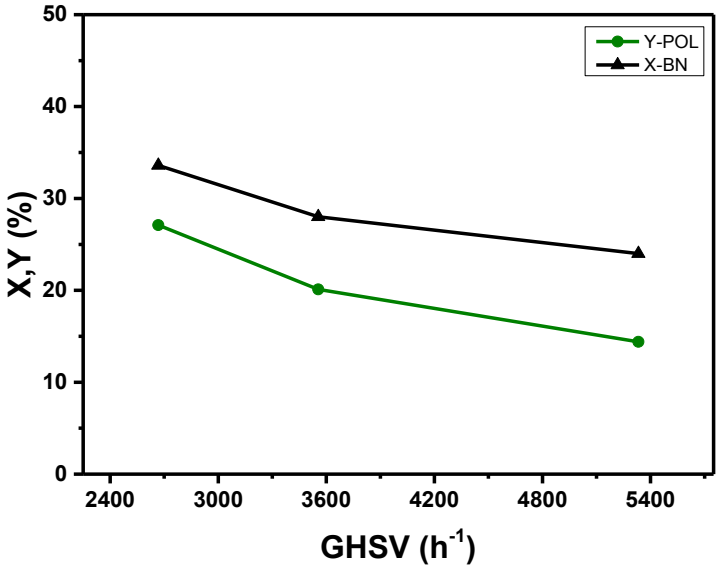

Figure 6.8. Effect of GHSV on the catalytic performance of V-Ti/Ga-ZSM-5 catalyst
(Reaction conditions: catalyst weight = 2 g; T = 410 °C; mole ratio of BN: N_2O: N_2 = 1: 1.5: 82.3; total flow: 12.8 l/h; τ = 0.7 to 1.4 s; benzene: 5 mmol/h)

6.4.1.4 Comparison of coke deposits in the spent V-Ti/S catalysts (S= support)

CHNS technique determines the elements such as carbon, hydrogen, nitrogen and sulphur. It is important to know the percentage of carbon in the spent catalysts. The amount of coke

deposits in the spent catalysts received after 4 hours of catalytic tests is compared in Figure. 6.9. For this study, the best V-Ti composition on different supports is selected. Mordenite support was not included here due to its inactive nature or poor performance compared to others. It can be seen that certain amount of coke deposition occurs in almost all catalysts. However, V-Ti/Beta catalyst has shown the highest carbon deposits (C = 13%) within 4 hours-on-stream studies while V-Ti/ZSM-5 and V-Ti/Ga-ZSM-5 samples have the lowest coke (ca. 7%) for the same period of catalytic testing. This fact suggests that the nature of support also plays a key role on the amount of carbon deposition during the course of the reaction. The results revealed that V-Ti/BEA catalyst revealed highest coke formation compared to other catalysts which demonstrated by changes in the zeolite pore volume or in the diffusivity of the reactants and hence coke formation over the catalysts exterior surfaces play a key role in reaction deactivation [153]. The fundamental reason of deactivation for acid zeolite catalyst is coke deposition which blocks the porous network and hence leads to reduced activity of catalysts.

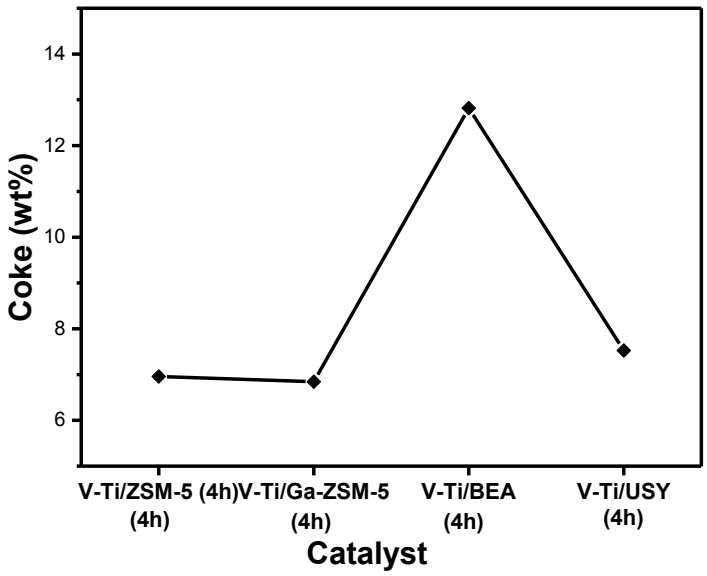

Figure 6.9. Comparison of amount of coke deposits in the spent V-Ti/S catalysts (S = support) (after 4 hours of catalytic tests)

6.5 Conclusions

Results revealed that the nature of support, redox properties as well acidity characteristics have shown strong influence on the catalytic performance of V-Ti bimetallic catalysts. It was

also observed that the nature of support also plays a key role even on the carbon deposition. Among the five different supports scrutinized, Ga-ZSM-5 has given the best performance with significantly high yields of phenol at acceptably high conversion of benzene. Nature of support also revealed substantial impact on the reducible properties and acidity characteristics. On the whole, 33.6% conversion of benzene with 27.2% yield of phenol could be successfully achieved over V-Ti/Ga-ZSM-5 catalyst. This is indeed a remarkable outcome of this study. The deactivation occurs due to coke deposition which in turn leads to pore blocking and reduced conversion of benzene and decreased yield of phenol as well.

Chapter 7

Overall summary and outlook

In this chapter, an appraisal of the entire study concerning catalyst preparation, characterization methods, catalytic results and outlook are summarized. The main focus was laid on the direct conversion of benzene to phenol using zeolite supported catalysts using N_2O as an oxidant.

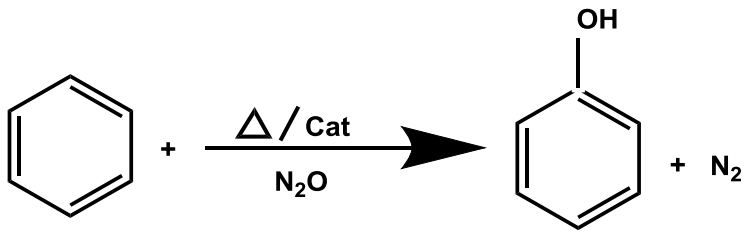

Overall summary

The goal of the present work is to provide a method for the direct synthesis of phenol from benzene by hydroxylation in a single step. In particular, this relates to a method for the manufacture of phenol in vapour phase continuous process, which comprises a reacting mixture of benzene, nitrous oxide and an inert gas (e.g. nitrogen) in presence of a solid heterogeneous catalyst. More particularly, the said reaction is carried out at a reaction temperature in the range of 300 to 450 °C using a zeolite supported transition metal containing catalyst in a fixed bed tubular reactor. A further objective of this study is to optimise the reaction conditions for improving the yield of phenol.

Calcination temperature, the resultant solid catalyst is calcined in a suitable atmosphere at a temperature in the range of 500 °C to 700 °C, a calcination temperature of 500 °C is found to be improved the physiochemical properties of V-Ti/ZSM-5 such as redox, metal oxide species and surface area and thus An increase of temperature of catalyst calcination more than 700 °C leads to decrease the phenol yield and increasing the conversion of benzene probably caused by demolition of zeolite structure. Therefore, Calcination temperature at 500 °C might enhance of efficiency and duration stability of zeolite catalyst which has a large influence on the surface area, lattice oxygen concentration and acidic of catalyst while the higher calcination temperature at 700 °C reduced the surface and hence the stability of catalyst might be low or non-existent and thus using different calcination temperature leads to improve the catalytic activity.

In the direction of developing novel catalyst compositions, it is decided to stick to metal-doped zeolite catalysts for initial catalyst screening tests. With this objective, all metals (1 wt% each) belonging to 3d series (i.e. starting from Sc to Zn) and Pd, Ru were impregnated separately onto ZSM-5 support and tested. ZSM-5 support applied is a commercial sample having a Si/Al ratio of 25. During the initial screening tests over Fe/ZSM-5 catalyst, a phenol yield of only 3% was achieved. Later on 12 different monometallic catalysts were investigated. Among the twelve different monometallic catalysts tested, vanadium doped catalyst (V/ZSM-5) was found to display the best catalytic performance followed by titanium (Ti/ZSM-5) doped one. As a result, optimization of reaction conditions was further carried out. The reaction variables such as i) effect of reaction temperature, ii) effect of benzene/N_2O mole ratio, iii) effect of benzene feed rate, iv) effect of space velocity on the conversion of benzene and yield of phenol were carried out. Additionally, a calcination temperature of 500 °C is found to be optimum to obtain improved catalytic properties. After optimizing the above

mentioned reaction conditions, a phenol yield of ~ 12% could be achieved over monometallic V/ZSM-5 catalyst. All these monometallic catalysts were characterized by various techniques such as ICP, BET-surface area, pore size distribution, XRD, NH_3-TPD, TPR and so on. Nature of metal doped has shown strong influence on the BET surface areas, reducible properties, as well as acidity characteristics. XRD analysis does not provide any hints on the presence of crystalline phases in these samples due to low concentration of metal contents (0.25 to 1.0 wt%) in these samples. All the catalyst samples were found to be X-ray amorphous. It has been observed that the reducible properties (TPR) and acidity characteristics (TPD) play a key role on the activity and selectivity properties. TPD-NH3 results of monometallic supported on ZSM-5 showed two peaks i.e., one at temperature of < 300 °C and other at temperature of > 300 °C depicting weak and strong acidic sites. In a Cr/ZSM-5 catalyst is easily reducible compared to other monometallic catalysts. TEM-EDX results of monometallic supported on ZSM-5 showed metal particles and these metal contents were confirmed through EDX. In view of the superior performance of V and Ti doped solids, it was decided to combine these two metals and further explore the beneficial effects of such combination on the yield of phenol. For this purpose, I moved from monometallic to bimetallic catalysts and then prepared six different bimetallic catalysts and tested. The catalyst compositions of bimetallic catalysts were selected purely based on their performance. Si/Al ratio of 25 modified with Vanadium and Titanium is highly active for hydroxylation benzene to phenol. TEM results of this catalyst revealed no clearly distinguishable morphology for the metal particles, which is probably due to low contents of metals doped. Of all these bimetallic compositions, V-Ti/ZSM-5 has given the superior performance. In subsequent runs, close optimization of V and Ti metal contents were further examined. For this study, three different concentrations of V and Ti such as V: Ti = 0.25: 0.25 wt%, 0.5: 0.5 wt% and 1.0: 1.0 wt% were selected. Among these three loadings, 0.25 wt%V-0.25 wt%Ti loading has given the best performance. Interestingly, phenol yield was improved from ca.12% (on the best monometallic V/ZSM-5 catalyst) to ca. 17% on the bimetallic V-Ti/ZSM-5 catalyst. Further optimization of reaction conditions led to the conclusion that a reaction temperature of 410 °C, benzene/N_2O mole ratio of 1: 1.5, a GHSV of 2612 h^{-1}, benzene feed rate of 5 mmol/h were optimum. These optimised conditions were further used in all subsequent screening tests. Up to now, we have found the right catalyst composition, and suitable reaction conditions to enhance the yield of phenol. In the last chapter, I have checked the effect of zeolite framework and for this study five different zeolites such as Ga-ZSM-5; ZSM-5, USY; BEA and Mordenite were selected using the best V-Ti composition.

TPR as well TPD characteristics have shown strong influence on the catalytic performance. Among them, Ga-ZSM-5 as a support improved the yield of phenol significantly while the Mordenite has given the worst catalytic performance. A conversion of 33.6% and a benzene yield of 27.2% were successfully achieved over 0.25V-0.25Ti/Ga-ZSM-5 catalyst. On the whole, the yield of phenol was improved from ca. 3% during the initial tests over Fe/ZSM-5 catalysts to an astonishing value of 27.2% over V-Ti/Ga-ZSM-5 catalyst. This is indeed a remarkable outcome of this study. High reaction temperatures more than 440 °C lead to deactivation catalyst. Deactivation of catalyst seems to be an important problem of this reaction due to coke deposition during the course of reaction and thus, the changes in the zeolite structure or formation on the surface such as carbonaceous deposit which cause for catalyst deactivation and some other factors such as diminution in quality of the active sites inside the zeolite catalysts, diminution of availability of pore space and diminution in the number of active sites which leads to catalytic activity. The advantages form direct conversion benzene to phenol is essentially no explosive intermediates, one direct conversion process and acetone is not observe in this reaction. The drawbacks from this reaction are follows as conversion is low, lifespan of zeolite catalyst is short and nitrous oxide is high cost.

Outlook

The results in the present work revealed the best catalytic performance in reaction benzene to phenol. Future work may be extended to investigate the influence of various other zeolite frameworks such as SSZ-13, LTA, FAU, and ZSM-10 under suitable reaction conditions. Additionally, the other support materials could be helpful to enhance the hydrothermal stability and catalytic performance. Future steps focusing on varying catalyst preparation methods, for instance sol-gel method and close optimization of concentration of transition metals, calcination atmosphere might also be useful. Further catalyst compositions consist of palladium Titanium silicate zeolite and even the application of membrane reactors could improve both the conversion of benzene and the yield of phenol. This approach particularly usage of membrane reactors may improve not only the activity/selectivity properties but also the long-term stability of the catalysts. There are various operating conditions which should be studied before starting the reaction as follows: Pressure, composition and feed flow rate and some optimization reaction. Moreover, this reaction is sentient to the porosity of catalyst and titanium atom. On the other hand, it might study the structure of catalyst such as framework, extra framework and pore sizes which attribute to the knowledge of the nature of

catalyst. In the contrast, the disadvantage of this catalyst is the diffusion of the reactants through catalyst which could be slow due to titanium silica zeolite has small pore size. There are two factors influence on this reaction effectiveness such as the porosity of the titanium silicate and membrane configuration. One of three different reactor configurations might be studied in direct conversion benzene to phenol i) membrane reactor in batch configuration (benzene as stripping stream) ii) membrane reactor in semi-batch configuration (water as stripping volume) iii) membrane reactor in continuous configuration. We seek to develop and enhance the reaction through increasing the phenol production. Our ongoing efforts are finding method for development of highly active such as increasing conversion, yield, enhance long term stability of catalyst and attempts to understand the cause of deactivation.

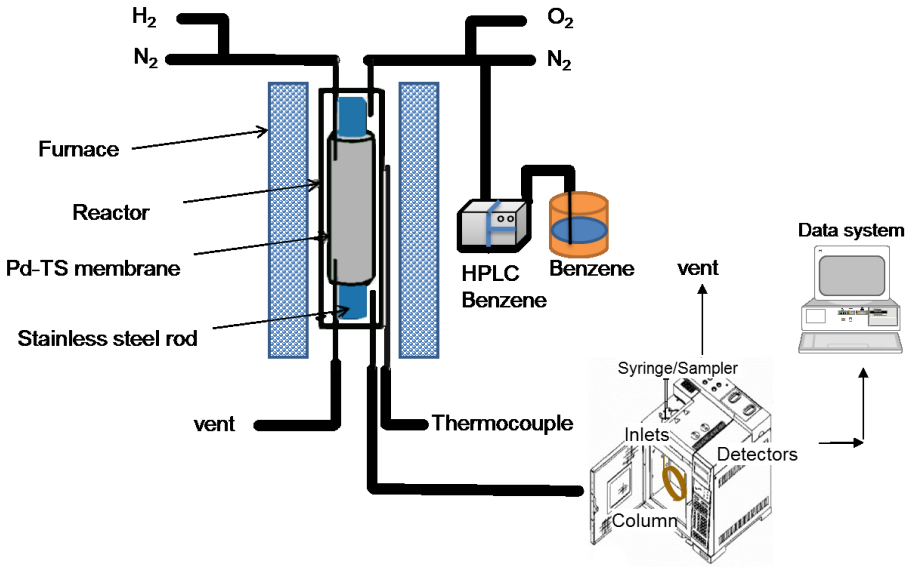

Figure 7.1. Direct hydroxylation of benzene to phenol using membrane reactor

8. References

[1] T. Dong, Z. Wang, T. Kan, Q. Li. Chin, J. Chem. Phys. 20 (2007) 297-304.

[2] R. Bal, S.A. Shankha, B. Sarkar, K. Singh Rawat, C. Pendem, US Patent, 2013/0096351 A1.

[3] C.A. Antonyraj, K. Srinivasan, Catal. Surv. Asia 17 (2013) 47-70.

[4] A. Tabler, A. Häusser, E. Roduner, J. of Mol. Catal A: Chem. 379 (2013) 139-145.

[5] R. Schmidt, Appl. Catal. A: Gen. 280 (2005) 89-103.

[6] P.R. Makgwane, Suprakas, S. Ray J. Mol. Catal. A: Chem. 398 (2015) 149-157.

[7] V.I. Sobolev, G.I. Panov, A.S. Kharitonov, V.N. Romannikov, A.M. Volodin, K.G. Ione, Kinet. Katal. 139 (1993) 435.

[8] G.A. Sheveleva, A.S. Kharitonov, G.I. Panov, V.I. Sobolev, N.L. Razdobarova, E.A. Paukshits, V.N. Romannikov, Neftekhimiya 33 (1993) 530.

[9] Krishnan S. Pillai, Jifei Jia, Wolfgang, M.H. Sachtler. Appl Catal A: Gen. 264 (2004) 133-139.

[10] G. I. Panov, *CATTECH* 4, 18 (2000).

[11] Z. Hua, Li. Feng, P. Ping, F. Shou, Chinese. J. Chem. 24 (2006) 1653-1656.

[12] P. Khatri, B. Singh, S. Jain, B. Saina, A. Sinha, Chem. Commun. 47 (2011) 1610-1612.

[13] T. Zhang, C. Gao, H. Yang, Y. Zhao, J Porous Mater. 17 (2010) 643-649.

[14] G. Shul'pin, D. Muratov, L. Shul'pina, A. Kudinov, T. Strelkova, P. Petrovskiy, Appl. Organometal. Chem. 22 (2008) 684-688.

[15] J. Chen, S. Gao, J. Xu, Catal. Commun. 9 (2008) 728-733.

[16] J. Pang, F. Shi, Y. Gu, Y. Deng, Green. Chem. 5 (2003) 224-226.

[17] Y. zhnog, G. Li, L. Zhu, Y. Yan, G. Wu, C. Hu, J. Mol. Catal. A: Chem. 272 (2007) 169-173.

[18] S. Song, H. Yang, R. Rao, H. Liu, A. Zhang, Appl. Catal. A: Gen. 375 (2010) 265-271.

[19] X. Qi, J. Li, T. Ji, Y. Wang, L. Feng, Y. Zhu, X. Fan, C. Zhang, Microporous and Mesoporous Mater. 122 (2009) 36-41.

[20] I. Yamanaka, M. Katagiri, S. Takenaka, K. Otsuka, Stud. Surf. Sci. Catal. 130 (2000) 809-814.

[21] R. J. Schmidt, Appl. Catal. A: Gen., 280, 89 (2005).

[22] https://www.acs.org/content/acs/en/pressroom/cutting-edge-chemistry/what-s-new-in-phenol-production-.html

[23] M. Zhang, L.Wang, H. Ji, B.Wu, X. Zeng, J. Nat. Gas. Chem. 16 (2007) 393-398.

[24] R. Morrison, R.T Boyd, 1992, Organic Chemistry, Sixth Edition, Prentice Hall, Englewood Cliffs, New Jersery.

[25] M. Weber,M. Weber,L. Pilato (2010) Phenolic Resins: a century of progress. Springer, Berlin, Heidelberg.

[26] D. Huang, M. Han, J. Wang, Y. Jin, Chem. Eng. J. 88 (2002) 215-223.

[27] J.F. Knifton, N.J. Grice, US Patent 4,876,397 (1989).

[28] A.A Chudinova., A.A. Salishcheva, E.N. Ivashkina, O.A. Reutova, K.S. Gulyaev, A.M. Demin, A.A. Syskina. Pro Chem. 10 (2014) 284-288.

[29] A. Chudinova, A. Salischeva, E. Ivashkina, O. Moizes, A. Gavrikov, *Pro. Chem. 15 (2015) 326-334*

[30] J. Remias, T. Pavlosky, A. Sen. J. Mol. Catal. A: Chem. 203 (2003) 179-192.

[31] A. Datta, S. Sakthivel, S. Kumar, US0234542A1 (2008).

[32] K. Lemke, H. Ehrich, U. Lohse, H. Berndt, K. Jähnisch, Appl. Catal. A: Gen. 243 (2003) 41-51.

[33] W. Laufer, W. Hoelderich, Chem. Commun. (2002) 1684-1685.

[34] Y. Gu, X. Zhao, G. Zhang, H. Ding, Y. Shan, Appl. Catal. A: Gen. 328 (2007) 150-155.

[35] Z. Hua, Li. Feng, P. Ping, F. Shou, Chinese. J. Chem. 24 (2006) 1653-1656.

[36] G. Centi, S. Perathoner, Catal. Today 143 (2009) 145-150.

[37] S. Nandi, P. Mukherjee, S. Tambe, R. Kumar, B. Kulkarni, Ind. Eng. Chem. Res. 41 (2002) 2159-2169.

[38] R. Leanza, I. Mazzola, L. Forni, Appl. Catal. A: Gen. 205 (2001) 93-99.

[39] G. Centi, S. Perathoner, R. Arrigo, G. Giordano, A. Katovic, V. Pedula, Appl. Catal. A: Gen. 307 (2006) 30-41.

[40] E. Hensen, Q. Zhu, R. Janssen, J. Catal. 233 (2005) 136-146.

[41] E. Hensen, Q. Zhu, R. Janssen, P. Magusin, P. Kooyman, R. Santen, J. Catal. 233 (2005) 123-135.

[42] S. Shevade, B. Rao, Catal. Lett. 66 (2000) 99-103.

[43] J. Yoo, A. Sohail, S. Grimmer, C. Feng, Catal. Lett. 29 (1994) 299-310.

[44] X. Ke, L. Xu, C. Zeng, L. Zhang, N. Xuet, Microporous and Mesoporous Mater. 106 (2007) 68-75.

[45] X. Wang, Y. Guo, X. Zhang, Y. Wang, H. Liu, J. Wang, J. Qiu, K. Yeung, Catal. Today 156 (2010) 288-294.

[46] Y. Li, H. Xia, F. Fan, Z. Feng, R. Santen, E. Hensen, C. Li, Chem. Commun. (2008) 774-776.

[47] M. Bahidsky, M. Hronec, Catal. Today 91-92 (2004) 13-16.

[48] Y. Gu, X. Zhao, G. Zhang, H. Ding, Y. Shan, Appl. Catal. A: Gen. 328 (2007) 150-155.

[49] H. Kanzaki, T. Kitamura, R. Hamada, S. Nishiyama, S. Tsuruya, J. Mol. Catal. A: Chem. 208 (2004) 203-211.

[50] T. Miyake, M. Hamada, Y. Sasaki, M. Oguri, Appl. Catal. A: Gen. 131 (1995) 33-42.

[51] A.V. Shijina, N.K. Renuka, React. Kinet. Catal. Lett. 98 (2009) 139-147.

[52] J.K. Joseph, S. Singhal, S.L. Jain, R. Sivakumaran, B. Kumar, B. Sain, Catal. Today 141 (2009) 211-214.

[53] M. Jian, L. Zhu, J.Wang, J. Zhang, G. Li, C. Hu, J. Mol. Catal. A: Chem. 253 (2006) 1-7.

[54] S. Feng, S. Pei, B. Yue, L. Ye, L. Qian, H. He, Catal. Lett. 131 (2009) 458-462.

[55] K. Sun, H. Xia, Z. Feng, R. van Santen, E. Hensen, C. Li, J. Catal. 254 (2008) 383-396.

[56] H.S. Abbo, S.J.J. Titinchi, Appl. Catal. A: Gen. 356 (2009) 167-171.

[57] I. Yuranov, A.D. Bulushev, A. Renken, L. Kiwi-Minsker, Appl. Catal. A: Gen. 319 (2007) 128-130.

[58] G.I. Panov, G.A. Sheveleva, A.S. Kharitonov, V.N. Romannikov, L.A. Vostrikova, Appl. Catal. A Gen. 82 (1992) 31-36.

[59] - V. Parmon, G. Panov, A. Uriarte, A. Noskov, Catal. Today 100 (2005) 115-131.

[60] E. Hensen, Q. Zhu, R. Van Santen, J. Catal. 220 (2003) 260-264.

[61] A. Ribera, I.W.C.E. Arends, S. de Vries, J. Perez-Ramírez, R.A. Sheldon, J. Catal.195 (2000) 287-297.

[62] J.Choi, T.Kim, K.Choo, J.Sung, M. Saidutta, S. Ryu, S. Song, B. Ramachandra, Y. Rhee, Appl. Catal. A: Gen. 290 (2005) 1-8.

[63] J. Remias, T. Pavlosky, A. Sen. J. Mol. Catal. A: Chem. 203 (2003) 179-192.

[64] A. Datta, S. Sakthivel, S. Kumar, US0234542A1 (2008).

[65] K. Lemke, H. Ehrich, U. Lohse, H. Berndt, K. Jähnisch, Appl. Catal. A: Gen. 243 (2003) 41-51.

[66] W. Laufer, W. Hoelderich, Chem. Commun. (2002) 1684-1685.

[67] Y. Gu, X. Zhao, G. Zhang, H. Ding, Y. Shan, Appl. Catal. A: Gen. 328 (2007) 150-155.

[68] J. Luo, B. V. Bhaskar, Y. Yeh, R. J. Gorte, Appl. Catal. A: Gen. 478 (2014) 228 233

[69] G. Centi, C. Genovese, G. Giordano, A. Katovic , S. Perathoner, Catal. Today 91-92 (2004) 17-26

[70] V. Rac, V. Rakic, D. Stosic, O. Otman, A. Auroux, Microporous Mesoporous Mater. 194 (2014) 126-134.

[71] N.Y. Topsøe, K. Pedersen, E.G. Derouane, J. Catal. 70 (1981) 41-52.

[72] Z. Sobalik, J.E. Sponer, Z. Tvaruzkova, A. Vondrova, S. Kuriyavar, B. Wichterlova, Stud. Surf. Sci. Catal. 135 (2001) 1545.

[73] S. Perathoner, F. Pino, G. Centi, G. Giordano, A. Katovic, J.B. Nagy, Topics Catal. 23 (2003) 125.

[74] K. Yoshizawa, T. Yumura, Y. Shiota, T. Yamabe, Bull. Chem. Soc. Jpn. 73 (2000) 29.

[75] G. Berlier, A. Zecchina, G. Spoto, G. Ricchiardi, S. Bordiga, C. Lamberti, J. Catal. 215 (2003) 264.

[76] Z. Sobalik, P. Kubanek, O. Bortnovsky, A. Vondrova, Z. Tvaruzkova, J.E. Sponer, B. Wichterlova, Studies Surf. Sci. Catal. 142 (2002) 533.

[77] A.L. Yakovlev, G.M. Zhidomirov, R.A. van Santen, J. Phys. Chem. B 105 (2001) 12297.

[78] P. Marturano, L. Drozdova, A. Kogelbauer, R. Prins, J. Catal. 192 (2000) 236.

[79] L.V. Pirutko, V.S. Chernyavsky, A.K. Uriarte, G.I. Panov, Appl. Catal. A: Gen. 227 (2002) 143.

[80] K.A. Dubkov, E.A. Paukshtis, G.I. Panov, Kinet. Catal. 42 (2001) 205.

[81] G.I. Panov, A.K. Uriarte, M.A. Rodkin, V.I. Sobolev, Catal. Today 41 (1998) 365.

[82] E.J.M. Hensen, Q. Zhu, R.A. van Santen, J. Catal. 220 (2003) 260.

[83] Q. Zhu, R.M. van Teeffelen, R.A. van Santen, E.J.M. Hensen, J. Catal. 221 (2004) 575.

[84] D.A. Bulushev, L. Kiwi-Minsker, A. Renken, J. Catal. 222 (2004) 389.

[85] R. Hamada, Y. Shibata, S. Nishiyama, S. Tsuruya, Chem. Phys. 5 (2003) 956-965.

[86] N. Kuznetsova, L. Kuznetsova, V. Likholobov. G. P. Pez, Catal. Today 99 (2005) 193-198.

[87] Y. Liu, K. Murata, M. Inaba, J. Mol. Catal. A: Chem. 256 (2006) 247-255.

[88] L. Passoni, A. T. Cruz, R. Buffon, U. Schuchardt, J. Mol. Catal. A: Chem. 120 (1997) 117-123.

[89] C. Lee, T. Lin, C. Mou, J. Phys. Chem. C. 111 (2007) 3873-3882.

[90] D. Tzoulaki, A. Jentys, J. Perez-Ramirez, K. Egeblad, J. A. Lercher, Catal. Today 198 (2012) 3-11.

[91] D. Liu, X. Zhang, A. Bhan, M. Tsapatsis, Microporous Mesoporous Mater. 200 (2014) 287-290.

[92] M. Moreno-Recio, J. Santamaría-González, P. Maireles-Torres, Chem. Eng. J. 303 (2016) 22-30.

[93] S. M. Opalka, T. Zhu, Microporous Mesoporous Mater. 222 (2016) 256-270.

[94] D. Barthomeuf, Acidic Catalysis with Zeolites, in Zeolites: Science and Technology, Ed. F. Ribeiro, A. Rodrigues, Martinus Nijhoff Publishers, The Hague, 1984.

[95] S. Li, A. Tuel, D. Laprune, F. Meunier, D. Farrusseng, Chem. Mat. 27 (2015) 276-282.

[96] P. J. Smeets, J. S. Woertink, B. F. Sels, E. I. Solomon, R.A. Schoonheydt, inorg. chem. 49 (2010) 3573-3583.

[97] E. Suzuki, K. Nakashiro, Y. Ono,*Chem. Lett. 6 (*1988) 953-956.

[98] A. Wacław, K. Nowinska, W. Schwieger, A. Zielinska, Catal. Today 90 (2004) 21-25.

[99] E. V. Kondratenko, V. A. Kondratenko, M. Santiago, J. Perez-Ramirez, Appl. Catal. B: Environ. 99 (2010) 66-73.

[100] M.M. Dubinin, Chem. Rev. 60 (1960) 235-241.

[101] C. Wang, L. Hu, Y. Hu, Y. Ren, X. Chen, B. Yue, H. He, Catal. Commun. 68 (2015) 1-5.

[102] Z. Wan, W. Wu, G. K. Li, C. Wang, H. Yang, D. Zhang, Appl. Catal. A: Gen. 523 (2016) 312-320.

[103] M. Perez-Page, J. Makel, K. Guan, S. Zhang, J. Tringe, R. H. R. Castro, P. Stroeve, Ceram. Int. 42 (2016) 15423-15431.

[104] Y. Cheng, L. Wang, J. Li, Y. Yang, X. Sun, Mater. Lett. 59 (2005) 3427-3430.

[105] H. Liu, S. Yang, J. Hu, F. Shang, Z. Li, C. Xu, J. Guan, Q. Kan, Fuel Process. Technol. 96 (2012) 195-202.

[106] S. Storck, H. Bretinger, W.F. Maier, Appl. Catal. A: Gen. 174 (1998) 137-146.

[107] X. Du, E. Wu, J. Phys. Chem. Solids 68 (2007) 1692-1699.

[108] T. Brian. Holland, L. Abrams, A. Stein, J. Am. Chem. Soc. 121 (1999) 4308-4309.

[109] M. Mihaylov, A. Penkova, K. Hadjiivanov, M. Daturi, J. Mol. Catal. A: Chem. 249 (2006) 40-46.

[110] M. Mhamdi, A. Ghorbel, G. Delahay, Catal. Today 142 (2009) 239-244.

[111] F.Z. Zhang, X.W. Guo, X.S. Wang, G.Y. Lia, Q. Zhao, X.H. Bao, X.W. Han, L.W. Lin, Mater. Chem. Phys. 60 (1999) 215-220.

[112] H. Liu, T. Shen, W. Wang, T. Li, Y. Yue, X. Bao, Appl. Clay Sci. 115 (2015) 201-211.

[113] W. Mozgaw, J. Mol. Struct. 555 (2000) 299-304.

[114] M. d. Arco, C. Martin, V. Rives, V. Sanchez-Escribano, J. chem. Soc. Faraday Trans. 89 (1993) 1071-1078.

[115] L. Lietti, I. Nova, G. Ramis, L. Dall'Acqua, G. Busca, E. Giamello, P. Forzatti, F. Bregani, J. Catal. 187 (1999) 419-435.

[116] L. Shirazi, E. Jamshidi, M. R. Ghasemi, Cryst. Res. Technol. 43 (2008) 1300-1306.

[117] L. Rodrıguez-Gonzalez, F. Hermes, M. Bertmer, E. Rodrıguez-Castellon, A. Jimenez-Lopez, U. Simon, Appl. Catal. A: Gen. 328 (2007) 174-182

[118] N. Katada, H. Igi, J. Kim, M. Niwa, J. Phys. Chem. B 110 (1997) 5969-5997.

[119] W. Fanchiang, Y. Lin, Appl. Catal. A: Gen. 419-420 (2012) 102-110.

[120] X. Niu, J. Gao, Q. Miao, M. Dong, G. Wang, W. Fan, Z. Qin, J. Wang, Microporous Mesoporous Mater. 197 (2014) 252-261.

[121] X. Zhao, L. Wei, S. Cheng, Y. Cao, J. Julson, Z. Gu, Appl. Catal. A: Gen. 507 (2015) 44-55.

[122] M. Mhamdi, S. Khaddar-Zine, A. Ghorbel, Appl. Catal. A: Gen. 357 (2009) 42-50.

[123] T. Okachi, M. Onaka, J. Am. Chem. Soc. 126 (2004) 2306-2307.

[124] S. Imachi, M. Onaka, Chem. Lett. 34 (2005) 708-709.

[125] F. Ayaria, M. Mhamdi, J. Alvarez-Rodriguez, A.R. Guerrero Ruiz, G. Delahayc, A. Ghorbel, Appl. Catal. B: Environ. 134-135 (2013) 367-380.

[126] A. De Lucas, J. L. Valverde, F. Dorado, A. Romero, I. Asencio, J. Mol. Catal. A: Chem. 225 (2005) 47-58.

[127] M.O. Daramola, K. Matamela, O.O. Sadare, J. Environ. Chem. Eng. 5 (2017) 54-62.

[128] J. Yuan, X. Huang, M. Chen, J. Shi, W. Shangguan, Catal. Today 201 (2013) 182-188.

[129] H. Huang, H. Huang, Q. Feng, G. Liu, Y. Zhan, M. Wu, H. Lu, Y. Shu, D. Y.C. Leung, Appl. Catal. B: Environ. 203 (2017) 870-878.

[130] F. Ayari, M. Mhamdi, J. Alvarez-Rodriguez, A.R.G Ruiz, G. Delahay, A. Ghorbel, Microporous Mesoporous Mater. 171 (2013) 166-178.

[131] J.H. Yun, R.F. Lobo, Microporous Mesoporous Mater. 155 (2012) 82-89.

[132] M. Liu, X. Guo, X. Wang, C. Liang, C. Li, Catalysis Today 93-95 (2004) 659-664.

[133] M. S. Kumar, M. Schwidder , W. Grünert, A. Brückner, J. Catal. 227 (2004) 384-397.

[134] B. Rhimi, M. Mhamdi, A. Ghorbel, V.N Kalevaru, A. Martin, M. Perez-Cadenas, A. Guerrero-Ruiz, J. Mol. Catal. A: Chem. 416 (2016) 127-139.

[135] Y. Zhang, Y. Zhou, Li Huang, S. Zhou, X. Sheng, Q. Wang, C. Zhang, Chem. Eng. J. 270 (2015) 352-361.

[136] J. Xu, R.D. Armstrong, G. Shaw, N.F. Dummer, S.J. Freakley, S.H. Taylor, G.J. Hutchings, Catal. Today 270 (2016) 93-100.

[137] E. Yuan, K. Zhang, G. Lu, Z. Mo, Z. Tang, J. Ind. Eng. Chem. 42 (2016) 142-148.

[138] M. Mhamdi, S. Khaddar-Zine, A. Ghorbel, Appl. Catal. A: Gen. 337 (2008) 39-47.

[139] J. Dedecek, D. Kaucky, B.Wichterlova, Microporous Mesoporous Mater. 35-36 (2000) 483-494.

[140] S.A. Yashnik, Z.R. Ismagilov, V. F. Anufrienko, Catal. Today 110 (2005) 310-322.

[141] T. Zhang, J. Liu, D. Wang, Z. Zhao, Y. Wei, K. Cheng, G. Jiang, A. Duan, Appl. Catal. B: Environ. 148-149 (2014) 520-531.

[142] C.M.A.S. Freitas, O.S.G.P. Soares, J.J.M. Orfao, A.M. Fonseca, M.F.R. Pereira, I.C. Neves, Green Chem.17 (2015) 4247-4254.

[143] M. Rutkowska, D. Macina, Z. Piwowarska, M. Gajewska, U. Diaz, L. Chmielarz, Catal. Sci. Technol. 6 (2016) 4849-4862.

[144] S. Sang, F. Chang, Z. Liu, C. He, Y. He, L. Xu, Catal. Today 93-95 (2004) 729-734.

[145] D.P. Serrano, R.A. Garcia, M. Linares, B. Gil, Catal. Today 179 (2012) 91-101.

[146] X. Lou, P. Liu, J. Li, Z. Li, K. He, Appl. Surf. Sci. 307 (2014) 382-387.

[147] I. Nowak, J. Quartararo, E.G. Derouane, J.C. Vedrine, Appl Catal. A: Gen. 251 (2003) 107-120.

[148] A. Durmus, S.N. Koc, G.S. Pozan, A. Kasgöz, Appl. Catal. B: Environ. 61 (2005) 316-322.

[149] I.E. Wachs, B.M. Weckhuysen, Appl. Catal. A: Gen. 157 (1997) 67-90.

[150] S. Youn, S. Jeong, D.H Kim, Catal. Today 232 (2014) 185-191.

[151] Z. Fu, D. Yin, Y. Yang, X. Guo, Appl. Catal. A: Gen. 124 (1995) 59-71.

[152] A. Ausavasukhi, T. Sooknoi, Appl. Catal. A: Gen. 361 (2009) 93-98.

[153] B. Liu, D. Slocombe, M. AlKinany, H. AlMegren, J. Wang, Arden, A. Vai, S. Gonzalez-Cortes, T. Xiao, V. Kuznetsov, P. P. Edwards, Appl. Petrochem. Res. 6 (2016) 209-215.

9. Appendices

Appendix A: List of supporting figures and tables

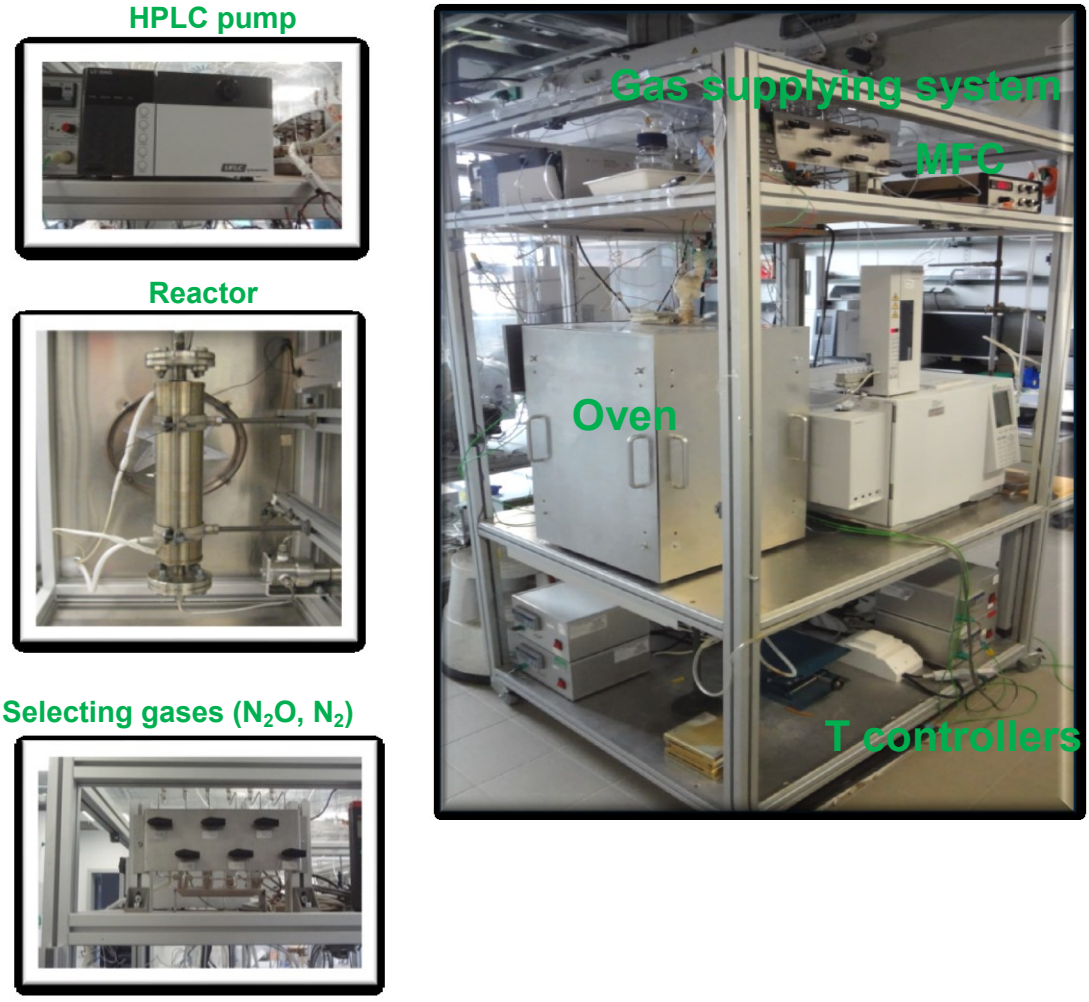

Figure A1. Experimental set up

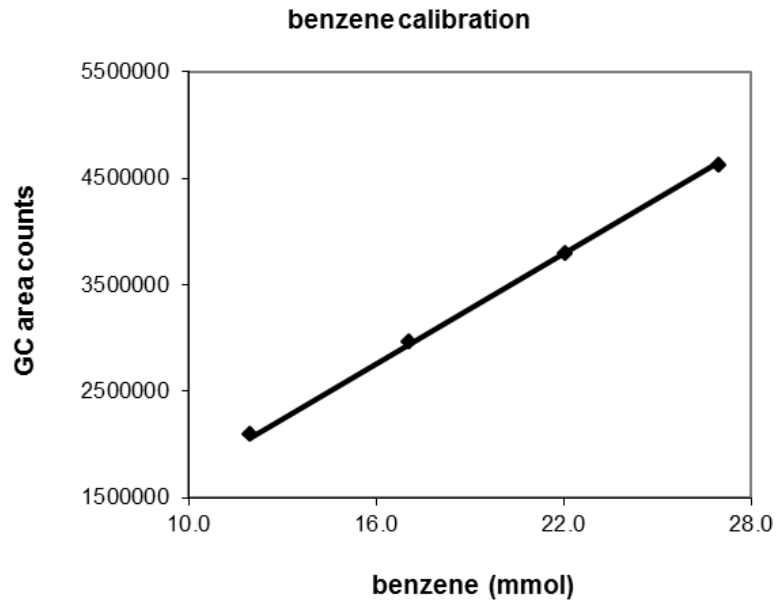

Figure A2.GC calibration plot for benzene (mmol vs GC area counts)

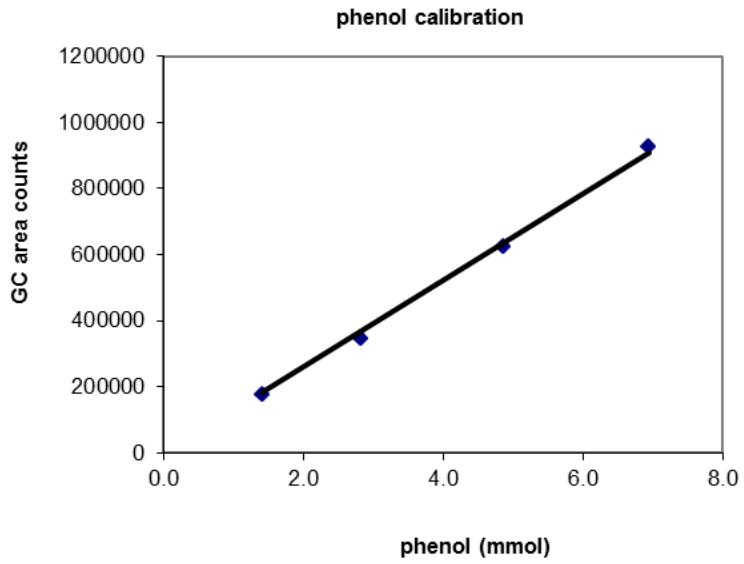

Figure A3.GC calibration plot for phenol (mmol vs GC area counts)

GC-Analysis: (Shimadzu GC-2010Plus).

- Liquid and gases samples
- Duration: 9 min.
- Method Aan3F, Split: 40, Inj. 0,2 µl (Auto sampler)
- Method Aan3F_TCD (gases N_2O, N_2, CO_2 and He)

- 4.4g benzene, 0.45g phenol
- samples are taken out by a syringe: 50 µl
- Collected in a cooling trap (washed by methanol at 0°C)
- Liquid product mixtures of the cooling trap are filled into a 50 ml flask.

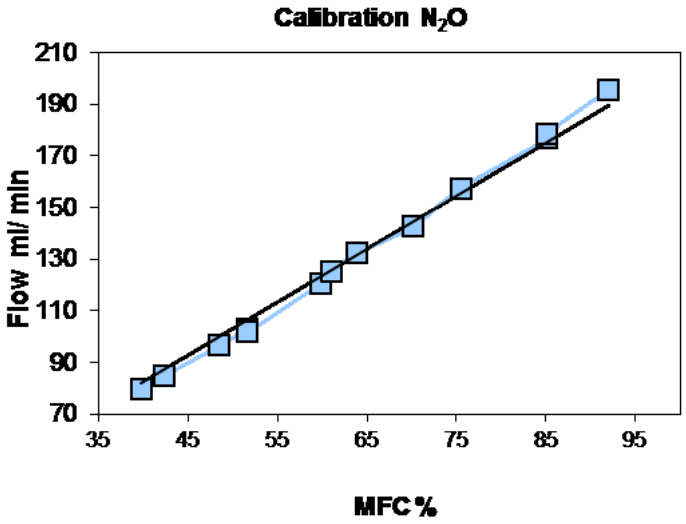

Figure A4. Calibration plot for N_2O MFC.

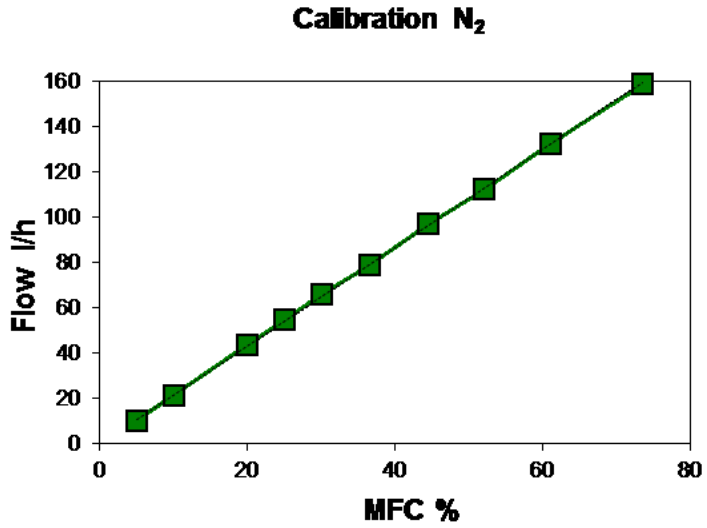

Figure A5. Calibration plot for N_2 MFC

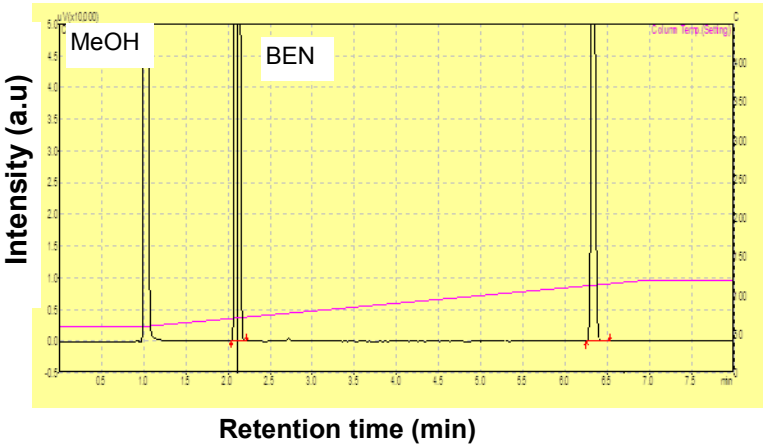

Figure A6. GC chromatogram showing the clear separation of benzene and phenol

Table A1. Phenol calibration by GC taking four different concentrations of phenol

Phenol (wt./g)	Phenol (mmol)	Average GC counts[b]
0.132	1.4	175520
0.265	2.8	345052
0.458	4.9	625712
0.652	6.9	928487

[b] average counts from 4 injections

Table A2. Benzene calibration by GC taking four different concentrations of benzene

Benzene (wt./g)	Benzene (mmol)	Average GC area counts[a]
2.104	26.9	4619435
1.718	22.0	3799874
1.329	17.0	2970432
0.933	11.9	2096127

[a] average counts from 4 injections

Appendix B: list of publications and conference contributions

M. Alotaibi, V.N. Kalevaru, H. Almegren, M. Alkinany, A. Martin, “An improved process for preparing a catalyst and its application for direct synthesis of phenol by hydroxylation of benzene’’, SA 115360683 (2015) (Patent).

M. Alotaibi, V.N. Kalevaru, H. Almegren, M. Alkinany, A. Martin, “Direct hydroxylation of benzene to phenol’’ US (submitted 2016) (patent).

M. Alotaibi, V.N. Kalevaru, H. Almegren, M. Alkinany, A. Martin, “Gas phase hydroxylation of benzene to phenol over M (Ti, V, Cr, Mn)/ZSM-5 using nitrous oxide’’ Catal. Commun (in preparation).

M. Alotaibi, V.N. Kalevaru, H. Almegren, M. Alkinany, A. Martin “One step hydroxylation of benzene to phenol using Fe-ZSM-5”.presented at 16th. Netherlands' Catalysis and Chemistry Conference (NCCC XVI), held at Noordwijkerhout, Netherlands during 2-4 Mar. 2015 (poster).

M. Alotaibi, V.N. Kalevaru, H. Almegren, M. Alkinany, A. Martin, “Direct hydroxylation of benzene to phenol using zeolite catalyst N2O as an oxidant” presented at 17th International Symposium on Relations between Homogeneous and Heterogeneous Catalysis (ISHHC) held at Utrecht, The Netherlands during 12-15 Jul. 2015 (poster).

M. Alotaibi, V.N. Kalevaru, H. Almegren, M. Alkinany, A. Martin, “Gas phase hydroxylation of benzene to phenol over M (Co, Ni, Cu, Zn) ZSM-5 using nitrous oxide” presented at European Congress on Catalysis (Europacat XII) held at Kazan, Russia during 30.08 to 04.09.2015 (poster).